

© Copyright by Pushpesh Sharma 2019
All Rights Reserved

Non-thermal Recovery of Bitumen using Cyclic Surfactant Solubilization

A Dissertation

Presented to

the Faculty of the Department of Chemical and Biomolecular Engineering

University of Houston

In Partial Fulfillment

of the Requirements for the Degree

Doctor of Philosophy

in Chemical and Biomolecular Engineering

by

Pushpesh Sharma

May 2019

Non-thermal Recovery of Bitumen using Cyclic Surfactant Solubilization

Pushpesh Sharma

Approved:

Chair of the Committee,
Dr. Konstantinos Kostarelos,
Associate Professor,
Petroleum Engineering

Committee Members:

Dr. Jeffrey Rimer,
Abraham E. Dukler Professor,
Chemical and Biomolecular Engineering

Dr. Jeremy Palmer,
E. J and B. M Henley Assistant
Professor,
Chemical and Biomolecular Engineering

Dr. S.M. Farouq Ali,
Distinguished Professor,
Petroleum Engineering

Dr. Mohamed Y. Soliman,
Professor & William C. Miller
Department Chair,
Petroleum Engineering

Dr. Suresh K. Khator,
Associate Dean,
College of Engineering

Dr. Michael P. Harold,
Chair & M.D. Anderson Professor,
Chemical and Biomolecular Engineering

Acknowledgments

I would like to express my sincere gratitude towards Dr. Konstantinos Kostarelos for his continuous support of my research, for his patience, motivation, and immense knowledge. His challenged me to continuously improve myself and to expand my knowledge. I am honored to have the opportunity to work under him.

I would also like to thank rest of my committee Dr. Jeffery Rimer, Dr. Jeremy Palmer, Dr. S.M. Farouq Ali, and Dr. Mohamed Y. Soliman for their time and insightful discussions throughout the course of this work. My sincere appreciation goes to Dr. Michael Myers, Dr. Lori Hathon, Prof. C.S. Kabir and Dr. Adry Bissada for sharing their wealth of knowledge, support, and guidance. I want to thank Ms. Yolanda Thomas, Ms. Anne Strum, and Ms. Trina Johnson for their help in managing my degree.

I would like to thank Dr. Sujeewa Palayangoda for his mentorship, without it my research work would not have been possible. I would also like to thank all undergraduate and graduate students in Petroleum Engineering Department that helped me along the way, particularly Mohamad Salman, Jae Ho Lee, Carlos Ortiz, Xiaonan Xiong, and Enjelia Veony.

I want to thank my parents, Shama and Om Prakash Sharma for their unconditional support and sacrifices. I also want to thank my uncle Dr. N.K. Sharma and aunt Dr. Indira Sharma for their guidance and motivation, as well as my sisters and cousins for supporting me throughout this work and my life in general.

I dedicate this work in loving memory of my grandfather Raghuveer Prasad Sharma, who believed in me and taught me to be a better human being.

Non-thermal Recovery of Bitumen using Cyclic Surfactant Solubilization

An Abstract

of a

Dissertation

Presented to

the Faculty of the Department of Chemical and Biomolecular Engineering

University of Houston

In Partial Fulfillment

of the Requirements for the Degree

Doctor of Philosophy

in Chemical and Biomolecular Engineering

by

Pushpesh Sharma

May 2019

Abstract

Natural bitumen and extra heavy oil resources accounts for approximately two-thirds of the known fossil fuel resources in the world. Existing recovery processes for these resources have been criticized for their negative impact on the environment. This study presents a novel approach - cyclic surfactant solubilization. The process involves solubilizing heavy oil in a low viscosity single phase microemulsion using a surfactant formulation. The surfactant formulation can be recovered for reinjection after oil separation and recovery. It is a non-thermal sustainable approach.

Initially, a proof-of-concept study was conducted using a model oil, namely coal tar. Based on phase behavior studies a suitable surfactant formulation was selected and flow experiments were conducted. The study established that oil recovery is possible by producing only single phase microemulsion.

The next step was to apply the process on real field samples. Oil sands samples were acquired from Alberta, Canada for that purpose. Bitumen was extracted from the sand to perform oil characterization and phase behavior studies. However, flow experiments performed with the selected surfactant formulation did not yield expected results, which led to phase behavior experiments with oil sands instead of extracted oil. The formulation was optimized based on these observations and a set of flow experiments were conducted which resulted in improved recoveries.

A part of the cyclic surfactant solubilization process is surfactant recovery and recycle. This study also explores various pathways to achieve this. The economics of the process may be improved with the development of surfactant recovery processes.

A green alternative to recover bitumen from these resources is key for fulfilling future energy demands and for keeping climate change in check. The cyclic surfactant solubilization process provides a feasible low-energy alternative to thermal processes especially in countries like Venezuela and Canada, where majority of fossil fuel resources are available in the form of natural bitumen or extra heavy oil.

Table of Contents

Acknowledgments	v
Abstract	viii
Table of Contents	x
List of Figures	xvi
List of Tables	xxi
Nomenclature	xxiii
Chapter 1 Introduction	1
1.1 Motivation	1
1.2 Research Objectives	2
Chapter 2 Background	4
2.1 Natural Bitumen and Extra Heavy Oil.....	4
2.2 Bitumen and Extra Heavy Oil Recovery Processes	6
2.2.1 In-situ Methods	6
2.2.2 Ex-situ Methods – Open Pit Mining	21
2.3 Surfactant Chemical EOR.....	23
2.3.1 Surfactants – Properties and Classification.....	23
2.3.2 Fundamentals of Surfactant EOR	25
2.3.3 Single Phase Microemulsion	29

2.3.4 Microemulsion Separation and Surfactant Recovery	30
Chapter 3	33
Chapter 4 Equipment and Materials	35
4.1 Equipment	35
4.1.1 Gas Chromatograph and Mass Spectrometer (GC-MS)	35
4.1.2 High Performance Liquid Chromatograph (HPLC)	36
4.1.3 Auto Titrator System	36
4.1.4 Mixer	36
4.1.5 Centrifuge.....	37
4.1.6 Pump	37
4.1.7 Fluid Reservoirs	37
4.1.8 Pressure Differential Transducers and Data Acquisition	37
4.1.9 Tubing.....	38
4.1.10 Valves and Fittings.....	38
4.1.11 Core Holder	39
4.1.12 Glass Column.....	39
4.1.13 Fractional Collector	39
4.1.14 Sealing Torch	39
4.1.15 Vacuum Pump	40

4.1.16 Glassware and Centrifuge Tubes.....	40
4.1.17 Viscometer	40
4.1.18 pH and Conductivity Meters	41
4.1.19 Water De-ionizer	41
4.1.20 Filtration Equipment	41
4.1.21 Scales.....	41
4.1.22 Water Bath Circulator	42
4.1.23 Benchtop Mixers	42
4.2 Materials.....	42
4.2.1 Oil Sands.....	42
4.2.2 Clean Sand.....	42
4.2.3 Gases	42
4.2.4 Chemical	43
4.2.5 Surfactants	44
Chapter 5 Experimental Procedures.....	46
5.1 Coal tar.....	46
5.1.1 Stock Solution Preparations	46
5.1.2 Phase Behavior Studies	47
5.1.3 Flow Experiment	49

5.2 Bitumen	51
5.2.1 Soxhlet Extraction	51
5.2.2 Bitumen Extraction from Oil Sands	52
5.2.3 Stock Solution Preparation.....	53
5.2.4 Phase Behavior Studies	54
5.2.5 Static Tests	55
5.2.6 Dynamic Tests	57
5.2.7 Sandpack Permeability Measurement	63
5.2.8 Polymer Solution Preparation and Characterization	64
5.3 Surfactant Recovery Experiments	64
5.3.1 Surfactant Behavior with pH Variations and Salt Concentration.....	64
5.3.2 Microemulsion Behavior with pH Variations and Salt Concentration	65
Chapter 6 Results and discussion	66
6.1 Coal tar.....	66
6.1.1 Surfactant Screening	66
6.1.2 Salinity Scans	70
6.1.3 Aqueous Stability Tests	72
6.1.4 Flow Experiment	73
6.2 Bitumen	79

6.2.1 Soxhlet Extraction	79
6.2.2 Bitumen Characterization	79
6.2.3 Phase Behavior Studies	82
6.2.4 Dynamic Tests 1 – 3.....	88
6.2.5 Static Tests	93
6.2.6 Dynamic Tests 4 – 8.....	99
6.3 Surfactant Recovery Experiments	116
6.3.1 Surfactant Behavior with pH Variations and Salt Concentration.....	116
6.3.2 Microemulsion Behavior with pH Variations	121
Chapter 7 Summary, Conclusions and Recommendations	125
7.1 Summary.....	125
7.1.1 Coal tar: Proof of Concept.....	125
7.1.2 Bitumen	126
7.1.3 Surfactant Recovery Experiments	128
7.2 Conclusions	130
7.3 Recommendations.....	131
References	133
Appendix A	143
A.1 Coal tar GC calibration.....	143

A.2 Bitumen GC calibration	145
----------------------------------	-----

List of Figures

Figure 2-1: Recovery methods for bitumen and extra heavy oil	8
Figure 2-2: Schematic diagram of CSS (imperialoil.ca, Canada)	14
Figure 2-3: SAGD Production Scheme (oilsandsmagazine.com).....	17
Figure 2-4: Mechanism of VAPEX process (Das 1998)	18
Figure 2-5: Schematic diagram of In-situ Combustion (insitucombustion.ca)	21
Figure 2-6: Flow scheme for the open pit mining process (2b1stconsulting.com)	22
Figure 2-7: Phase change from type I to type II through different types of type IV microemulsion (Winsor, 1948)	29
Figure 3-1: Cyclic surfactant solubilization flow schematic.....	34
Figure 5-1: Flow experiment setup for coal tar recovery	51
Figure 5-2: Soxhlet Extractor (source blogspot.com)	52
Figure 5-3: Solvent recovery setup	53
Figure 5-4: Flow diagram for dynamic tests, blue colored loop highlights the bypass loop	58
Figure 5-5: Glass Column used in all dynamic tests except test 3.....	59
Figure 6-1: Surfactant screening tubes for 2 wt.% C24-28 IOS surfactant formulation with coal tar at 25°C.....	67
Figure 6-2: Solubilization of nine coal tar components with 2 wt.% C24-28 IOS surfactant formulation. The nine components are 1) azulene, 2) 2-methyl naphthalene, 3) acenaphthene, 4) dibenzofuran, 5) fluorene, 6) phenanthrene, 7) fluoranthene, 8) pyrene, and 9) benzopyrene.....	67

Figure 6-3: Solubilization of nine coal tar components with 2 wt.% alcohol propoxy sulfate, 1 wt.% C15-18 IOS, 1 wt.% C12-13 AAS, and 4 wt.% 2-butanol surfactant formulation. The nine components are 1) azulene, 2) 2-methyl naphthalene, 3) acenaphthene, 4) dibenzofuran, 5) fluorene, 6) phenanthrene, 7) fluoranthene, 8) pyrene, and 9) benzopyrene 68

Figure 6-4: Surfactant screening tubes for 4 wt.% alcohol propoxy sulfate and 4 wt.% sodium dioctyl sulfosuccinate with 4 wt.% tri-ethylene glycol monobutyl ether as co-solvent and 0.5 wt.% Na₂CO₃ with coal tar at 25°C. The picture at the bottom is taken under UV light 69

Figure 6-5: Solubilization of nine coal tar components with 4 wt.% alcohol propoxy sulfate and 4 wt.% sodium dioctyl sulfosuccinate with 4 wt.% tri-ethylene glycol monobutyl ether and 0.5 wt.% Na₂CO₃ formulation. The nine components are 1) azulene, 2) 2-methyl naphthalene, 3) acenaphthene, 4) dibenzofuran, 5) fluorene, 6) phenanthrene, 7) fluoranthene, 8) pyrene, and 9) benzopyrene 70

Figure 6-6: Salinity scan for 4 wt.% alcohol propoxy sulfate and 4 wt.% sodium dioctyl sulfosuccinate with 4 wt.% tri-ethylene glycol mono-butyl ether and 0.5 wt.% Na₂CO₃ formulation at 25°C..... 71

Figure 6-7: Salinity scan for selected formulation at 25°C. From top left, four WOR are shown a) WOR=1, b) WOR=2, c) WOR=3, and d) WOR=4 72

Figure 6-8: Aqueous stability for selected surfactant formulation at 25°C, no separation or instability was observed 73

Figure 6-9: Produced microemulsion from the flow experiment under UV light 74

Figure 6-10: Viscosity of produced microemulsion at 25°C.....	75
Figure 6-11: Coal tar recovered with pore volumes of microemulsion produced	76
Figure 6-12: Concentration of coal tar in produced microemulsion, measured using GC77	
Figure 6-13: Comparison of sand (OK-75) before and after the flow experiment	78
Figure 6-14: Bitumen viscosity variations at shear rate = 10 s^{-1} with temperature	80
Figure 6-15: Bitumen viscosity at multiple temperature and shear rates, notice the shear thinning behavior	81
Figure 6-16: Surfactant screening tubes for 0.5 wt.% C12-13 sulfate (7 PO), 0.5 wt.% C12-13 AAS (13 PO), 1 wt.% 2-butanol, and 0.5 wt.% Na_2CO_3	83
Figure 6-17: Surfactant screening tubes for 0.5 wt.% C20-24 IOS, 0.5 wt.% C13 13 PO sulfate, 1 wt.% 2-butanol and 0.5 wt.% Na_2CO_3	83
Figure 6-18: Salinity scan for 0.50 wt.% C20-24 IOS and 0.50 wt.% C13 13 PO alcoxy sulfate, with 1 wt.% 2-butanol and 0.2 wt.% NaCl with bitumen	85
Figure 6-19: Salinity scan for 0.25 wt.% C20-24 IOS and 0.25 wt.% C13 13 PO alcoxy sulfate, with 0.5 wt.% 2-butanol and 0.2 wt.% NaCl with bitumen	86
Figure 6-20: WOR scan for 0.25 wt.% C20-24 IOS and 0.25 wt.% C13 13 PO alcoxy sulfate, with 0.5 wt.% 2-butanol, 0.5 wt.% Na_2CO_3 , and 0.2 wt.% NaCl with bitumen.....	87
Figure 6-21: Aqueous stability tubes for surfactant formulation, notice cloudy solution for salinities 4 and 5 wt.% NaCl	88
Figure 6-22: Bitumen concentration and oil recovery dynamic test 2	91
Figure 6-23: Concentration and pressure profile during dynamic test 3	93

Figure 6-24: Static test result for oil sand mixed with 0.25 wt.% C20-24 IOS, 0.25 wt.% C13 13 PO sulfate, 1 wt.% 2-butanol and 0.5 wt.% sodium carbonate	94
Figure 6-25: Surfactant adsorption with respect to sodium carbonate concentration, notice the inflection point at 2 wt.%	96
Figure 6-26: Alkali scan for 0.25 wt.% C20-24 IOS and 0.25 wt.% C13 13 PO alcoxy sulfate, and 0.5 wt.% 2-butanol, notice the phase separation in tubes higher than 4 wt.% Na ₂ CO ₃	98
Figure 6-27: Static test for 1 wt.% C20-24 IOS and 1 wt.% C13 13 PO alcoxy sulfate, 1 wt.% TEGMBE, and 4 wt.% Na ₂ CO ₃	99
Figure 6-28: Concentration profile for bitumen in test 1, concentrations are normalized by the highest concentration which was 30,000 mg/L.....	101
Figure 6-29: Picture of the flow setup during the test. Notice the microemulsion moving through the column, circled in red	102
Figure 6-30: Top left – Original sand sample, Top right – Inlet sand sample after test, Bottom left – Side view of outlet sand sample, and Bottom right – Top view of outlet sand sample	103
Figure 6-31: Concentration profile for test 5, concentrations are normalized by the highest concentration 37,700 mg/L.....	104
Figure 6-32: Top – Original sand sample, bottom left – Inlet sand sample after test, and bottom right outlet sand sample after test	106
Figure 6-33: Concentration profile test 6, concentrations are normalized by the highest concentration 35,500 mg/L	108

Figure 6-34: Top left – original sand sample, top right – inlet sand sample after test, bottom left – side view of outlet sand sample, and bottom right – top view of outlet sand sample	109
Figure 6-35: Bitumen concentration profile of test 7, concentrations are normalized by the highest concentration 35,000 mg/L	110
Figure 6-36: Top – Original oil sand, Bottom left – Inlet sand, and Bottom right – Outlet sand.....	112
Figure 6-37: Top - original oil sand, bottom left – Inlet sand, and bottom right – outlet sand.....	115
Figure 6-38: Left – Microemulsion mixture produced from dynamic test. Right – Separated phases after acid addition and equilibration	122
Figure 6-39: Left – Produced microemulsion from dynamic test. Right – Microemulsion after base addition, notice black droplet on the glass wall, indicating unstable solution	123
Figure 6-40: Microemulsion from Triton X-100 static tests. Right – Separated phases after salt addition and equilibration.....	124
Figure A-1: Gas chromatograph peak area for azulene for different coal tar concentrations	144
Figure A-2: Peak area for retention time 20-40 mins, for different bitumen concentration in DCM.....	147
Figure A-3: Peak area for retention time 20-40 mins, for lower bitumen concentration in DCM.....	148

List of Tables

Table 4-1: GC-MS specification	35
Table 4-2: HPLC System description	36
Table 4-3: PFA tubing specifications	38
Table 4-4: Laboratory gases	43
Table 4-5: Anhydrous salts and their vendors	44
Table 4-6: Surfactant types and activity	45
Table 5-1: GC-MS method used for microemulsion analysis with coal tar	48
Table 5-2: GC method for microemulsions bitumen concentration measurement.....	55
Table 5-3: HPLC method for surfactant detection	56
Table 5-4: Sandpack properties for dynamic tests	61
Table 6-1: Results of Soxhlet extraction for oil sand	79
Table 6-2: SARA results for bitumen and coal tar.....	80
Table 6-3: Bitumen viscosity at 10 s^{-1} shear rate at different temperatures	81
Table 6-4: Results of Dynamic test 1.....	90
Table 6-5: Results of Dynamic test 2.....	92
Table 6-6: Results of dynamic test 4.....	92
Table 6-7: Synthetic sand static test design and results.....	95
Table 6-8: Surfactant adsorption with respect to the amount of alkali added	96
Table 6-9: Properties of sandpack in dynamic test 4.....	100
Table 6-10: Properties of dynamic test - 5.....	104
Table 6-11: Sandpack composition and properties for test – 6	107

Table 6-12: Sandpack properties and composition for test 7	110
Table 6-13: Viscosity of different polymer concentration solution at 20°C and 1/s shear rate	113
Table 6-14: Sandpack properties and composition for test 8	113
Table 6-15: Observations of acid addition to surfactant stock solutions	118
Table 6-16: Observations of base addition to surfactant stock solutions	120
Table 7-1: Summary of dynamic tests	128
Table 7-2: Results summary of dynamic tests	128
Table A-1: Compound names and retention time for coal tar	143
Table A-2: Conversion factor for selected compound from coal tar	145
Table A-3: Bitumen calibration GC method	146

Nomenclature

Acronyms

AAS	Alkyl aryl sulfonates
API	American Petroleum Institute
AS	Alkali surfactant
ASP	Alkali surfactant polymer
bbls	Barrels
BPR	Backpressure regulator
CHOPS	Cold Heavy Oil Production with Sand
cm	Centimeters
DI	De-ionized water
EO	Ethylene oxide
EOR	Enhanced oil recovery
g	Grams
GC	Gas chromatography
GC-MS	Gas chromatography and mass spectrometry
GOR	Gas oil ratio
HPLC	High performance liquid chromatography
IFT	Interfacial tension, dynes/cm
IOR	Improved oil recovery
IOS	Internal olefin sulfonate
ISC	In-situ combustion
L	Liters
M	Mole per liter
ME	Microemulsion
ml	Milliliter
mm	Millimeter

MPa	Megapascals
MSD	Mass selective detector
N	Gram equivalent per liter
OOIP	Original oil in place
PO	Propylene oxide
PPM	Parts per million
psig	Pounds per square inch, gauge
psia	Pounds per square inch, absolute
PV	Pore volume
ROIP	Residual oil in place
RPM	Revolutions per minute
SAGD	Steam Assisted Gravity Drainage
SOR	Steam oil ratio
TAN	Total acid number
TDS	Total dissolved solids
TGMBE	Triethylene glycol monobutyl ether
UV	Ultraviolet
VAPEX	Vapor Extraction
WAG	Water Alternating Gas
wt.	Weight

Symbols

<i>A</i>	Area, cm ²
<i>C</i>	Concentration, wt% or ppm
cP	Centipoise
cSt	Centistokes

C_H	Huh constant, 0.3 dynes/cm
g	acceleration due to gravity, m/s ²
h	Height, inch or cm
k	permeability, md
L	Length, inch or cm
M	Mobility ratio
N_{\square}	Dimensionless Bond Number
N_{\square}	Dimensionless capillary number
N_{\square}	dimensionless Trapping Number
p	pressure, psia or psig
Δp	pressure gradient, psi
q	rate, cm ³ /min
RF	Recovery Factor
S	Saturation
SP	Solubilization parameter
T	Temperature; Kelvin, Celsius, or Fahrenheit
u	Superficial velocity, ft/d
V	Volume, cm ³

Greek

λ	Mobility, md/cp
μ	viscosity, cp
ρ	density, g/cm ³
σ	interfacial tension, dynes/cm
W_f	bulk water fraction

Chapter 1

Introduction

This study explores a novel application of chemical Enhanced Oil Recovery (EOR) principles to develop a non-thermal method of oil recovery from natural bitumen and extra heavy oil reservoirs. The chemical EOR approach implemented in this work differs significantly from conventional chemical methods.

1.1 Motivation

Natural bitumen and extra heavy oil make up approximately two thirds of the fossil fuel resources in the world. Due to physical characteristics such as high viscosity and density, recovery of oil from these resources becomes challenging. Oil viscosity decreases exponentially with the temperature, hence thermal methods of recovery are prevalent. Thermal methods are responsible for a significant portion of heavy oil produced all over the world.

Thermal methods, such as open pit mining, Steam Assisted Gravity Drainage (SAGD), Vapor Extraction (VAPEX) etc., have a larger carbon footprint. These processes have been criticized for heating permafrost, extensive use of freshwater resources, and land stripping. The produced oil from thermal methods is still highly viscous and needs to be diluted with solvents to be transported to refineries. These methods are being applied predominantly in the fields of Canada and Venezuela.

The non-thermal methods utilized for bitumen and extra heavy oil recovery are Cold Heavy Oil Production with Sands (CHOPS), and chemical EOR. The CHOPS method is

generally applied for depositions with higher temperature and in the presence of solution gas. CHOPS is being utilized in Canada and the Orinoco belt Venezuela, where conditions are suitable. Current chemical EOR research is predominantly focused on mobility control by either alkali addition or polymer injection. Chemical EOR approach is mostly in research or pilot phase. There are some efforts towards a thermal chemical application which is a combination of thermal and chemical (surfactants) methods, but these alternatives are also still in the research phase.

Provided the adverse effect of recovery methods on the environment and the size of the resource, it is essential for future energy demand to develop a more sustainable non-thermal method of oil recovery from natural bitumen and extra heavy oil reservoirs.

1.2 Research Objectives

The objective of the work presented in this dissertation involves conceptualization and development of a sustainable non-thermal process for oil recovery from natural bitumen and extra heavy oil reservoirs. Specifically, this study proposes a novel approach of Cyclic Surfactant Solubilization. Initially, a proof-of-concept study was conducted using synthetic oil. Based on phase behavior studies a suitable surfactant formulation was selected and flow experiments were conducted. The study established that oil recovery is possible by producing only single phase microemulsion. The next step was to apply the process on real field samples. Oil sands samples were acquired from Alberta, Canada for that purpose. Bitumen was extracted from the sands to perform oil characterization and phase behavior studies. However, flow experiments performed with the selected surfactant formulation did not yield expected results, which led to phase behavior

experiments with oil sands instead of extracted oil. The formulation was optimized based on these observations and a set of flow experiments were conducted which resulted in improved recoveries. A critical part of the cyclic surfactant solubilization process is surfactant recovery and recycle. A variety of different approaches were employed. These processes are still being investigated.

Chapter 2

Background

2.1 Natural Bitumen and Extra Heavy Oil

Oil resources are classified based on their API gravity and viscosity. Conventional oils have API gravity higher than 22.3°API and viscosity less than 100 cP. Oil with API between 10 to 22.3°API and viscosity higher than 100 cP are considered as 'heavy oil'. If the crude oil is less than 10°API and a viscosity higher than 10,000 cP, it is considered to be 'extra heavy oil'. Natural bitumen is generally refers to an oil that has an API gravity less than 7°API (Fassihi and Kovscek, 2017).

According to a study by the International Energy Agency, unconventional oil (including bitumen, extra-heavy oil, and kerogen) accounts for two-thirds of the recoverable oil resources in the world (International Energy Agency, 2013). There are 598 and 162 deposits reported for natural bitumen and extra-heavy oil respectively (WEC, 2010). The Orinoco Oil Belt in Eastern Venezuela is the largest deposit of extra-heavy oil in the world, 1.9 trillion bbls of original oil in place (Fassihi and Kovscek, 2017). The Western Canada Sedimentary Basin contains a vast deposit of natural bitumen predominantly in the form of oil sands, approximately 1.73 trillion bbls (WEC, 2010). Other significant deposits of natural bitumen are Grosmont carbonate in Alaska, North Caspian basin in Kazakhstan, and Timan-Pechora basin in Russia (Fassihi and Kovscek, 2017).

Most of these accumulations are broad, shallow deposits trapped on the flanks of foreland basins. Foreland basins are depressions formed by the depression of the earth's crust during orogeny. Marine sediments buried in these basins became the source rock for hydrocarbon (Alboudwarej et al., 2006). These hydrocarbons move up dip into the eroded formation which often lacks any sealing caprocks. These shallow and cool accumulations provide perfect conditions for biodegradation.

Microorganisms degrade the light and medium hydrocarbons over geological time scales, producing methane and leaving heavy hydrocarbons. Biodegradation leads to oxidation of the oil, decreased GOR, increased density, viscosity, acidity, sulfur content, and metal content. The main limiting factor for biodegradation is temperature. The microbial degradation is feasible in reservoirs at less than 80°C but it is effective up to 65-70°C and above 90°C the depositions are considered sterilized. The second limiting factor is the presence of inorganic nutrients, which is present in the formation water. The extent of biodegradation can be assessed by a scale ranging from 1 to 10 proposed by Peters, Walters, and Moldowan (Peters et al., 1993). According to the scale biodegradation levels (PM levels) are light (1-2), moderate (4-5), heavy (6-7), very heavy (8-9), and severe (10). Some physical processes such as water washing, and phase separation also contribute to separating light fractions from oil.

The composition of heavy oil depends on the depositional environment, extent of microbial degradation, pressure, and temperature of the deposition. The properties of bitumen can vary spatially in a given accumulation; this is attributed to more degradation

near the oil water contact resulting in highly viscous oil at the deeper section (Gates et al., 2010).

2.2 Bitumen and Extra Heavy Oil Recovery Processes

Based on reservoir characteristics (depth, thickness, rock type, temperature, and dynamic properties such as permeability, and porosity) and crude oil properties (composition, viscosity, and solution gas oil ratio etc.), an optimal heavy oil recovery method is selected. Various recovery methods are shown in the Figure 2-1.

2.2.1 In-situ Methods

2.2.1.1 Non-thermal In-situ Methods

Non-thermal methods can be sub-divided into primary recovery and improved/enhanced oil recovery processes (IOR/EOR).

Primary Recovery

Primary recovery is defined as the oil recovery achieved without any external energy added into the reservoir. Primary production is achieved by conventional oil production techniques utilizing either high density vertical wells (due to low mobility of the oil) or horizontal wells. The pressure reduction created by production liberates the solution gas present in the oil, which aids in recovery by way of volume replacement due to the higher compressibility of gas compared to liquid.

Primary methods usually result in 4 to 12% average recovery. In addition to the oil properties, the recovery efficiency is also dependent upon reservoir permeability, solution gas oil ratio and reservoir heterogeneity.

Cold Heavy Oil Production with Sand (CHOPS)

Sand production is not desirable in conventional oil production, but this may be desirable for heavy oil recovery. The CHOPS method is based on the fact that sand production modifies the near-wellbore geometry resulting in wormholes, dilated zones, and cavities, leading to increased porosity and permeability. Frictional drag on the oil is reduced because of the sand flow resulting in increased productivity. The CHOPS process is applicable for unconsolidated sands with heavy oil containing solution gas. CHOPS wells are vertical or slightly deviated wells. There are three main mechanism for oil production from CHOPS. Solution gas drive, wormholes activation and a delayed water-drive (Fassihi and Kavscek, 2017). Solution gas evolution from heavy oil provides a drive called “foamy flow”.

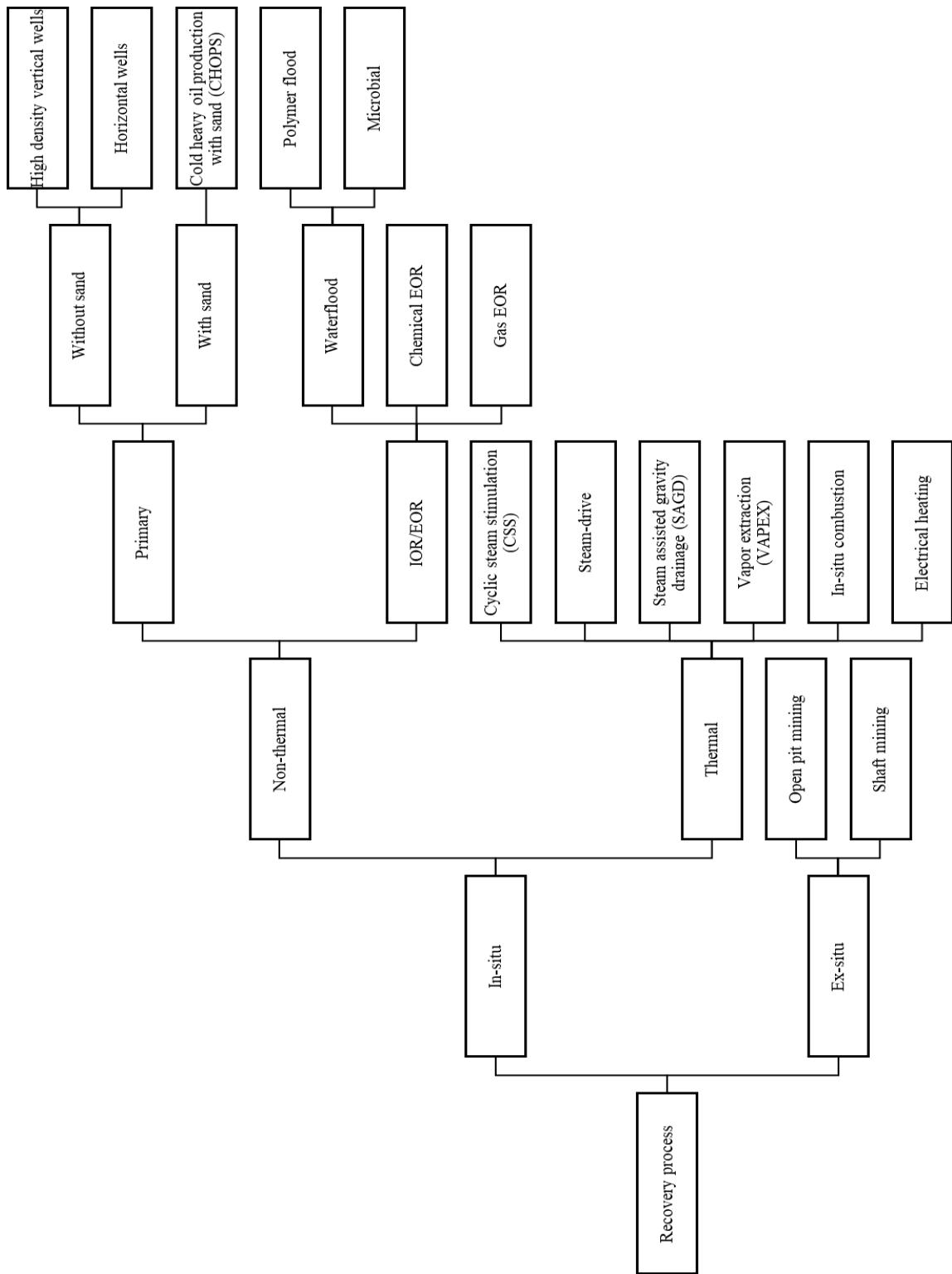


Figure 2-1: Recovery methods for bitumen and extra heavy oil

A downhole pump creates an aggressive pressure differential between the formation and wellbore. The pressure drop forces the solution gas evolution from the heavy oil solution and create foams. In the later phase of operation, it is observed that the recovery mechanism changes from solution gas drive to water drive. Initial sand production is around 10%, which decreases to 2% with stable production (Speight, 2009). CHOPS has been successfully applied at multiple locations in Venezuela and Canada. Sand separation, handling and disposal are economic and operational challenges for CHOPS.

Another important group of non-thermal processes are termed improved and enhanced oil recovery processes. This category includes waterflooding, surfactant-polymer flooding and gaseous processes. These processes are applied in reservoirs where thermal methods are either not required or inefficient due to heat losses and/or deep formations.

Waterflooding and Polymer Flooding

Waterflooding is challenging in heavy oil reservoirs, due to an unfavorable very high mobility ratio caused by a vast difference between displacing and displaced fluid viscosities. The mechanism of recovery is the immiscible displacement (piston-like) of oil by injected water, but instead, due to highly unfavorable mobility ratio, injected water tends to finger through highly-permeable zones leading to very high water cut in production. Examples of waterflooding application for heavy oil in literature are mostly limited to oil less than 1000 cP viscosity (Beliveau, 2009).

The presence of polymer improves the mobility ratio which can significantly improve the recovery efficiency when compared with waterflooding. Studies have shown that polymer injection also results in reduction in residual oil saturation due to their viscoelastic nature (J. J. Sheng et al., 2015; Qi et al., 2017). However, polymer flooding has been shown to be more effective for intermediate viscosity oils (between 10 to 150 cP) (Seright, 2010). Higher viscosity oil requires more viscous polymer solution which, in turn, requires a high injection pressure.

Chemical EOR Processes

Chemical EOR processes are gaining attention for heavy oil fields due to their minimal environmental impact and energy efficiency. Chemical EOR for heavy oil research is currently focused primarily on injection of alkalis. There are some examples of combinations of alkali with surfactants and polymers. Common examples of alkali, used in chemical EOR, are Na_2CO_3 , NaBO_2 , NaOH , and KOH . Alkali is used to control surfactant adsorption and to generate in-situ soaps. For heavy oil, the major advantage of alkali use is the generation of in-situ surfactant. Heavy oils generally have a high amount of naphthenic acids; it is quantified by total acid number (TAN). It is the amount (mg) of KOH required to neutralize one gram of oil. Crude oils with TAN higher than 1 mg KOH/g are considered to be high-TAN crude.

McAuliffe showed that injection of oil-in-water emulsion improved the oil recovery (McAuliffe, 1973). Based on these observations, it is proposed that the emulsion generated from the in-situ surfactants will also improve recovery. Jennings et al. explained that in-situ surfactants generated by the alkali reduce the interfacial tension

between oil and water (Jennings et al., 1974). This results in the emulsification of oil in water. The emulsion droplets are larger and become entrapped in the smaller pore throat leading to a decrease in the mobility of the water phase. Low mobility water provides better sweep efficiency, resulting in improved oil recovery.

Alkali injection with a synthetic surfactant is also suggested to further increase the emulsification. The effects of other parameters such as surfactant addition are contradictory in the literature. Liu et al. (Liu et al., 2006) and Bryan et al. (Bryan and Kantzas, 2007) discussed alkaline surfactant (AS) flooding for Canadian heavy oil. They reported that surfactants with alkali injection resulted in an oil-in-water emulsion and improved sweep efficiency. Bryan et al. found that only surfactant injection was not sufficient to emulsify oil, alkali injection is necessary (Bryan and Kantzas, 2009). Zhang et al. reported that addition of surfactant to alkali does not improve the recovery efficiency (Zhang et al., 2010). They reported that mobility control is critical in the process instead of IFT reduction. Pei et al. also observed that there is no significant benefit of adding surfactant (Pei et al., 2012). Tang et al. reported a different mechanism for the alkali process, that water-in-oil emulsion is responsible for sweep efficiency improvement (Tang et al., 2013). Kumar showed that the salinity of the reservoir affects the type of emulsion formed (Kumar, 2013). High salinity will lead to highly viscous water-in-oil emulsion leading to better sweep efficiency than oil-in-water emulsion at low salinity. Pei et al. reported that addition of low molecular weight alcohol would improve the recovery efficiency (Pei et al., 2014).

Kumar and Mohanty applied a traditional alkali-surfactant-polymer (ASP) flooding for medium-heavy oil (330 cP) (Kumar and Mohanty, 2010). Sim et al. reported improved oil recovery for heavy oils (>10,000cP) with ASP as compared to polymer flooding (Sim et al., 2014). Another work compared polymer and ASP floods for heavy oils of different viscosities (Fortenberry et al., 2015). ASP improved the performance in every case but both polymer and ASP process performance was still poor for higher viscosities. A modification of the ASP technique was proposed as alkali cosolvent polymer (ACP) flooding (Fortenberry et al., 2015). Mechanisms of chemical EOR processes are discussed in detail in section 2.3.

Another chemical approach discussed in the literature is to inject oil and water emulsion into the subsurface. The injection of emulsions led to improvement in recovery for intermediate viscosity oils. Injection of water-in-oil emulsion found to be more effective than oil-in-water emulsion (Farouq Ali et al., 1979), which suggests that the recovery mechanism is better sweep as experienced for alkali injection. A refinement of this approach called as oil external solid stabilized emulsions, was suggested (Kaminsky et al., 2011). They added small quantities of various minerals such as kaolinite, bentonites, and surface-fumed silica, to improve the stability of the injected emulsion. The emulsion injection approach is generally not accepted by operators due to their unwillingness to inject oil back into the reservoir.

Gaseous Injection Processes

Carbon dioxide (CO₂) has overtaken thermal processes to become the largest EOR technique in the United States. The application of CO₂ EOR has been focused on lighter

oils, however there are some examples in literature for its application in heavy oil reservoirs (Sobers et al., 2010; Araghi, 2010). The most significant challenge with gas injection processes is mobility control. Foam generation is being studied as a possible mobility control mechanism (Emadi et al., 2011). Gas injection processes for heavy oil are at very early stage of research and need to be investigated more before applying for heavy oil.

2.2.1.2 Thermal In-Situ Methods

Thermal EOR methods are the most applied methods in the field for bitumen and extra heavy oil recovery. Steam injection heats up the reservoir and formation fluids, leading to an exponential decrease in the oil viscosity. Low viscosity oil flows easily through the subsurface to the production well. Thermal processes can be either: steam-injection based such as cyclic steam stimulation, steam flooding etc.; solvent-injection based such as vapor extraction, or; air-injection based such as In-situ combustion.

The steam injection application depends on multiple factors such as reservoir depth, reservoir thickness and presence of an aquifer. Deeper reservoirs require high-pressure steam, which is not cost effective (Fassihi and Kovscek, 2017). Also, longer wellbore travel distance in deeper reservoirs experience heat loss prior to reaching the formation. Some major steam, solvent, and air injection applications in extra heavy oil are discussed in detail here.

Cyclic Steam Stimulation (CSS)

Cyclic steam stimulation, also known as the Huff and Puff method, uses a combination of viscosity reduction, wettability alteration and gas expansion as recovery mechanisms (Alvarez and Han, 2013).

CSS is a three-stage cyclic process, which utilizes one well as both injector and producer (Figure 2-2). The three stages of a cycle are injection, soaking, and production. During the first stage, high pressure and temperature steam is injected into the well to heat the oil. At the second stage, the well is closed to let the formation soak the steam. Finally, the well is opened to produce lower viscosity oil. A cycle generally has 10% of days for injection, 10% for soaking and 80% for production (Alvarez and Han, 2013). As the reservoir temperature decreases to pre-steam injection level, a new cycle is started. Cycles are repeated until the production rates are uneconomical. For heavier oils, artificial lift is required to bring the oil to the surface.

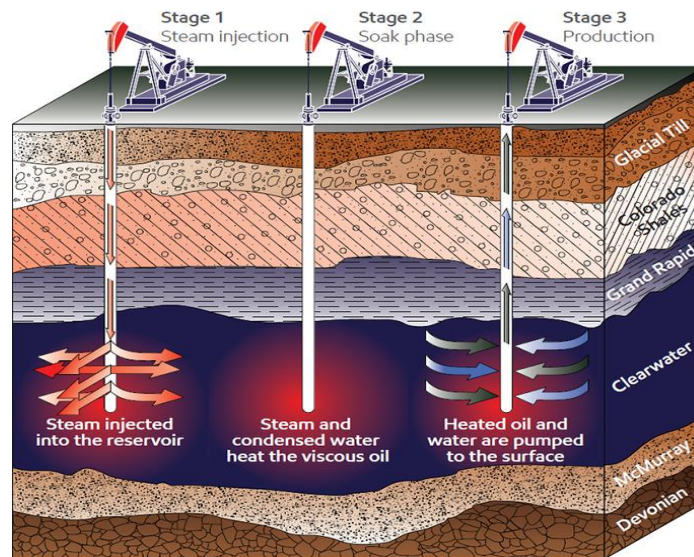


Figure 2-2: Schematic diagram of CSS (imperialoil.ca, Canada)

Although heavy oil reservoirs, that can contain the high pressure steam without fracturing are best candidates for CSS, there are examples of injecting steam at pressure higher than fracturing pressure to improve injectivity. Typically, CSS works best with the thick pay zones (>10 m) and high porosity sands (>0.3) (Speight, 2009). Most of the field applications for CSS have been for vertical wells.

The CSS method is extensively applied in the field making it very attractive for new projects due to the availability of data from different field developments. It is also used to improve injectivity before steam-flooding and in-situ combustion. CSS recovers oil from one wellbore while steam-flooding produces between wells.

Low recovery, steam generation and treatment of the produced water are major challenges for the process. The steam to oil ratio for the process is 3 to 5 bbls of steam per bbl of oil. Oil recoveries from CSS are lower than SAGD, and steam flooding, typically on the order of 20% to 35%.

The conventional CSS process has been modified to achieve higher recovery factors. Some examples in literature are CSS with chemical additives (solvents and surfactants) (Srivastava and Castro, 2011) and CSS with horizontal wells (Chang et al., 2009).

Steamflooding

Steamflooding also known as continuous steam injection is a process similar to waterflooding, where steam is injected through several injection wells and the heated,

low viscosity oil is pushed towards production wells. Steamfloods lead to evaporation of the lighter components present in the oil, which move towards the colder sections of the formation and condense to create a solvent bank followed by condensed water and steam fronts (Renard and Nauroy, 2011). This phenomenon helps reduce residual oil saturation and improve oil recovery. The mechanism for oil recovery in steamflooding is gravity drainage. The injected steam goes to the top of the zone, creating a steam chest. Oil recovery rates are not affected in large part by steam injection rate if a certain steam chest pressure is maintained (Vogel, 1984). Like cyclic steam process, steamflooding is adversely affected by the presence of an aquifer. Gravity override and the presence of natural fractures will also lead to early breakthrough of steam leading to low recovery.

Steam Assisted Gravity Drainage (SAGD)

Steam Assisted Gravity Drainage, commonly known as SAGD, is currently one of the most widely applied, thermal, heavy oil recovery techniques in oil sands reservoirs, especially in Canada. The recovery mechanism is a combination of thermal conduction and gravity; steam injection into a horizontal well heats the bitumen until its viscosity is low enough to drain downward to a lower horizontal production well.

As depicted in the Figure 2-3, two horizontal wells are drilled in the oil sand reservoir, the lower well (production well) is drilled near the bottom of the productive zone, and the injection well is drilled at the top of the production well. High temperature steam is injected through the injection well, and heavy oil and water condensate are produced from the production well. The steam injection pressure is decided based on the reservoir fracture pressure.

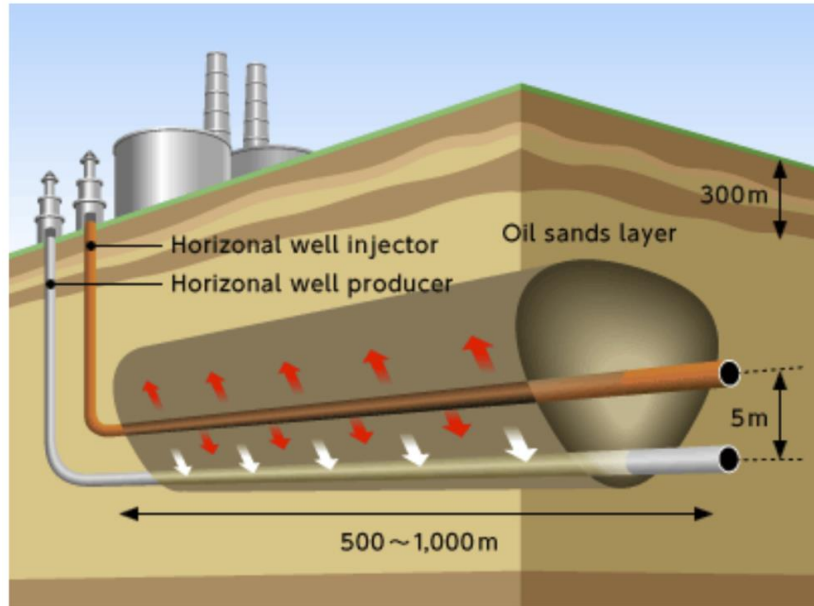


Figure 2-3: SAGD Production Scheme (oilsandsmagazine.com)

In the SAGD process steam injected into the injection well creates a steam chamber above the injector which grows vertically and laterally until it reaches the upper limit of the reservoir structure, and downwards until it reaches the proximity of the production well. As heavy oil is being drained and produced, the steam takes its space in the reservoir pores and maintains drive pressure. The typical steam-oil-ratio (SOR) is 3:1, meaning that it takes 3 barrels of water equivalents of steam to recover 1 barrel of bitumen (Butler, 1994). Oil recoveries for SAGD are usually high due to gravity drainage.

SAGD is not applied for conventional vertical wells due to the limited contact area and resistance to flow due to high viscosity (Butler, 1994). The presence of an aquifer complicates the process; if steam contacts the aquifer, steam will be lost due to high relative permeability of steam within the aquifer. Oil produced from SAGD requires the

addition of solvent for transportation. A major disadvantage of SAGD is low energy efficiency due to heat losses to the formation. Treatment and disposal of effluents are also challenging for SAGD. These factors lead to a high fresh water requirement and increased CO₂ emission making SAGD environmentally critical.

Vapor Extraction (VAPEX)

The fundamental principle behind VAPEX is viscosity reduction of heavy oil due to dilution with vaporized hydrocarbon solvents. This process is still in the research phase; experimental studies are conducted using either propane or butane as solvent.

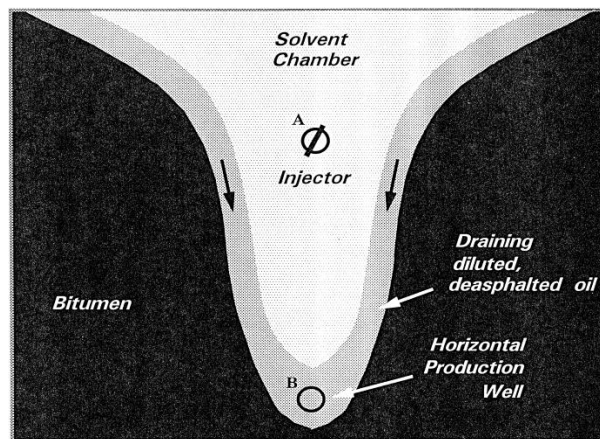


Figure 2-4: Mechanism of VAPEX process (Das 1998)

The VAPEX production scheme is similar to SAGD: two horizontal wells are used as injection and production wells. As shown in the Figure 2-4, horizontal injection well (A) is used to inject vaporized solvent into the reservoir. The vaporized solvent dissolves the heavy oil near the injection well and creates a solvent-heavy oil interface. The solvent diffuses into the bulk of heavy oil and dilutes it. The diluted oil drains to the horizontal

production well located vertically below the injection well due to the gravity difference. Vaporized solvent provides a higher driving force for gravity drainage in comparison to liquid solvent.

The VAPEX process is considered more energy efficient than the steam processes, it uses only 3% of the energy compared to steam processes (Das, 1998). The solvent to oil ratio is 0.5 in case of VAPEX, compared to SAGD's SOR of 3 (Das and Butler, 1998). The solvent that is produced with oil can be recycled and re-injected. VAPEX process can be modified to produce in-situ upgraded oil. Injection of solvent at a pressure near its saturation pressure will lead to de-asphalting, leading to the production of less viscous oil (Das and Butler, 1998).

De-asphalting precipitates asphaltenes from the oil, depositing them within the pore space, which will lead to a reduction in permeability, plugging of wells and other flow issues. The VAPEX process is a molecular diffusion-controlled process, so the production rates are slower than the conventional thermal methods. The economic viability of the VAPEX process will depend on the amount of solvent used per barrel of oil produced and amount of energy required per barrel of oil recovered. Pilot scale testing of VAPEX was conducted during early 2000s in Dover VAPEX project. The recovery rates observed were very low.

In-situ Combustion (ISC)

In-situ combustion is a recovery process where air or any oxygen-containing gas is injected into the reservoir, which in turn reacts with the hydrocarbon present in the

reservoir leading to combustion. Heat generated due to combustion is utilized in recovering oil. It is also known as fireflooding or in-situ burning.

Ignition is the first step of the process. Spontaneous ignition normally occurs when reservoir temperature is above 60°C. Artificial ignition can be achieved by an electric heater, burner, hot-fluid injection or injection of highly oxidizable chemicals.

The most common ISC method is when air is injected into the reservoir, it is known as dry combustion. Air mixed with water is also injected in some cases, known as wet combustion. The combustion front moves from injection well to production well, pushing the unburned hot oil ahead of it. The combustion can be either forward combustion or backward combustion. When combustion front moves in the same direction as the airflow it is known as forward combustion, in reverse combustion the combustion front moves in the opposite direction to air flow. A general flow profile for in-situ combustion is drawn in Figure 2-5.

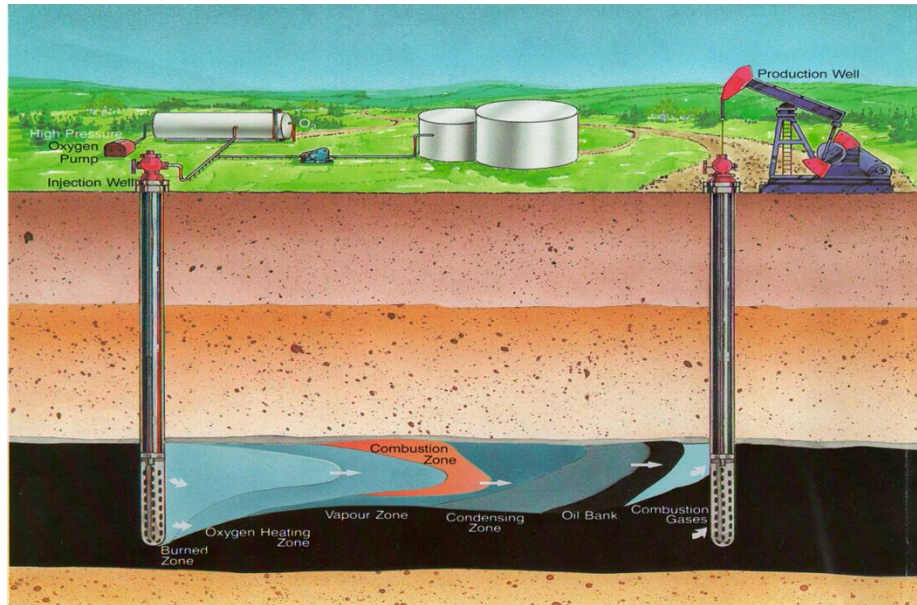


Figure 2-5: Schematic diagram of In-situ Combustion (insitucombustion.ca)

ISC provides heat to mobilize heavy oil and provides in-situ upgrading of the heavy oil, but the combustion front can be difficult to control, and can result in early breakthrough to the production well. It can also damage the well and can result in hot flammable gases leaking to surface.

2.2.2 Ex-situ Methods – Open Pit Mining

Open pit mining is a commonly-used bitumen extraction technique; it consists of excavating the oil sands and separating the bitumen from the water and sand/inorganic composites. Oil sands excavated are usually 10%-18% bitumen, 3%-5% water and 75%-80% inorganic composites (Speight, 2009).

Tons of oil sands are excavated with mining shovels and transported in trucks to a crusher where the oil sands are broken down into smaller pieces. Warm water is added

to the sand and mixed with rotating drums to further reduce their size to about 5cm. This slurry mixture is then transported by pipeline to a primary separation cell, where air is injected to make bitumen froth. The bitumen froth, being less dense settles on top, while the water and sand stay at the bottom due to gravity. The water and sand particles are moved to a cyclone separator, from which most of the water is removed for treatment and recycling. The wet sand is disposed of into tailing ponds. A hydrocarbon solvent, usually naphtha, is added to the bitumen froth to clean it. The mixture is fed to a centrifuge; where any remaining solids are removed at this stage. At the final separation stage, naphtha is removed, and bitumen is sent to storage tanks. A diluent is added in order to transfer the viscous bitumen to the refineries.

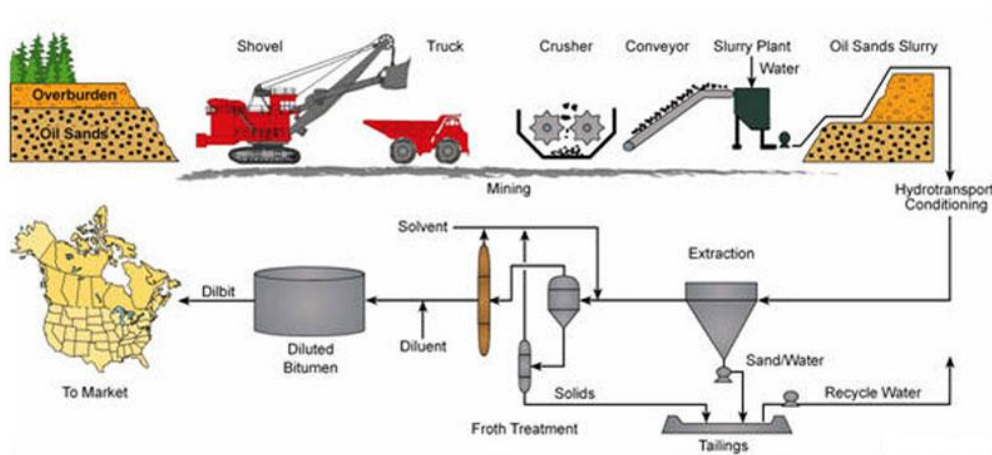


Figure 2-6: Flow scheme for the open pit mining process (2b1stconsulting.com)

This technique has high recovery efficiency, recovering most of the bitumen from the oil sands (~90%) in contrast with thermal in-situ bitumen recovery and hydrocarbon

recovery in conventional oil wells. Water-treatment and recycling recover 90% of water used.

However, it has several disadvantages; it has an immense environmental footprint compared to other bitumen extraction techniques. It strips large acres of land and vegetation. Another disadvantage is that it requires vast amounts of hot water: to process 4 tons of tar sands, approximately 1 ton of hot water is needed (Banerjee, 2012). The creation of tailing ponds also poses a negative environmental impact that affects wildlife, vegetation, and air.

2.3 Surfactant Chemical EOR

Surfactants are surface active compounds, amphiphilic consisting a hydrophilic polar head and a non-polar hydrophobic tail. Surfactants aggregate at the interface of oil and water phases reducing the IFT between them. Surfactants are classified based on the polarity of the hydrophilic group (head). Surfactants can be anionic, cationic, nonionic and zwitterionic.

2.3.1 Surfactants – Properties and Classification

The fundamental property of the surfactant(s) is to aggregate at the surfaces/interfaces. They exist as monomers at lower concentrations but above a certain concentration, surfactant monomers form aggregates in the solution known as micelles. The concentration above which micelle formation start is known as critical micelle concentration (CMC). Only surfactant monomers contribute towards lowering surface (surfactant solution with air)/interfacial tension (between oil and surfactant solution), so

above CMC the surface tension/interfacial tension stays constant. For EOR applications, surfactants are utilized above the CMC.

In addition to CMC, there are two more properties of surfactants which affect their surface properties. The Krafft point is defined as the temperature below which surfactant does not form micelles; below this temperature, surfactants will precipitate out of the solution. For non-ionic surfactants, solubility decreases with increase in temperature. Above a certain temperature, non-ionic surfactants lose their surface activity and precipitate out of solution, which is known as cloud point.

Anionic surfactants are the most important surfactants for EOR application. Anionic surfactants are less susceptible to adsorption on negatively-charged sandstone surface. Some examples of anionic surfactant head groups are sulfate, sulfonate, carbonate, and phosphate. They exhibit excellent IFT reduction capabilities. Surface properties of anionic surfactants are affected by salinity of the solution; higher salinity makes them more hydrophobic. Anionic surfactants especially sulfates are generally adversely affected by the presence of bivalent cation salts (such as calcium) and hydrolysis at higher temperature in the reservoir brine. Research has exhibited that sulfonates and carboxylates are more suitable to work in the harsher environment (high salinity, high temperature).

Non-ionic surfactants are generally long chain alcohols. Non-ionic surfactants are generally compatible with other surfactants; hence they are often used as co-surfactants. The properties of non-ionics are not affected by the salinity of the mixture but are

affected by temperature. An increase in temperature makes them more hydrophobic. Ethoxylated alcohols with varying numbers of oxyethylene units are examples of commonly utilized non-ionic surfactants.

Cationic surfactants generally consist of a nitrogen atom carrying a positive charge. They are only stable at low pH environment, which lead to higher adsorption in formations. They are not compatible with anionic surfactants, so their use is limited in oil and gas industry. Some proposed applications of cationic surfactants are surface modification and wettability alteration (Somasundaran and Zhang, 2006).

Zwitterionic surfactants contain both positively and negatively charged groups. Zwitterionic surfactants have very good dermatological properties making them a useful in cosmetics industry (Holmberg et al., 2003). Zwitterionic surfactants are often confused with amphoteric surfactants, which changes their properties from cationic-zwitterionic-anionic as pH is increased. Zwitterionic surfactant properties are similar to non-ionic surfactant due to having net-zero charge. A commonly used zwitterionic surfactant is betaine.

2.3.2 Fundamentals of Surfactant EOR

When an aqueous solution containing surfactant above CMC is mixed with oleic phase, it generates a thermodynamically-stable dispersion phase, known as microemulsion. Based on the solution properties such as salinity (for ionic surfactants) and temperature (for non-ionic), the microemulsion phase can transition from water

continuous to oil continuous. Winsor classified these microemulsion in four categories (Winsor, 1948).

Winsor type I – It is also known as type II (-), water continuous microemulsion and water external microemulsion. In this system surfactant stays in the aqueous phase and solubilizes oil in an oil-in-water microemulsion and remains in equilibrium with the excess oil phase. Oil droplets stay in micelles, where oil drops stay surrounded by surfactant molecules with their polar head towards the aqueous phase. Type I microemulsion is favored at low salinity (for ionic surfactants) or low temperature (non-ionic surfactants).

Winsor type II – Also known as type II (+), is an oil continuous microemulsion and oil external microemulsion. Surfactant prefer the oleic phase in this case and solubilizes water in water-in-oil microemulsion which stays in equilibrium with the excess water phase. Type II forms at higher salinity (ionic) and higher temperature (non-ionic). In this type of microemulsion, micelles solubilize water, with their hydrophobic tail towards the oil phase. These are called reverse micelles.

For intermediate salinity (or temperature) surfactant creates a separate microemulsion phase, which stays in equilibrium with both excess water and excess oil phases. It is known as Winsor type III microemulsion or bi-continuous microemulsion. If a sufficient amount of surfactant is added into the mixture, then the microemulsion phase can consume the excess phase completely. This type is known as Winsor type IV or single phase microemulsion. Single phase microemulsion are discussed in detail in section 2.3.3.

The solubilization parameter of oil in microemulsion is defined as the ratio of volume of oil solubilized to the volume of surfactant,

$$SP_o = \frac{V_o}{V_s} \Big|_{ME\ phase} . \quad (2.1)$$

Similarly, solubilization parameter of water in microemulsion is defined as the ratio of volume of water solubilized to the volume of surfactant,

$$SP_w = \frac{V_w}{V_s} \Big|_{ME\ phase} . \quad (2.2)$$

Chun Huh (Huh, 1979) proposed a correlation between IFT and solubilization parameter of any phase,

$$\sigma = \frac{C_H}{SP^2}, \quad (2.3)$$

where σ is the IFT, C_H is a constant that is approximately 0.3 dynes/cm, and SP is the solubilization parameter.

Ultra-low IFT can be achieved when surfactant is equally soluble in oleic and aqueous phases, meaning the solubilization parameter is same for both oil and water. The salinity at which the solubilization parameter of oil and water equates is known as optimum salinity. Optimum salinity is very critical to oil and gas applications. Capillary forces are responsible for the trapping of large quantities of oil in waterflooded reservoirs. Interfacial tension (IFT) between oil and water results in capillary forces that act to trap the oil within the pore spaces. The fundamental principle behind the surfactant process

is the reduction in IFT through micelles formation. The mechanism is related to the Capillary number, defined as the ratio of viscous forces to capillary forces.

$$N_c = \frac{v\mu}{\sigma}, \quad (2.4)$$

where:

N_c - Capillary number,

μ - viscosity of the displacing phase,

v - velocity of the displacing phase, and

σ - IFT between displacing and displaced fluid.

As the capillary number increases the residual oil saturation is initially constant until reaching a critical value after which it decreases, this behavior is depicted in capillary desaturation curve. The most practical way to increase the capillary number is to reduce IFT. Surfactant flooding conducted at optimum salinity reduces the IFT to ultra-low values, which enables the movement of capillary trapped oil.

The Chun Huh relation has been beneficial to surfactant screening process and for numerical simulations since IFT estimation can be done based on easily determined solubilization parameter. Experimentally, IFT can be measured using the spinning drop tensiometer to verify adherence to the Chun Huh equation. In most of the EOR applications, co-surfactant is added into the formulation to optimize the surfactant slug.

Co-solvents, generally low molecular weight alcohols (secondary butanol, isopropyl alcohol etc.), are added to decrease the viscosity of the microemulsion, reduce the equilibration time and to prevent gel formation.

Alkali is also a very important additive in surfactant formulation. They are primarily used to control the adsorption of surfactant in reservoir. They are used to alter the wettability of the formation (Hirasaki et al., 2011). Alkali converts naphthenic acid present in the crude to in-situ surfactants. Linkers are sometimes added to improve the solubilization of oil (hydrophobic linkers) or water (hydrophilic linkers) such as 1-octanol as hydrophobic linker. Recent advances and best practices of chemical EOR work can be found in review paper by Hirasaki et al. (2011).

2.3.3 Single Phase Microemulsion

Single phase microemulsion also known as Winsor type IV, is achieved when sufficient amount of amphiphiles (surfactant/co-surfactant/co-solvent) is present in the mixture to consume both excess water phase and excess oil phase.

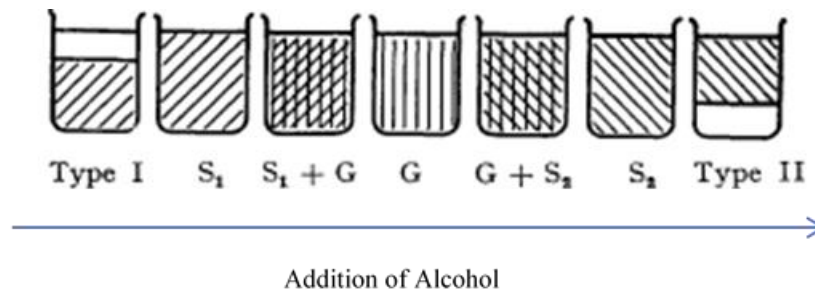


Figure 2-7: Phase change from type I to type II through different types of type IV microemulsion (Winsor, 1948)

Winsor explained different phases present during a transition from type I- type IV- type II (Winsor, 1948). In Figure 2.7, S1 and S2 denotes clear single phase microemulsion, whereas G phase is a gel phase. Gel phase is highly undesirable for any kind of flow process. S1 solution will be achieved when surfactants prefer aqueous phase (lower salinity) and S2 solution when surfactant prefer oleic phase (higher salinity). The type IV (single phase microemulsion) was suggested in the remediation of non-aqueous-phase-liquid (NAPL) from the superfund sites (Rhue et al., 1999), but the focus of this application was environmental clean-up only and solubilization achieved was not very high.

2.3.4 Microemulsion Separation and Surfactant Recovery

2.3.4.1 Microemulsion Separation

There are several examples in literature of the use of various demulsifiers for separation of emulsion formed during oil production due to the presence of surface active components (Sjöblom et al., 2003; Sullivan et al., 2010; Goldszal and Bourrel, 2000). The micellar emulsion generated due to the application of EOR techniques is generally more stable. Hirasaki et al. observed that conventional demulsifiers are not very effective in dealing with stable emulsions, they suggested use of cationic surfactant lead to a better and faster separation (Hirasaki et al., 2011).

Based on the stability of anionic surfactants, hydrolysis can also lead to separation. Specifically, anionic surfactants with sulfate head group are prone to hydrolyze under acidic conditions at higher temperatures due to the presence of weak carbon oxygen bond. Sulfonates and carboxylates are generally considered stable, however ester-based

sulfonates such as sulfosuccinates are also very susceptible to hydrolysis under both acidic and basic conditions due to the presence of ester linkage (Tyagi, 2006).

For non-ionic surfactant, the cloud point can be varied by the addition of salt. This phenomenon is known as salting in or salting out based on the effect of addition of salt. Emulsions containing non-ionic surfactants can be separated by salting the surfactant out. In fact, both anionic and non-ionic surfactants are likely to be ineffective at higher salinity and temperature. Anionic surfactants are more likely to interact with the bi-valent cations present in the system and precipitate out of the solution rendering them ineffective.

2.3.4.2 Surfactant Recovery

Methods to separate oleic and aqueous phase mentioned in the previous section focus more on the proper separation of the phases. Surfactant recovery and reuse has been an interest in the environmental remediation field. Surfactant-enhanced aquifer remediation (SEAR) process utilizes surfactants to solubilize toxic chemicals from contaminated sites. The recovery techniques were investigated to make cleaning process more economical. The surfactant recovery techniques were classified based on the nature of the contaminant (oleic phase) (Lowe et al., 2000). For volatile organic contaminants (VOCs):

- Air stripping with antifoaming agents;
- Membrane air stripping;
- Flash vacuum stripping and vacuum distillation;

- Membrane liquid-liquid extraction;
- Pervaporation; and
- Precipitation

For non-volatile contaminants:

- Membrane liquid-liquid extraction; and
- Precipitation

In addition, Lee et al. reported a solvent extraction method. They used three different solvents to extract toluene from a mixture (Lee et al., 2002).

Surfactant recovery methods mentioned here are designed for applications where the contaminant solubilization in the aqueous phase is very low, hence recovery of contaminant was not considered. The focus was on developing techniques that could only recover surfactant. The recovery methods were designed to handle small quantity of mono-component oleic phase, which cannot be scaled up to handle large amount of multi-component oil.

Chapter 3

Cyclic Surfactant Solubilization

Existing recovery methods for bitumen and extra heavy oil applicable in field are open pit mining, CHOPS, and thermal methods. Open pit mining is criticized for its carbon footprint, it destroys the vegetation and tailing ponds potentially contaminate the soil. Thermal methods are highly energy inefficient and have a large carbon footprint. Thermal methods require fresh water for steam generation and produced water is contaminated which needs to be treated before reinjection.

A sustainable non-thermal method of bitumen recovery is proposed, that relies on solubilizing bitumen in a single phase microemulsion. This approach is designed to only solubilize the oil, not mobilize. Only single phase microemulsion is produced, which will have lower viscosity being the oil-in-water microemulsion. The produced microemulsion can be transported easily. After transportation microemulsion can be separated to recover oil and surfactant can be recycled for re-injection. This is a benefit, since existing methods require addition of solvent in order to transport the oil, which add to the carbon footprint for solvent separation. The flow schematic is shown in Figure 3-1.

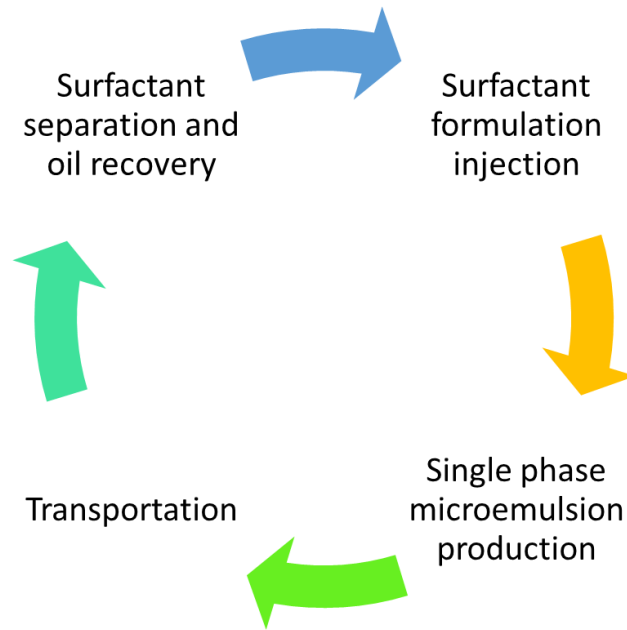


Figure 3-1: Cyclic surfactant solubilization flow schematic

Cyclic surfactant solubilization can be a game changer in places like Canada, Venezuela, and Columbia. Current recovery methods are detrimental to for the environment and are creating hazardous conditions. Cyclic surfactant solubilization provides a greener alternative. Surfactant recycle could help to improve the sustainability and the economics of the process.

Chapter 4

Equipment and Materials

This chapter presents a brief description of all the experimental equipments and materials utilized for the work.

4.1 Equipment

4.1.1 Gas Chromatograph and Mass Spectrometer (GC-MS)

A GC-MS system by Agilent Technologies was used to analyze microemulsion samples for oil solubilization. The specification of system is reported in Table 4.1. The chromatograph is generated using a flame ionization detector (FID). The oven temperature range is 4 – 450°C. The MSD has an electron ionization (EI) source with ion source temperature range from 150 – 350°C and quadrupole temperature 106 – 200°C. Helium was used as carrier gas. Air and hydrogen mixture served as fuel for the flame in FID.

Table 4-1: GC-MS specification

gas chromatograph and mass spectrometer	
gas chromatograph (GC)	7890B
autosampler	7693A
mass selective detector (MSD)	5977A
column	19091S-433UIHP-5MS Ultra Inert 30 m length, 0.25 mm diameter, 0.25 μ m coating

4.1.2 High Performance Liquid Chromatograph (HPLC)

The HPLC system 1260 Infinity by Agilent Technologies was used to analyze surfactant solutions related to both surfactant synthesis and surfactant recovery. HPLC system description is listed in Table 4-2. The HPLC was used with Acclaim Surfactant column by Thermo Fisher. The column was silica-based column with 5 μm particle size, 4.6 mm diameter, 250 mm length. Nitrogen served as nebulizer inert gas for ELSD system.

Table 4-2: HPLC System description

high performance liquid chromatograph	
autosampler	1260 Infinity II
quaternary pump	1260 Infinity
diode array detector (DAD)	1260 DAD
evaporative light scattering detector (ELSD)	1260 ELSD

4.1.3 Auto Titrator System

Metrohm 888 Titrando with Tiamo Light was used for titration. This setup was useful for measuring surfactant concentrations and total acid number (TAN). For surfactant analysis surfactant electrode purchased from Van London Co. was used. TAN measurement was performed with Metrohm Solvotrode Easyclean electrode. Hyamine (0.05 M) was used as a titrator for anionic surfactant titration.

4.1.4 Mixer

SCIOGEX MX-RD-Pro tube rotator was used for mixing centrifuge tubes, phase behavior tubes, and surfactant recovery work. It has adjustable speed from 10 to 70 RPM. The rotation angle can be changed from 0 to 90°.

4.1.5 Centrifuge

Clay Adams Dynac centrifuge was used to separate solutions. It is capable of holding 8, 15 ml centrifuge tubes. It has a speed range of 500-3600 RPM and time can be set up to 30 minutes.

4.1.6 Pump

Jasco PU -2086 Semi-preparative HPLC pump was used for flow experiments. It has a dual-piston pump capable of 1 $\mu\text{L}/\text{min}$ to 20 ml/min rates and was rated for 40 MPa (5800 psig).

4.1.7 Fluid Reservoirs

The flow experiments were conducted at low pressures so low-pressure accumulators were utilized. Several 2000 ml acrylic floating piston accumulators (FPAs) rated for 100 psig from Core Laboratories LP were used during the flow (core flood) experiments. Floating piston accumulators are useful in pumping corrosive liquids into the columns without exposing the pump to corrosion or damage. De-ionized (DI) water is pumped to the bottom of the pump and piston drives the process fluid to the column. Large Mariotte devices (20-gallon polyacrylate fluid accumulators) tapped with 1/8-inch swage fittings were fabricated at the University of Houston and utilized as reservoir of DI water for the dual-piston pumps.

4.1.8 Pressure Differential Transducers and Data Acquisition

Several pressure differential transducers were used in the experiments depending on the expected pressure for the experiment. Pressure transducers were PX26 series

manufactured by Omega. They were rated for 200 psi total. A DC power source PSS10 from Omega was used to provide 10 V excitation voltage to the pressure transducers. Pressure transducers were calibrated to convert the output of mV to a pressure (psig) measurement. A multimeter GDM-8351 by GwInstek was used to sense the voltage response of the transducers.

4.1.9 Tubing

Perfluoroalcoxy (PFA) tubing rated as per ASTM – D3307 type II, was used to build the flow loop for the experiments. Tubing was supplied by Swagelok. The dimensions and other specification are listed in Table 4-3.

Table 4-3: PFA tubing specifications

PFA tubing specification	
outer diameter	1/8 inch
wall thickness	0.03 inch
pressure rating	275 psig
temperature rating	400 F

4.1.10 Valves and Fittings

Multiple two- and three-way valves were utilized in the flow loop. All valves were stainless steel – 316 (SS316) suitable for 1/8-inch fitting, rated for 300°F and 2500 psig. Nylon ferrules were used for fittings which are compatible for the tubing and had similar pressure and temperature rating. Apart from that all other fittings (union, tee, plugs etc.) were SS316. All fittings and valves were purchased from Swagelok.

4.1.11 Core Holder

Core holder was used to conduct flow experiment under high pressure. Hydrostatic core holder from Vince Technologies rated for 10,000 psig with Hastelloy-wetted parts was used for experiments. Hydrostatic core holders can provide both radial and axial confining stress. It was capable of accommodating 1.5 inches diameter cores of up to 12 inches length. One end, the end piece was fixed while, the other end is adjustable to accommodate different sized cores. Core was held inside a removable Viton sleeve, which has three tapping for recording intermediate pressures.

4.1.12 Glass Column

For low pressure sandpack experiments, Kimble Chase Kontes Chromoflex columns were used. Multiple columns with different heights were purchased to conduct flow tests. Longer columns have one adjustable end to adjust the height of the sandpack. The columns are jacketed to maintain the temperature of the experiments. These columns are all rated for 50°C temperature and 100 psig pressure.

4.1.13 Fractional Collector

A Teledyne ISCO 500 fractional retriever was used for outlet sample collection. The collector is capable of moving at variable rates and held up to 72 centrifuge tubes.

4.1.14 Sealing Torch

A Bernzomatic acetylene sealing torch which consumes MAP-Pro gas and oxygen cylinders was used to seal borosilicate pipettes for surfactant phase behavior studies. The

torch was setup in an isolated hood vent and pipettes were handled using tongs during sealing.

4.1.15 Vacuum Pump

A Welch 1400B-01 vacuum pump capable of 1×10^{-4} torr ultimate pressure, was used to pull vacuum for bulk water fraction measurements.

4.1.16 Glassware and Centrifuge Tubes

VWR-brand 10 ml borosilicate pipettes were used in the surfactant phase behavior portion of the work; the ends were sealed using an acetylene torch. Fisherbrand 20x125 and Fisherbrand 16x100 mm test tubes were used for phase behavior work involving bitumen. Fisherbrand 16x100 mm screw-top test tubes were used to collect the flow samples. Falcon 15 ml high-clarity polypropylene conical centrifuge tubes were utilized in various lab activities related to surfactant analysis and recovery. Several other glasswares (various beakers, Erlenmeyer flasks, round bottom flasks, etc.) were purchased from VWR and Fisher Scientific.

4.1.17 Viscometer

Brine and surfactant formulation viscosity measurements were performed using a Koehler KV3000 series kinematic viscosity bath set to room temperature (25°C) and Fisherbrand Size 50 and 200 glass kinematic viscometer tubes. Kinematic viscosity measurements were performed and converted to dynamic viscosity by multiplying the solution density at the same temperature to the measured kinematic viscosity value

(ASTM D445-17a 2016). Bitumen viscosity was measured using Anton Paar MCR 302 with standard CC27 Single Gap Measuring System.

4.1.18 pH and Conductivity Meters

The pH measurement was very critical for surfactant work. pH was measured using a Mettler Toledo S220 SevenCompact pH/Ion meter. Salinity tracer effluent was measured using a Hanna Instruments HI 5321 laboratory research grade benchtop EC/TDS/Salinity/Resistivity Meter.

4.1.19 Water De-ionizer

A Millipore Sigma Milli-DI wall-mounted water purification system capable of producing Type 2 de-ionized lab water was used to prepare stock brine and surfactant solutions. DI water quality was indicated live via the green LED indicator on the unit. In addition, the water quality was checked periodically using pH and conductivity meters.

4.1.20 Filtration Equipment

An Advantec MFS KP47H 47 mm filter holder was used with a filter flask for filtration and clarification of stock brine solutions. Batches of 400 ml of brine solution were filtered using the filter holder passed through Millipore Sigma 1.2-micron nitro cellulose filter paper using a filter flask connected to house vacuum.

4.1.21 Scales

A Mettler Toledo PE 3600 DeltaRange precision balance capable of 0.1 g/0.01 g readability was used during the analytical portion of the work. An Ohaus Explorer analytical balance (120 g capacity) was used to weigh chemicals for analytical work.

4.1.22 Water Bath Circulator

Water bath circulator was used to circulate water in the glass column jacket. A Fisherbrand Isotemp 6.8 L was setup for that purpose. It is suitable for -48 to 200°C temperature range and is able to pump 21 L/min.

4.1.23 Benchtop Mixers

VWR International multi-position hotplate stirrers were used in the preparation of stock brine and surfactant solutions. The hotplate function was disabled during the operation of the mixing unit.

4.2 Materials

4.2.1 Oil Sands

Two oil sands samples were acquired from Alberta Innovates Technology Futures, Alberta, Canada: “Athabasca oil sands low” and “Athabasca oil sands high”. Oil sands samples are characterized as low or high quality based on the fines content; higher fines content correlates with lower quality of sand.

4.2.2 Clean Sand

High purity sand samples were bought from US Silica to prepare sandpack. Multiple grades of sands were purchased but, in this work, OK-75 grade was used. OK-75 is 99.8% silicon dioxide and white in color. The specific gravity of OK-75 is 2.65.

4.2.3 Gases

Lab gases nitrogen, argon, helium, hydrogen, and air were purchased from Matheson gas and shipped in industrial cylinders. Connections to the cylinders were

initiated via dual-stage regulators purchased from Matheson gas. Various gases and their purity grades are listed in Table 4-4.

Table 4-4: Laboratory gases

gas	grade
nitrogen	Ultra-High Purity
helium	High Purity
argon	Ultra-High Purity
hydrogen	Ultra-High Purity
air	Zero Gas

4.2.4 Chemical

Laboratory grade chemicals were purchased from VWR International, Alfa Aesar, and Sigma Aldrich are listed in Table 4.5.

Table 4-5: Anhydrous salts and their vendors

chemical	vendor
sodium hydroxide	VWR
hydrochloric acid	VWR
sodium carbonate	VWR
2-butanol	Alfa Aesar
iso-propyl alcohol	Alfa Aesar
tri-ethylene glycol mono butyl ether	Alfa Aesar
sodium chloride	Sigma Aldrich
calcium chloride	Sigma Aldrich
magnesium chloride	Sigma Aldrich
sodium monochloracetate	Sigma Aldrich
dichloromethane	Alfa Aesar
sulfamic acid	Sigma Aldrich
potassium chloride	VWR
methylene chloride	Alfa Aesar
toluene	Alfa Aesar
coal tar	Alfa Aesar
n-octanol	Alfa Aesar
hyamine (0.05M) titrant	Alfa Aesar
acetonitrile	VWR
ammonium acetate	VWR
urea	Sigma Aldrich
KemSweep A-5903 Polymer	Kemira

4.2.5 Surfactants

A summary of surfactants used in the work are listed in Table 4-6. All surfactants were used “as received”, except Soloterra 938 which was received as an acid, requiring neutralization with sodium hydroxide to a desired surfactant concentration.

Table 4-6: Surfactant types and activity

Surfactant	Type	Vendor	Activity	MW
Aerosol OT 100	Sulfosuccinate	Cytec	100.0%	444
Aerosol OT 75	Sulfosuccinate	Cytec	75.0%	444
Aerosol MA-80	Sulfosuccinate	Cytec	80.0%	388
Aerosol MA-80 I	Sulfosuccinate	Cytec	80.0%	388
Alfoterra 145-8S 90	Propoxysulfate	Sasol	90.0%	787
Alfoterra 123-8S 90	Propoxysulfate	Sasol	90.0%	761
ENORDET O352-9	C24-C28 IOS	Shell	69.4%	498.1
ENORDET O242	C20-24 IOS	Shell	19.0%	407
ENORDET J13131	C12-C13 AAS, 13 PO	Shell	29.2%	1090
ENORDET O342	C19-C23 IOS	Shell	31.4%	414.9
ENORDET J771	Branched C12-13, 7 PO Sulfate	Shell	30.0%	700
ENORDET O332	C15-C18 IOS	Shell	28.0%	350
NEODOL 25-3	Alcohol (C12-C16)poly(1-6)ethoxylates	Shell	100.0%	331
NEODOL 25-7	Alcohol (C12-C16)poly(7-19)ethoxylates	Shell	100.0%	525
Petrostep A6	C16-18 AAS	Stepan	50.0%	NA
Petrostep S13D HA	C13 13 PO Alcoxy Sulfate	Stepan	81.2%	850*
Petrostep S3B HA	C20-24 IOS	Stepan	57.9%	450*
Petrostep S2	C15-20 IOS	Stepan	21.9%	NA
SDS	Sodium Dodecyl Sulfate	Sigma Aldrich	100.0%	288.3
Polysorbate (Tween 80)	Non-ionic	Alfa Aesar	100.0%	1310
Triton X100	Non-ionic	Sigma Aldrich	100.0%	647
IGEPAL CO 720	Non-ionic	Sigma Aldrich	100.0%	735
Brij O20	Non-ionic	Sigma Aldrich	100.0%	1149
Brij L23	Non-ionic	Sigma Aldrich	100.0%	1199

*Estimated molecular weight. NA – Not Available

Chapter 5

Experimental Procedures

The experimental procedures employed for preliminary, “proof-of-concept” work with coal tar and the later work with bitumen samples are discussed in this section. This section also details the surfactant recovery experiments.

5.1 Coal tar

Coal tar was used as a model oil for heavy oil due to similarities in the properties. Coal tar provided a source for tar/bitumen in enough quantity which can be used for the total duration of the project, so the properties would be consistent and allow for comparison of results. Although the viscosities of the coal tar and bitumen are different, the mechanism of the process is based on solubilizing the tar/bitumen in the microemulsion rather than mobilizing the oleic phase, hence the effects of viscosity on the recovery efficiencies will not be significant.

5.1.1 Stock Solution Preparations

Concentrated surfactant stock solutions were prepared in glass jar with de-ionized water and desired co-solvent, and co-surfactants. Surfactants were prepared by weight by diluting according to the manufacturer-specified activity percentage. Solutions were homogenized using stir bars and a stir plate overnight. Various salt stock solutions were prepared in volumetric flasks to perform phase behavior work.

5.1.2 Phase Behavior Studies

Phase behavior studies comprised of surfactant screening, salinity scans, and aqueous stability. The methods employed to conduct these experiments have been discussed thoroughly in literature (Kostarelos et al., 2013; Dwarakanath et al., 1999; J. Sheng, 2010).

5.1.2.1 Surfactant Screening

Surfactant screening experiments were conducted to identify effective surfactant formulation. These are conventionally done in 5 ml glass pipettes, but 20 ml test tubes were used for coal tar due to higher viscosity of the sample. Coal tar and stock solutions were mixed at a water-oil-ratio (WOR) of 1 in a test tube. Test tubes were sealed with aluminum foil and cap. They were mixed and allowed to equilibrate at desired temperature. The suitability of the surfactant formulation was determined by visually examining the tubes. Volume of the microemulsion phase and excess phases were measured to ensure that equilibrium is achieved.

Microemulsion was darker in color so distinguishing the coal tar and microemulsion phase was difficult in natural light. Ultraviolet light was utilized to properly determine the interface between tar and microemulsion. For the formulations where visual analysis showed some potential for high solubilization of tar, additional GC-MS analysis was conducted to ensure no *preferential solubilization* in the microemulsion. Some surfactant formulations may solubilize only a narrow range of the crude oil (lighter components), which is known as preferential solubilization (Kostarelos et al., 2013). Preferential solubilization of the lighter components can lead to precipitation of heavier

compounds causing subsurface pore plugging and flow problems. The details of GC-MS method used for microemulsion analysis are mentioned in Table 5-1.

Table 5-1: GC-MS method used for microemulsion analysis with coal tar

GC-MS Method	
inlet	250°C
column	He Constant Flow 1 ml/min
oven	Initial temperature 80°C for 1 min ramp of 5°C per min to 275°C hold up time 40 mins
front detector	300°C, Hydrogen 30 ml/min, Air 350 ml/min
MS quad	150°C
MS source	230°C

5.1.2.2 Salinity Scans

Salinity scans were performed on surfactant formulations selected based on the surfactant screening tests. Scans were conducted in 10 ml glass pipettes. Coal tar (4 ml) was first pipetted and surfactant formulation (4 ml) was delivered on top of that. These pipettes were sealed at the top and allowed to equilibrate at desired temperature. After equilibration, levels of tar and microemulsion phases were measured to calculate solubilization parameter (SP). Salinity scans for the most promising surfactant formulations were conducted at WOR of 1, 2, 3, and 4.

5.1.2.3 Aqueous Stability Tests

Aqueous stability tests were conducted to measure the stability of the surfactant solution with brine at reservoir temperature. They were performed in 5 ml glass pipettes. Surfactant stock solution was mixed with varying amount of brine solution to achieve full

spectrum of the salinity. These pipettes were sealed and stored at desired temperature. The pipettes were inspected regularly for any instability and phase separation for a long period.

5.1.3 Flow Experiment

After phase behavior studies, the most suitable surfactant formulation was used in a one-dimensional flow experiment. The main objectives of this test were to ensure production of single phase microemulsion and recovery of solubilized oil with low pressure differentials; high pressure would indicate the formation of undesirable gel or other viscous phases. The test was performed in the Kimble-Kontes Chromaflex glass column, 60 cm long and 2.5 cm in diameter. An end piece with the adjustable length was used to keep the sand tightly packed. A synthetic oil sand sample was prepared by mixing 530 g of sand and 74.8 g of coal tar (12.4 wt.%). The column was packed to 6-inch height with the synthetic tar sand and the remaining space was filled with clean sand.

The glass column, being 60 cm (23.6 inches) in length, is much longer than needed to prove the concept—that solubilization of the tar could be achieved under dynamic conditions. The 15.24 cm long (6-inch) synthetic oil sand specimen was an adequate size on the basis of test duration, pore volume, etc., and while the end-piece of this column is adjustable, it does not extend enough to make-up the empty space within the glass column. Clean sand (the same as used to prepare the synthetic oil sand) was used to fill the space. The use of sand to fill the space is a safe choice that would not have any negative effect on the flow of the injected surfactant formulation.

A Mariotte bottle was used to establish constant inlet pressure for the flow into the column. The device was placed at the height of 203 cm (80 inches), resulting in a head of 20.7 kPa (3 psi) at inlet. Because the tar is heavier than water, the flow was maintained from top to bottom. Figure 5-1 shows the flow experiment setup. The produced samples were analyzed by GC to calculate the tar recovery. A total 730 ml (approximately 32 PV) of surfactant solution was injected into the column and chased with 180 ml (approximately 8 PV) of brine at the same salt concentration (0.15 wt.%) to ensure the removal of the remaining surfactant solution/microemulsion from the column. Viscosities of the produced microemulsions were measured using Cannon Fenske viscometer. After the test, the sand was removed from the column and washed with methylene chloride to dissolve any tar remaining in the sand, and this extract was analyzed using GC.

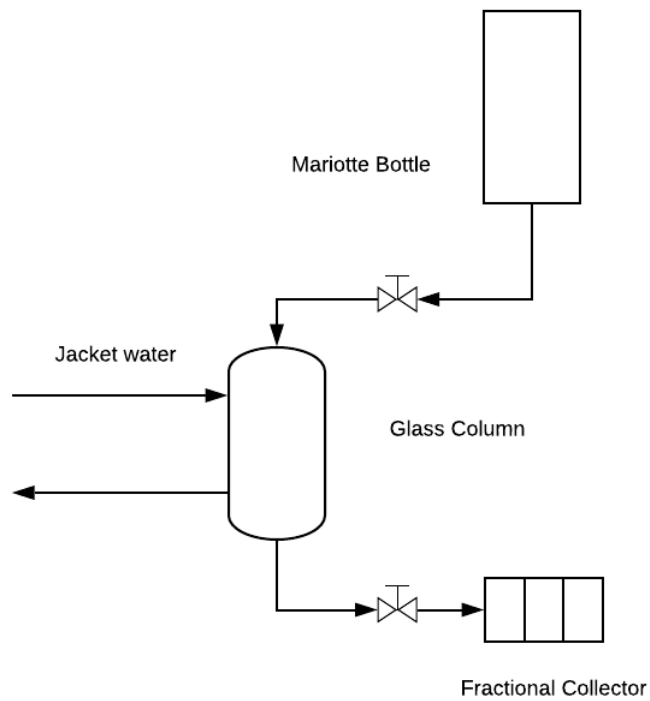


Figure 5-1: Flow experiment setup for coal tar recovery

5.2 Bitumen

5.2.1 Soxhlet Extraction

Soxhlet extraction was conducted to quantify the amount of bitumen present in the field obtained sample. A Soxhlet extractor was setup and known amount of oil sand sample wrapped by filter paper was placed in the main chamber of Soxhlet extractor. Toluene was used as a solvent in the distillation flask. Extraction was conducted for a day to ensure all the bitumen have been recovered from the sand. After extraction, the sand sample was dried and weighed. The difference in the weight was used to calculate bitumen content of oil sand. Description of Soxhlet extractor is shown in Figure 5-2.

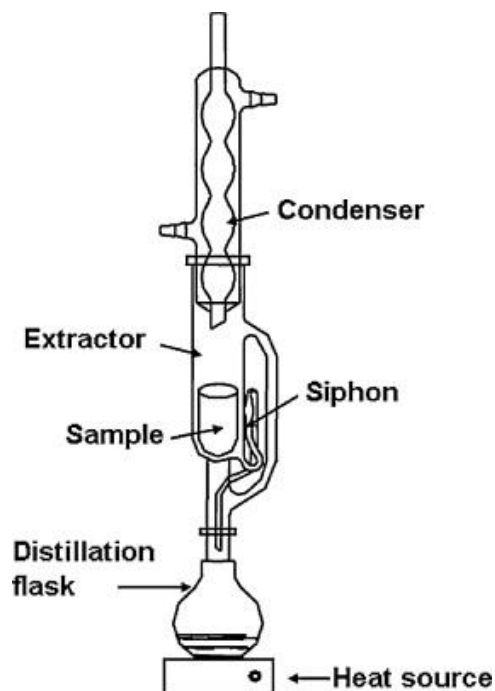


Figure 5-2: Soxhlet Extractor (source blogspot.com)

5.2.2 Bitumen Extraction from Oil Sands

Bitumen in oil sand was extracted using solvent extraction to be used in phase behavior studies. Methylene chloride (dichloromethane) was used as a solvent because of its low boiling point (39.6°C). High-grade oil sand sample was mixed with methylene chloride and left for settling. After settling the extract was transferred to a round bottom flask. The solvent was boiled off at 39.6°C from the extract and collected for re-use; the remaining bitumen in the flask was transferred to a collection vessel. The collected solvent was analyzed in GC-MS to ensure no bitumen component was evaporated. This process was repeated to collect 1000 ml bitumen sample for phase behavior studies. Figure 5-3 shows the solvent recovery setup utilized after each solvent extraction cycle.



Figure 5-3: Solvent recovery setup

5.2.3 Stock Solution Preparation

Brine stock solutions were prepared at injection and concentrated values by individually weighing salts on anti-static weigh boats and adding them to 2L Erlenmeyer flasks or screw-top sealed bottles. De-ionized water was then added to achieve a weight/weight percent solution, typically in g/kg. Solutions were mixed with magnetic stir bars until thoroughly homogenized. Brine stock solutions were degassed for 8 hours using argon gas.

Concentrated surfactant stock solutions were prepared in glass jar with de-ionized water and desired co-solvent, and co-surfactants. Surfactants were prepared by weight

by diluting according to the manufacturer-specified activity percentage. Solutions were homogenized using stir bars and a stir plate overnight.

5.2.4 Phase Behavior Studies

Bitumen extracted from oil sands was too viscous to conduct conventional phase behavior studies using the small-diameter, 5 ml pipettes, so glass tubes were used instead. Phase behavior work consisted of surfactant screening, salinity scans, and aqueous stability. Aqueous stability studies were conducted in the 5 ml glass pipettes.

5.2.4.1 Surfactant Screening

Surfactant screening was conducted to identify suitable surfactant formulations qualitatively. These tests were performed in 12 ml glass tubes. Screening was done at a water oil ratio (WOR) of 1. Tubes were filled with 4 ml of extracted bitumen and 4 ml of surfactant formulation was added. Tubes were sealed with aluminum foil and plastic cap. Suitable surfactant formulations were selected after visually examining the tubes.

5.2.4.2 Salinity Scans

Surfactant formulations selected based on the screening tests were studied further in more detailed salinity scans. Scans were also performed in 12 ml glass tubes. The glass tubes do not have any volumetric gradation, so it was not possible to simply record the volume changes for the bitumen and aqueous phases to determine the amounts solubilized. Instead, the microemulsion was analyzed by GC to calculate bitumen solubilized in microemulsion phase, GC method is listed in Table 5-2. Salinity scans were performed for WOR of 1, 2, 3, and 4.

Table 5-2: GC method for microemulsions bitumen concentration measurement

GC-MS Method	
inlet	250°C
column	He Constant Flow 1 ml/min
oven	Initial temperature 50°C for 1 min ramp of 5°C per min to 300°C hold up time 40 mins
front detector	300°C, Hydrogen 30 ml/min, Air 350 ml/min
MS quad	150°C
MS source	230°C

5.2.4.3 Aqueous Stability Tests

Aqueous stability tests were performed on the most promising surfactant formulation. Selected surfactant formulation was mixed with range of salt concentration in 5 ml glass pipettes. These pipettes were sealed and stored at desired conditions. They were checked every day for a month for phase separation or solution instability.

5.2.5 Static Tests

Static tests were designed to study the effect of sand particles on the solubilization of bitumen into the microemulsion. They were conducted in 20 ml glass tubes. Each tube was filled with 10 g of oil sand sample and 10 ml of the desired surfactant formulation was added to the tube. Tubes were sealed with aluminum foil and plastic cap. Tubes were mixed gently and then allowed to equilibrate for 24 hours. After equilibration and

settling, the supernatant was collected and analyzed by GC. Static tests were also performed with synthetic oil sands. Synthetic oil sands were created by mixing extracted bitumen and clean (OK-75) sand using a similar oil:sand mass fraction of the actual oil sand. The synthetic oil sand, being prepared as a control using clean quartz sand, was designed to determine whether components in the actual oil sand—other than the sand particles—may play a role in the solubilization of the oil.

Surfactant adsorption was also studied as part of the static tests. Different surfactant solutions were mixed with specific amount of clean oil sands or OK-75 sand in 15 ml centrifuge tubes. The amount is a function of the degree of adsorption and, since the adsorptivity is not known *a priori*, it was adjusted after initial testing. The tubes were rotated for 3 days to mix, after three days the tubes were centrifuged and the supernatant (surfactant solution) was analyzed in HPLC to measure the change in concentration. HPLC methods are unique to the surfactant type, the method most utilized in this study is described in Table 5-3.

Table 5-3: HPLC method for surfactant detection

HPLC Method	
injector	0.2 µL
solvent A	Acetonitrile
solvent B	Ammonium acetate 0.1 M
pump	1 ml/min
solvent ratio	00:00 50:50 15:00 90:10 25:00 90:10
column temperature	40°C
	ELSD
evaporator	60°C
nebulizer	60°C
gas flow rate	1.6 SLM

5.2.6 Dynamic Tests

5.2.6.1 Dynamic Test Setup

A flow diagram for dynamic tests is shown in Figure 5-4. The setup consisted of an HPLC pump as described in section 4.1.1. Multiple floating piston accumulators were prepared for various liquids (brine, surfactant formulations, etc.). The oil sand was packed into a Kimble Kontes Chromoflex glass column, 15 cm in length and 2.5 cm diameter. One dynamic test was performed under confining pressure; for that, a core holder described in section 4.1.9 was used. A water circulator (ISOTEMP 6200) was used to maintain the required flow temperature. The Omega PX-26 pressure transducers were used to measure pressure drop across inlet and outlet. A vacuum pump was used to pull vacuum during measurements of the bulk water fraction (W_f).

The setup was designed to have a by-pass to have the ability to change the flow direction from bottom-top to top-bottom (shown in Figure 5-4 in blue color). Microemulsion produced from these tests were collected in 12 ml glass tubes using the fractional collector. The photograph in Figure 5-5 depicts the actual glass column used for flow experiments. Experimental design and conditions for each flow experiment were different and are described in subsequent sections.

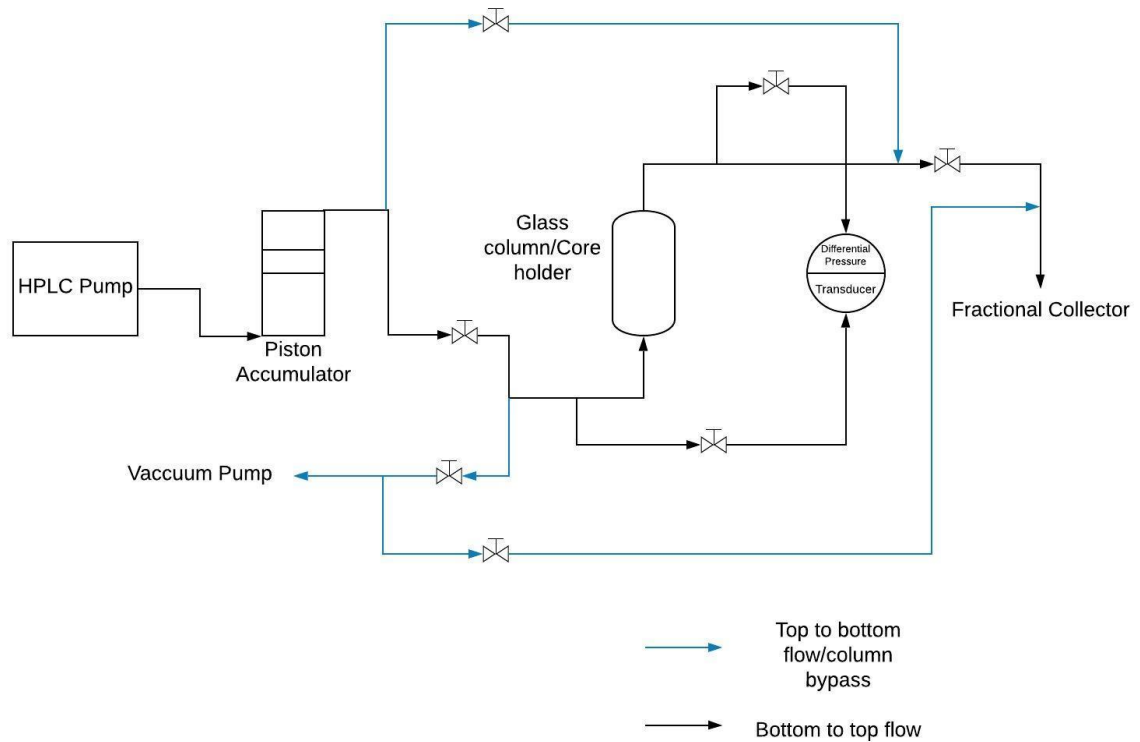


Figure 5-4: Flow diagram for dynamic tests, blue colored loop highlights the bypass loop

5.2.6.2 Dynamic Test 1

Field obtained high grade oil sand sample was used for the first flow experiment. The glass column was packed with 130 g of oil sand. The flow direction was maintained from top to bottom. Column temperature was maintained at 20°C and pressure drop was recorded. Microemulsion produced from the experiment was analyzed in GC-MS for bitumen solubilization.

5.2.6.3 Dynamic Test 2 and 3

These two tests were conducted using synthetic oil sands. Synthetic oil sand was prepared by mixing OK-75 sand with extracted bitumen to achieve 13 wt.% bitumen

content. Synthetic sand was prepared to eliminate the potential effects of the actual oil sand composition on the solubilization process. For test 2, 148 g of synthetic sand was packed in the glass column.

Test 3 was performed in a core holder (section 4.1.9). A confining pressure of 500 psig was applied to eliminate the possibility of flow channeling along the walls of glass column. The sandpack was prepared using 330 g of synthetic oil sand, which was 6 inches in length and 1.5 inches in diameter. For both tests the flow was maintained from bottom to top at 20°C temperature and produced samples were analyzed in GC-MS for solubilization calculations.



Figure 5-5: Glass Column used in all dynamic tests except test 3

5.2.6.4 Sandpack Bulk Water Fraction Measurements

Bulk water fraction of the sandpack denotes the available pore volume for flow and it was measured in a similar manner as porosity for consolidated cores. Bulk water fraction is analogous to water saturation in the case of consolidated cores.

Bulk water fraction measurements for dynamic test setup was critical for flow rate estimation and quantification of performance of the flood. Dead volume is defined as the volumes of the setup (volume of fluid in tubing, valves, etc.) that should not be included in the calculation. Dead volume of the flow setup was calculated by connecting column outlet and inlet together without the column. Vacuum was pulled for 1 hour in the setup using the vacuum pump (section 4.1.13) to remove any material from the setup. Inlet valve was opened after 1 hour to allow brine into the system and setup was allowed to equilibrate for 15 mins. The amount of brine consumed to saturate the setup was noted as dead volume of the setup (V_d).

Column packed with sand was connected to the system and system was checked for leaks. The setup was isolated, and vacuum was pulled for 2 hours. After 2 hours brine was allowed to flow inside the setup and equilibrate for 1hr. The volume of brine (V_{brine}) consumed to completely saturate the system was noted. Pore volume of the column was calculated by subtracting dead volume from the brine volume measured,

$$V_p = V_{brine} - V_d. \quad (5.3)$$

5.2.6.5 Dynamic Tests 4 – 8

Dynamic tests 4 – 8 were conducted in the glass column; sandpacks were prepared using the field obtained oil sand sample. Flow direction was maintained from top to bottom in these experiments. The sandpack description and conditions are listed in Table 5-4.

Table 5-4: Sandpack properties for dynamic tests

dynamic test	sand type	sand, grams	bitumen, grams	diameter, cm	length, cm
1	field sample	130.0	16.6	2.5	15
2	synthetic sample	148.0	19.2	2.5	15
3	synthetic sample	330.0	42.9	3.8	15.24
4	field sample	132.1	16.9	2.5	15
5	field sample	137.8	17.6	2.5	15
6	field sample	138.2	17.7	2.5	15
7	field sample	138.4	17.7	2.5	15
8	field sample	147.3	18.9	2.5	15

Dynamic test 4 was conducted with the improved surfactant formulation based on static tests at 20°C. Produced microemulsion was analyzed in GC, and the injection was stopped when bitumen concentration in microemulsion reached below 10,000 ppm. Test 5 was performed with the same formulation but with thermal enhancement at 40°C. Injection was stopped at 10,000 ppm bitumen concentration. Test 6 was conducted with huff and puff type of injection scheme. One PV of the surfactant formulation was injected, and column was isolated for 13 hours (the same amount of time as injection). This scheme was repeated until outlet concentration reached below 10,000 ppm. Test 7 was designed to study the effect of flow rate on oil recovery and was done at same conditions

as test 4 but with faster injection rate. As in the previous flow experiments and, for better comparison, the injection was stopped when outlet concentration reached below 10,000 ppm.

For test 8, the surfactant formulation was modified by adding 2000 ppm of A-5903 polymer solution. The stopping criterion of 10,000 ppm outlet concentration was not followed in this case because, in the presence of polymer, the GC method was not able to provide correct estimate of bitumen concentration and the test was continued longer than was likely needed.

After stopping each dynamic test, a 1 wt.% NaCl solution was injected to remove all the remaining microemulsion remaining in the system. The bulk water fraction was re-measured after the test. This bulk water fraction change was converted into weight of bitumen recovered to calculate the recovery of bitumen.

$$\Delta PV = W_{f,final}V_{total} - W_{f,initial}V_{total} \text{ and} \quad (5.1)$$

$$\% \text{ Recovery} = \frac{(\Delta PV)\rho_{bitumen}}{\text{bitumen weight}} \times 100, \quad (5.2)$$

where $W_{f,initial}$ is bulk water fraction before the test, $W_{f,final}$ is bulk water fraction after the test, V_{total} is the total volume of the column, ΔPV is the change in pore volume due to bitumen recovery, $\rho_{bitumen}$ is the density of bitumen.

Weight of the dry, packed column was used to calculate the % OOIP recovery from the test. Bitumen concentration measured with GC, was not used to calculate the

recovery because the surfactant peaks were interfering with bitumen peaks. So, GC concentration was used as a comparison for relative concentration changes but was not used to quantify the recovery from the tests.

5.2.7 Sandpack Permeability Measurement

Sandpack permeability was measured using Darcy's law, which relates flow in porous media to pressure drop.

$$q = \frac{k}{\mu} (\nabla\Phi), \quad (5.4)$$

where

q – flow rate, m/sec

k – permeability, m^2

μ - viscosity of brine, Pa.s

Φ - potential or P- ρZ using positive values of Z downward.

Since the values of Z are small in comparison to P, the pressure drop alone was used for the potential drop. In addition, the values of were graphed and the slope used, so the constant elevation difference does not affect the measured slope used to calculate the permeability.

Brine was injected into the sandpack at various flow rates and pressure drop was recorded between inlet and outlet. The pressure drop was plotted with flow rate, and a

straight line fit to those points was calculated. The slope of the line was used to calculate the permeability of the sandpack. Field unit for permeability is darcy, so calculated number was converted from m² to darcy.

5.2.8 Polymer Solution Preparation and Characterization

Dynamic test 8 was performed with a surfactant formulation with 2000 ppm of A-5903 polymer. The polymer solution was created for 2000, 4000, 6000, and 10,000 ppm with selected surfactant formulation to identify suitable polymer concentration. The solution was hydrated for 24 hrs. A filtration test was conducted to ensure proper injectivity of the solution as described in Koh et al.(Koh et al., 2017).

5.3 Surfactant Recovery Experiments

Recovery experiments were limited to specific anionic surfactants: sulfate and sulfonates and to non-ionic surfactants. Surfactant behavior was first studied without oil phase present. The emphasis was to study the behavior of anionic surfactants in presence of acid and bases. Another set of experiments were performed with non-ionic surfactant to study the salting-out phenomenon. After studying surfactant behavior in aqueous phase, some tests were conducted with the produced microemulsion from the flow experiments.

5.3.1 Surfactant Behavior with pH Variations and Salt Concentration

Stock solutions were prepared with various anionic surfactants. The pH of the stock solution was measured. For acidic treatment, 10 ml of each surfactant stock solution was mixed with 1 ml of 1 N HCl in Falcon 15 ml centrifuge tubes and pH was

measured after acid addition. For basic treatment, 10 ml of surfactant stock solution was mixed with 0.2 g of NaOH in 15 ml centrifuge tubes. The pH of the mixture was measured, and tubes were allowed to equilibrate. After equilibration, the tubes were analyzed with both titration and HPLC for surfactant composition. If there was phase separation, the phases were analyzed for surfactant composition. These experiments were repeated with the selected surfactant formulation as well. Salt treatment (“salting out”) was conducted for non-ionic surfactants only, where they were mixed with different amount of NaCl in a 15 ml centrifuge tube. If phase separation was observed, the phases were analyzed for surfactant composition.

5.3.2 Microemulsion Behavior with pH Variations and Salt Concentration

Microemulsion generated during phase behavior, static tests, and dynamic tests were also subjected to pH and salt concentration treatment to understand how the behavior will change in presence of oil phase. Microemulsion pH was measured and desired amount of acid or base was added. The pH of the mixture was measured, and it was allowed to equilibrate. The initial goal for these treatments were to achieve separation of oil and aqueous phase, so the amount of acid or base added was varied to achieve separation. After phase separation aqueous phase was analyzed with auto titrator and HPLC to understand the composition of aqueous phase.

Chapter 6

Results and discussion

6.1 Coal tar

6.1.1 Surfactant Screening

A total of 60 surfactant screening tests were performed using both single and various surfactant combinations. These tests indicated the qualitative behavior of the surfactant solution mixed with tar. A GC calibration curve was prepared to analyze 9 components of coal tar, and used to determine preferential solubilization in the microemulsion. The GC calibration method and the calibration curves are described in Appendix A1. The photograph in Figure 6-1 showed very low solubilization using 2 wt.% C24-28 IOS surfactant solution, and the GC analysis presented in Figure 6-2 indicated that it also preferentially solubilized the lighter components. Microemulsion formed with 2 wt.% alcohol propoxy sulfate, 1 wt.% C15-18 IOS, 1 wt.% C12-13 AAS, and 4 wt.% 2-butanol did not exhibit preferential solubilization (Figure 6-3), but the amount of coal tar solubilized was low. Solubilization was around 250,000 mg/L, it was a suitable formulation based on no preferential solubilization and absence of gel, but further investigation led to even better formulation in terms of solubilization.

Figure 6-4 shows a photograph of surfactant mixture of 4 wt.% alcohol propoxy sulfate sodium and 4 wt.% sodium dioctyl sulfosuccinate with 4 wt.% tri-ethylene glycol mono-butyl ether (TEGMBE) as co-solvent and 0.5 wt.% Na₂CO₃ that resulted in single phase microemulsion behavior. It showed very high solubilization of 500,000 mg/L and

no preferential solubilization as shown in Figure 6-5. Similar results were observed for the same surfactant formulation with 2-butanol as co-solvent. This surfactant formulation was selected to do salinity scans and aqueous stability tests.

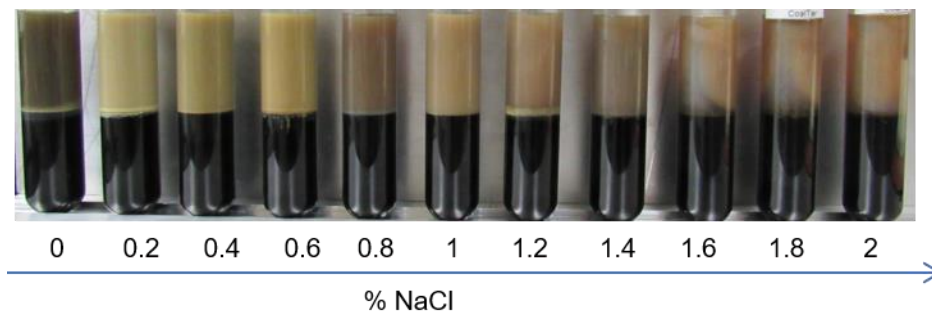


Figure 6-1: Surfactant screening tubes for 2 wt.% C24-28 IOS surfactant formulation with coal tar at 25°C

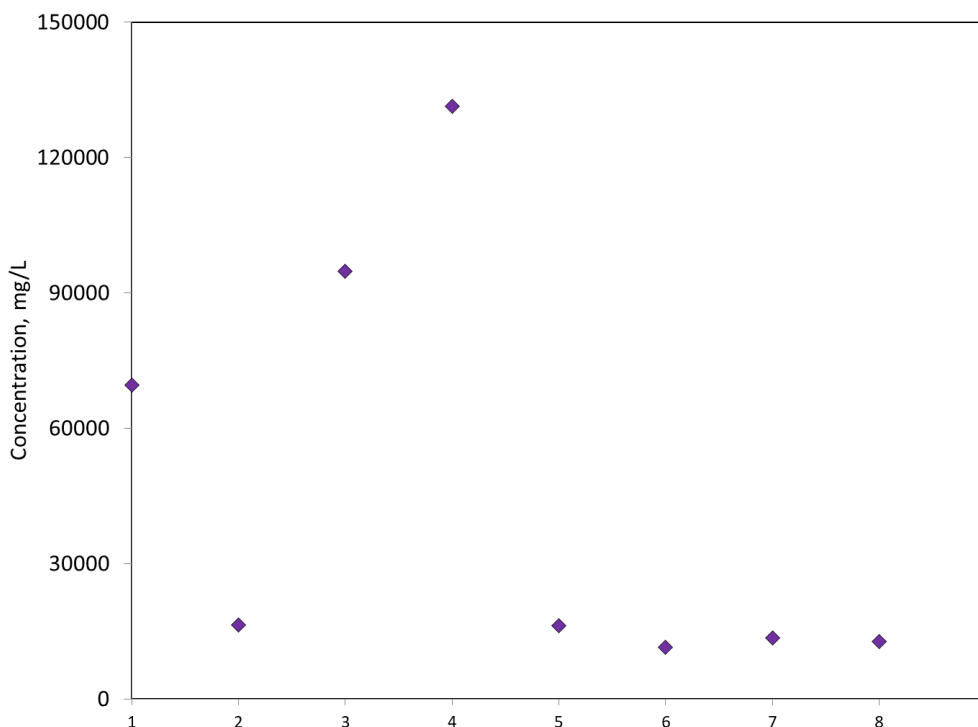


Figure 6-2: Solubilization of nine coal tar components with 2 wt.% C24-28 IOS surfactant formulation. The nine components are 1) azulene, 2) 2-methyl naphthalene, 3) acenaphthene, 4) dibenzofuran, 5) fluorene, 6) phenanthrene, 7) fluoranthene, 8) pyrene, and 9) benzopyrene

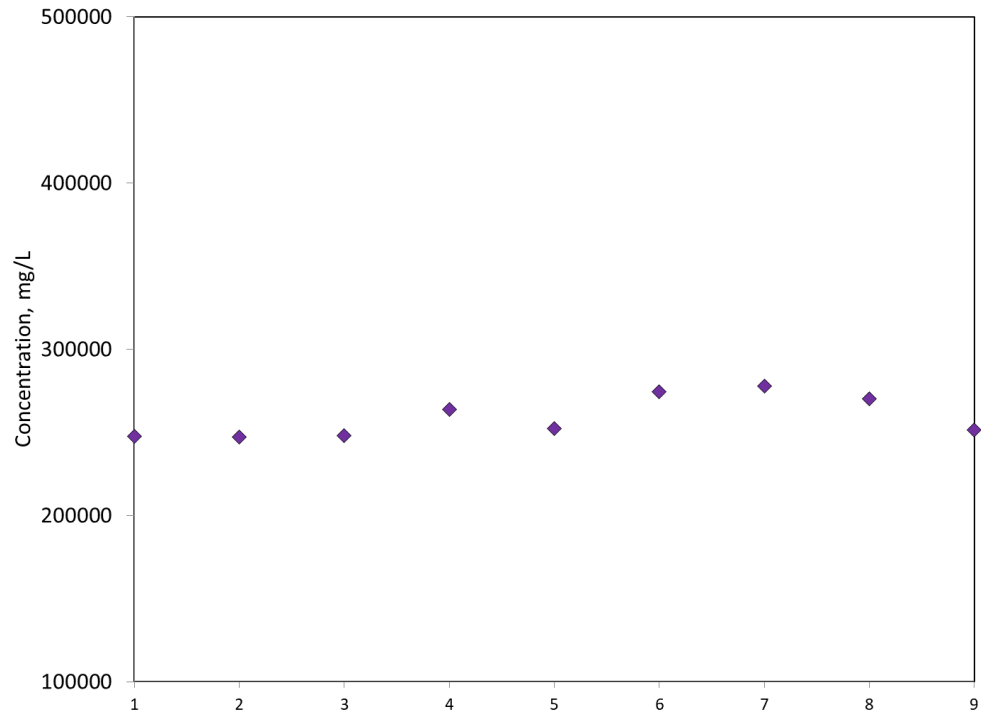


Figure 6-3: Solubilization of nine coal tar components with 2 wt.% alcohol propoxy sulfate, 1 wt.% C15-18 IOS, 1 wt.% C12-13 AAS, and 4 wt.% 2-butanol surfactant formulation. The nine components are 1) azulene, 2) 2-methyl naphthalene, 3) acenaphthene, 4) dibenzofuran, 5) fluorene, 6) phenanthrene, 7) fluoranthene, 8) pyrene, and 9) benzopyrene

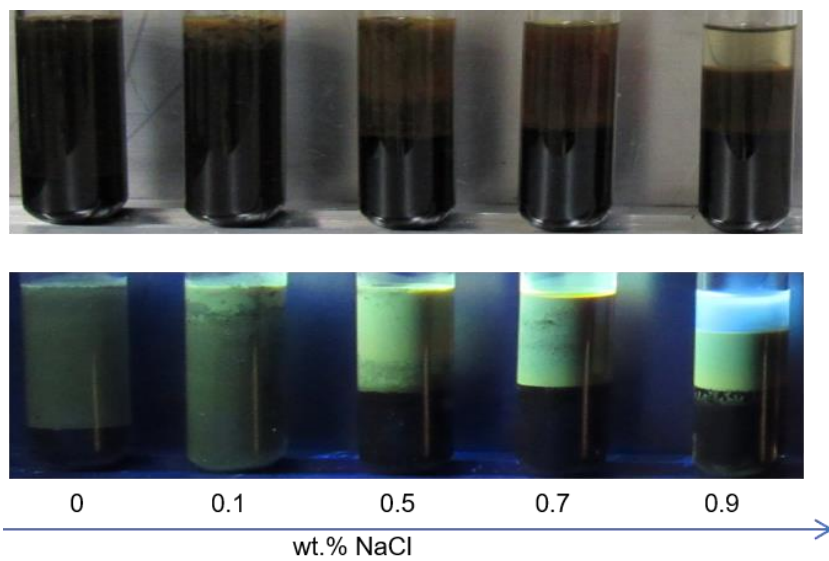


Figure 6-4: Surfactant screening tubes for 4 wt.% alcohol propoxy sulfate and 4 wt.% sodium dioctyl sulfosuccinate with 4 wt.% tri-ethylene glycol monobutyl ether as co-solvent and 0.5 wt.% Na_2CO_3 with coal tar at 25°C. The picture at the bottom is taken under UV light

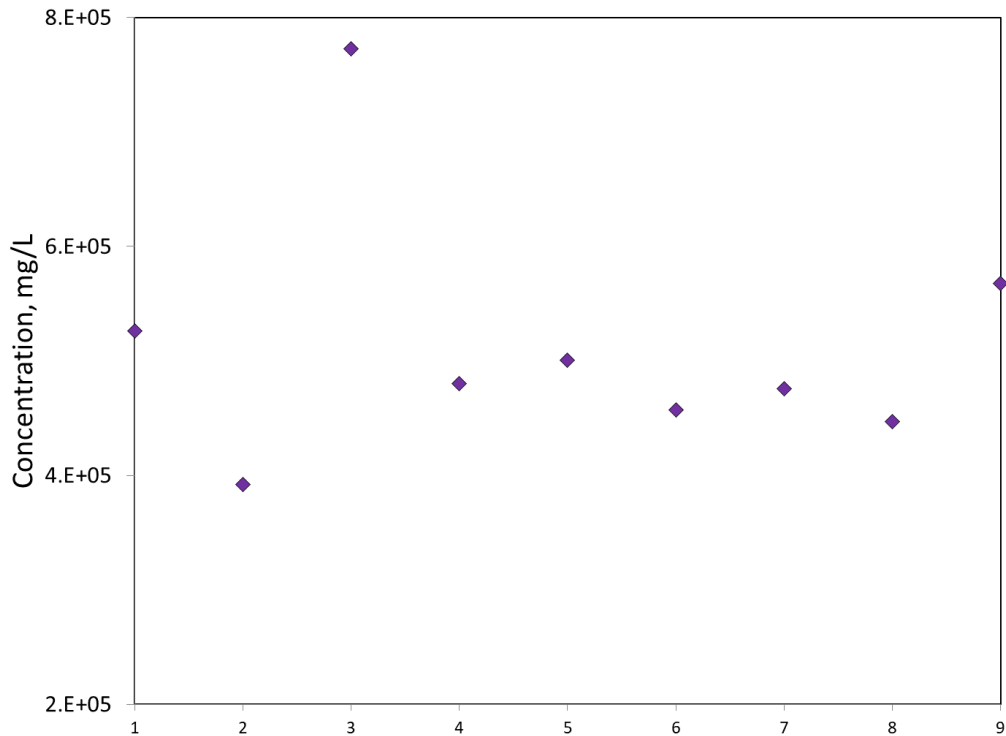


Figure 6-5: Solubilization of nine coal tar components with 4 wt.% alcohol propoxy sulfate and 4 wt.% sodium dioctyl sulfosuccinate with 4 wt.% tri-ethylene glycol mono-butyl ether and 0.5 wt.% Na_2CO_3 formulation. The nine components are 1) azulene, 2) 2-methyl naphthalene, 3) acenaphthene, 4) dibenzofuran, 5) fluorene, 6) phenanthrene, 7) fluoranthene, 8) pyrene, and 9) benzopyrene

6.1.2 Salinity Scans

Salinity scans were performed using pipettes at a WOR=1 for the selected surfactant composition to determine the salinity range for single phase microemulsion of the mixture. Figure 6-6 is an image under UV light of the pipettes after equilibration. Single phase microemulsion with high coal tar solubilization was observed at salinities 0.1, 0.15, and 0.2 wt.% NaCl. In addition, salinity scans were performed in test tubes at WOR of 1, 2, 3 and 4, and are presented in Figure 6-7 under UV light. Tubes with salinities of

0.1 and 0.15 wt.% yielded single phase microemulsion for the WOR tested (1, 2, 3 and 4); the solubilization parameter was calculated for all salinities at WOR=1.

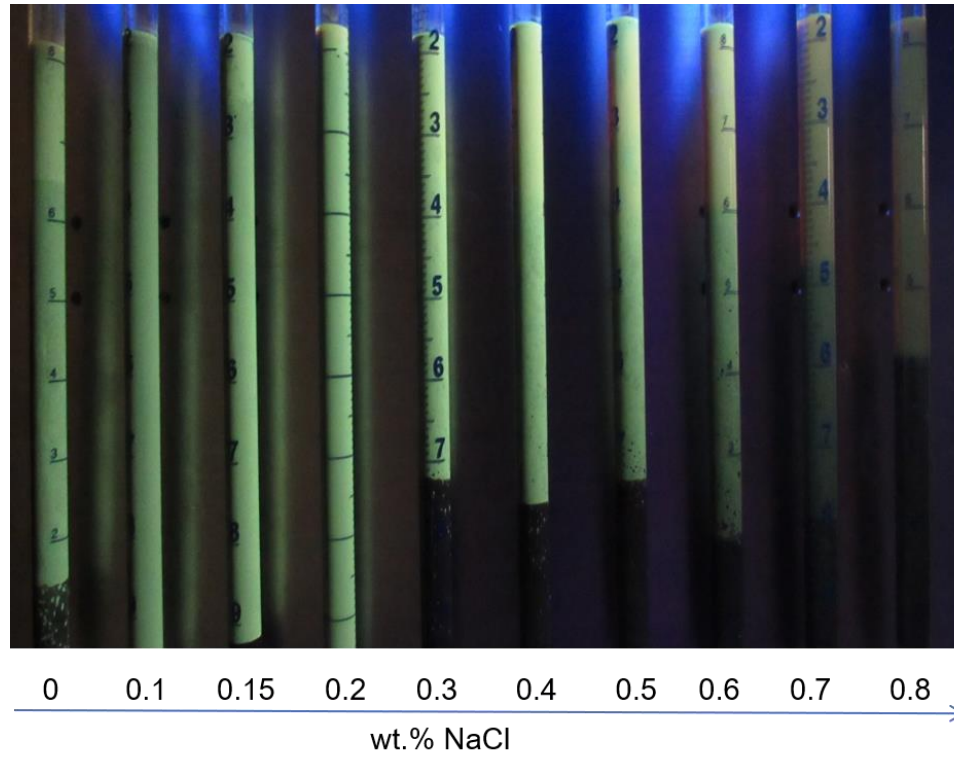


Figure 6-6: Salinity scan for 4 wt.% alcohol propoxy sulfate and 4 wt.% sodium dioctyl sulfosuccinate with 4 wt.% tri-ethylene glycol mono-butyl ether and 0.5 wt.% Na_2CO_3 formulation at 25°C

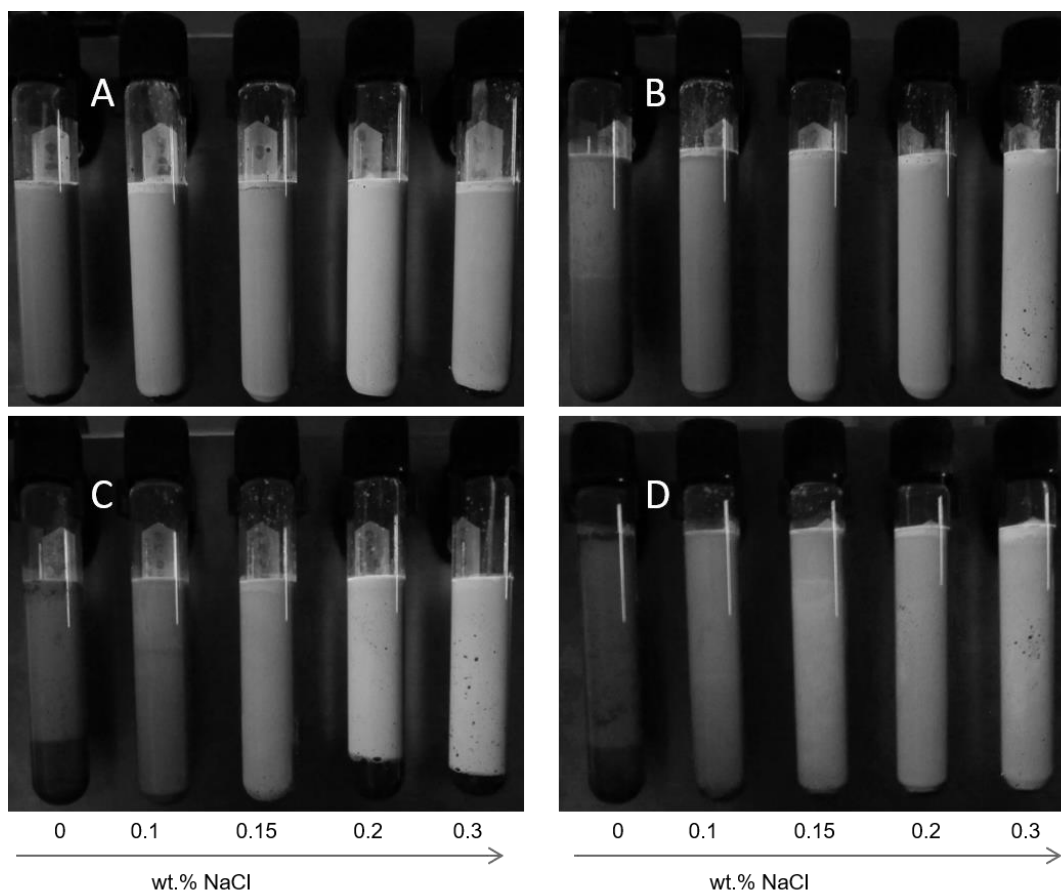


Figure 6-7: Salinity scan for selected formulation at 25°C. From top left, four WOR are shown a) WOR=1, b) WOR=2, c) WOR=3, and d) WOR=4

6.1.3 Aqueous Stability Tests

These tests examined the stability of the surfactant stock solution with time. Surfactant solution was observed to be stable after 1 month for a range of salinity. No phase separation or precipitation was observed, as shown in the photograph (Figure 6-8).

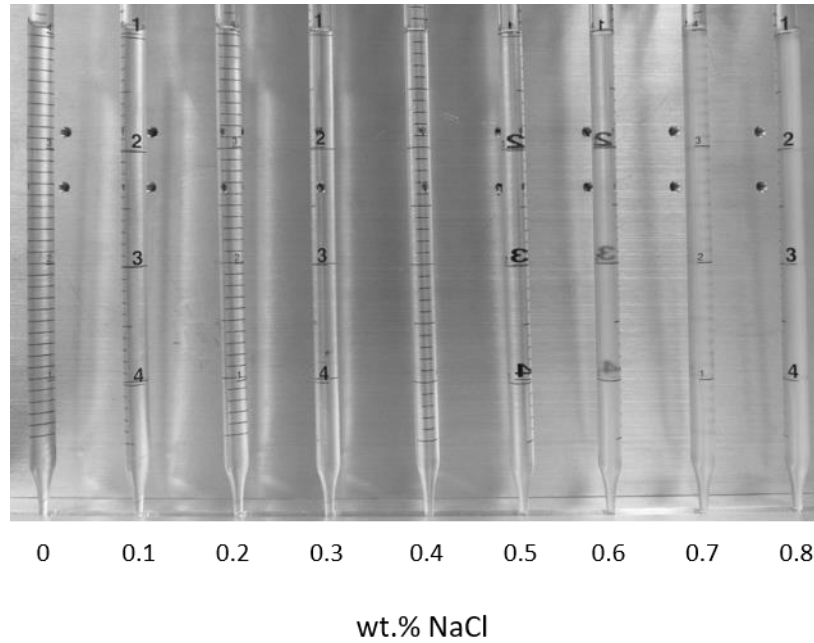


Figure 6-8: Aqueous stability for selected surfactant formulation at 25°C, no separation or instability was observed

6.1.4 Flow Experiment

The selected surfactant formulation was injected at a constant pressure into the glass column containing the synthetic oil sand and the produced liquid was collected in glass test tubes. No gel formation was observed in the produced liquid, which was confirmed based on the higher flow rates achieved using a low pressure gradient. Coal tar was not produced during the experiment indicating that it was not mobilized. Only single phase microemulsion was produced during the flow experiment from the beginning as observed in the concentration history in Figure 6-9. The microemulsion was lower in viscosity than the actual coal tar. The viscosity of the produced microemulsions are plotted with PV produced in Figure 6-10 and follow the trend in concentration. Initial

samples were black in color indicating high solubilization, followed by dark brown and light brown in later stages.

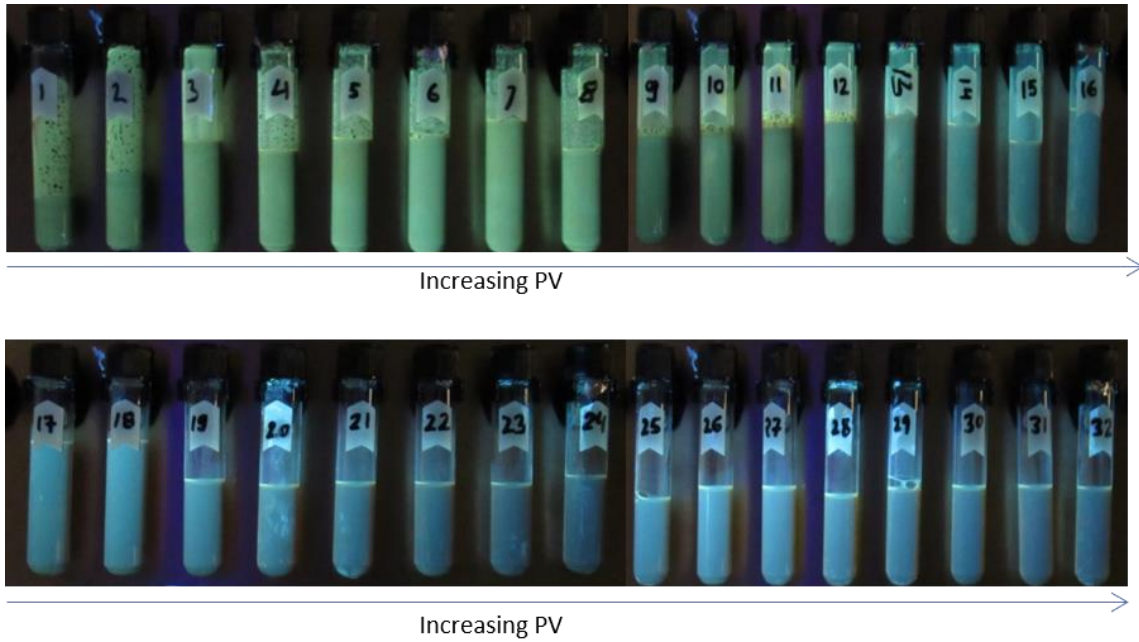


Figure 6-9: Produced microemulsion from the flow experiment under UV light

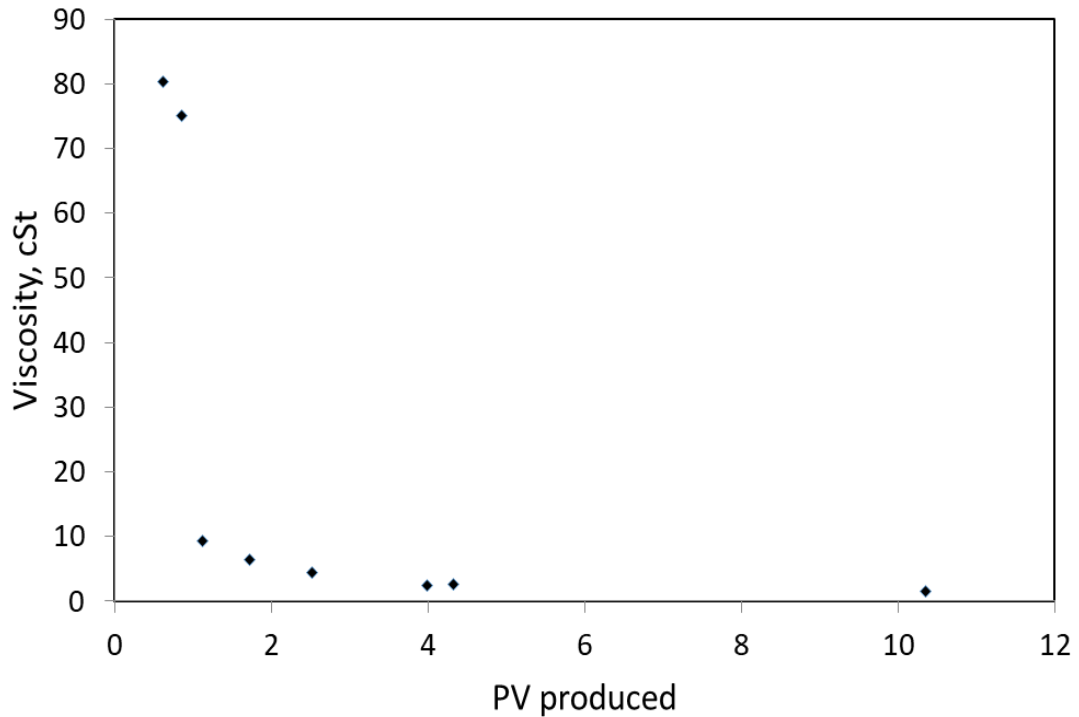


Figure 6-10: Viscosity of produced microemulsion at 25°C

Produced microemulsion was analyzed by GC to calculate the amount of oil produced in each glass collection tube. A low, constant pressure drop of only 20.7 kPa (3 psi) was used for the surfactant injection vertically downward and it was sufficient to induce flow. After approximately 32 PV (730 ml) of surfactant flood, 8 PV (183 ml) of brine (0.15 wt.%) was injected to displace the surfactant/microemulsion from the column. In examining the oil recovery history (Figure 6-11), note that the flow rate increased from 0.26 ml/min to 2.96 ml/min during the experiment due to microemulsion production; oil occupies pore space at the start of the experiment and results in a low relative permeability. Thus, the slower, initial flow rate correlates with the highest solubilized tar concentrations—on the order of 300,000 mg/L—with faster rates correlating with

significantly lower solubilized tar concentrations. The concentration of tar in produced microemulsion is plotted with PV injected in Figure 6-12. The flow rate increased by an order of magnitude during the experiment.

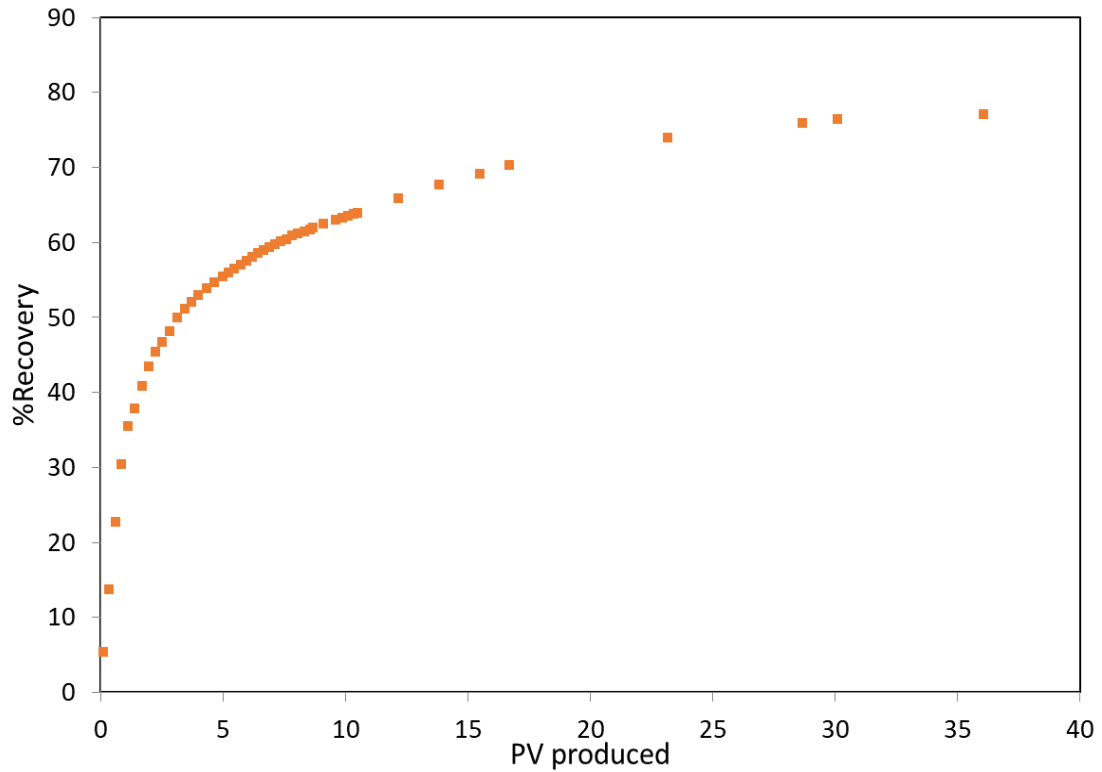


Figure 6-11: Coal tar recovered with pore volumes of microemulsion produced

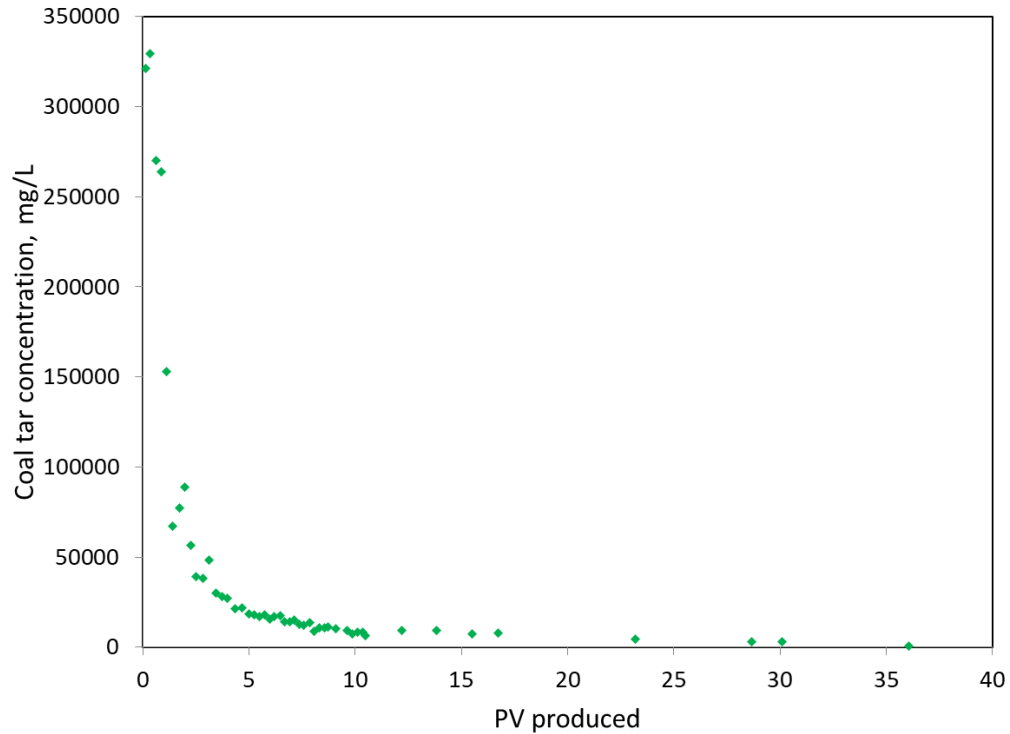


Figure 6-12: Concentration of coal tar in produced microemulsion, measured using GC

The viscosity of the microemulsion (produced fluid) correlates directly with solubilized tar concentration; the viscosity was initially about 80 cSt and fell to only 1–2 cSt after about 4PV of surfactant throughput, when more than half of the tar was recovered from the sandpack. Note that, although a low-pressure drop was used for the flow experiment, the flow rates near the end of the experiment were rather high (6.1 m/day or 77 ft/day average). Although this rate is higher than could be achieved in the field, no tar was produced at the higher shear rates associated with this rate. A slower, constant flow rate throughout the experiment would have likely resulted in higher recovery using less throughput; a shut-in for approximately 1 hour resulted in an increase in oil solubilization from 6,594 mg/L to 9,477 mg/L, indicating that the process could have

achieved higher oil recovery at slower rates that allowed for longer hydraulic residence time.

Oil recovery was calculated based on GC analysis of the microemulsion samples produced to determine the concentration and hence mass sample volume. The oil recovery was also calculated based on the analysis of the remaining sand using methylene chloride extraction. A recovery of 77 % OOIP is estimated based on the microemulsion analysis by GC; the recovery is estimated to be 78 % OOIP by methylene chloride extraction. Figure 6-13 shows a visual comparison of sand samples before and after the flow experiment.



Figure 6-13: Comparison of sand (OK-75) before and after the flow experiment

The flow experiment proved that significant oil recovery is possible through the use of single phase microemulsion. Next, a set of experiments were designed to develop the single phase microemulsion approach for oil sands.

6.2 Bitumen

6.2.1 Soxhlet Extraction

Oil was extracted from both high and low grade oil sand using the Soxhlet procedure; it was performed on three samples of each grade to ensure consistent results. For high grade sand, the bitumen content was found to be 12.8 wt.% on average, while the low grade sand had 13.5 wt.% on average bitumen content. High grade sand was used for all the experiments performed in this work. Results of each Soxhlet extraction are listed in Table 6-1.

Table 6-1: Results of Soxhlet extraction for oil sand

experiment	wt.% bitumen	
	high grade	low grade
1	13.1	13.5
2	12.6	14.1
3	12.8	13.3
average	12.8	13.6

6.2.2 Bitumen Characterization

The extracted bitumen was analyzed to characterize its properties and composition. The API gravity of bitumen was measured to be 6.8 °API. Results of SARA (Saturates, Aromatics, Resins, and Asphaltenes) analysis of bitumen and coal tar is listed in Table 6-2. The SARA analysis also supports the statement made earlier that coal tar is

comparable to bitumen. SARA and API gravity analysis was conducted at Center for Petroleum Geochemistry at University of Houston.

Table 6-2: SARA results for bitumen and coal tar

	saturates (%)	aromatics (%)	resins (%)	asphaltenes (%)
bitumen	23.85	28.21	15.13	32.81
coal tar	17.4	26.2	20.2	36.2

Total Acid Number (TAN) for bitumen was measured to be 2.94 mg of KOH per g of oil using ASTM – D664 – 18e2 (Drews, 2008). Viscosity of the bitumen sample was measured at multiple temperatures and multiple shear rates. The bitumen displays shear thinning behavior. In addition, the bitumen viscosity decreases drastically with temperature increase. Figure 6-14 and 6-15 shows the rheological properties of bitumen. The viscosity data with temperature is listed in Table 6-3.

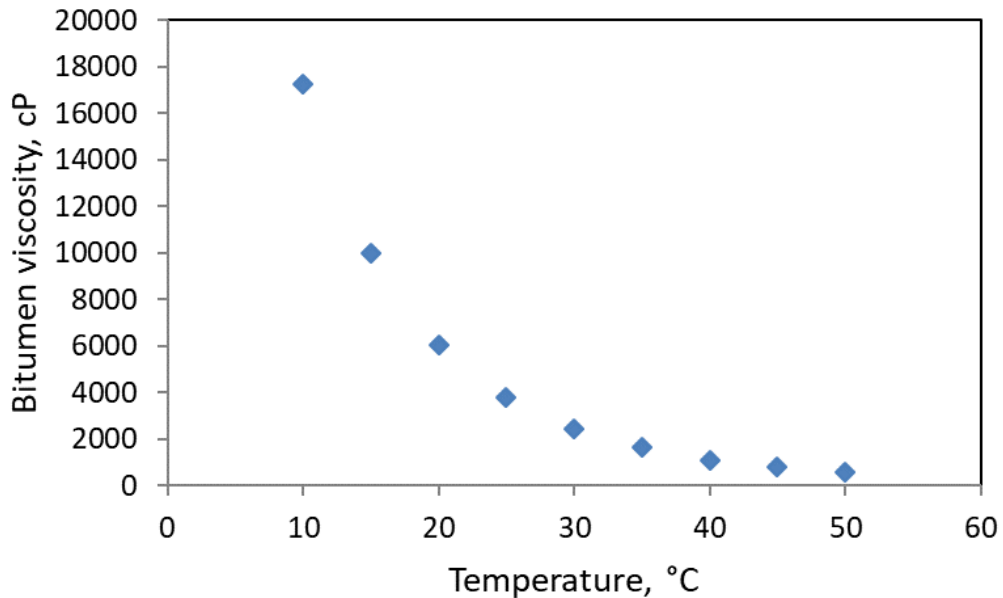


Figure 6-14: Bitumen viscosity variations at shear rate = 10 s^{-1} with temperature

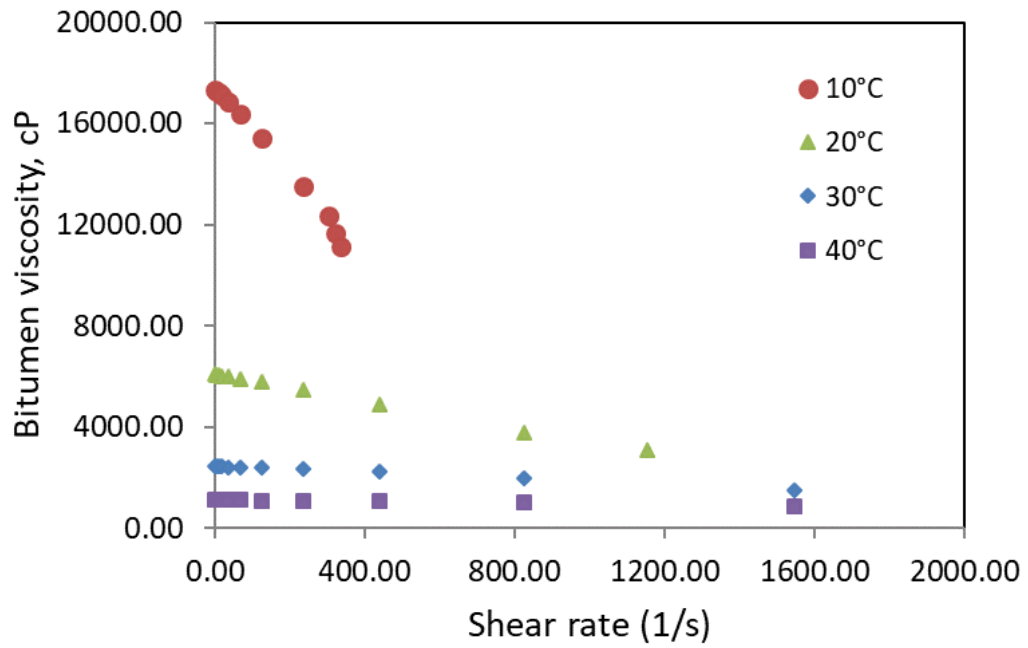


Figure 6-15: Bitumen viscosity at multiple temperature and shear rates, notice the shear thinning behavior

Table 6-3: Bitumen viscosity at 10 s⁻¹ shear rate at different temperatures

temperature [°C]	viscosity [mPa·s]
10	17248
15	10001
20	6039
25	3777
30	2440
35	1631
40	1120
45	792
50	572

6.2.3 Phase Behavior Studies

Phase behavior studies were performed on the extracted bitumen to identify surfactant formulations for single phase microemulsions. Oil sands deposits generally contains very small amount of formation brine, so the focus of the phase behavior was to identify the formulation suitable for this application and no attempt was made to find optimum salinity of the system.

6.2.3.1 Surfactant Screening

Surfactant screening was performed to identify surfactant formulation qualitatively. A total of 30 surfactant combinations were used. Sodium carbonate was an important constituent of the formulations due to the high TAN of bitumen. Figure 6-16 shows a picture of surfactant screening test tubes for bitumen with a mixture of 0.5 wt.% C12-13 sulfate (7 PO), 0.5 wt.% C12-13 AAS (13 PO), 1 wt.% 2-butanol, and 0.5 wt.% sodium carbonate. The formulation did not exhibit good solubilization with bitumen. Microemulsions at higher salinities were not required because oil-in-water microemulsions were suitable for the process.

A formulation of 0.50 wt.% C20-24 IOS and 0.50 wt.% C13 13 PO alcoxy sulfate, 1 wt.% 2-butanol, and 0.5 wt.% sodium carbonate exhibited good solubilization of bitumen. A photograph of the surfactant screening tubes is shown in Figure 6-17, where transition from type I to type II can be noted. Type I tubes (0.2 and 0.4 wt.% NaCl) showing good degree of solubilization.

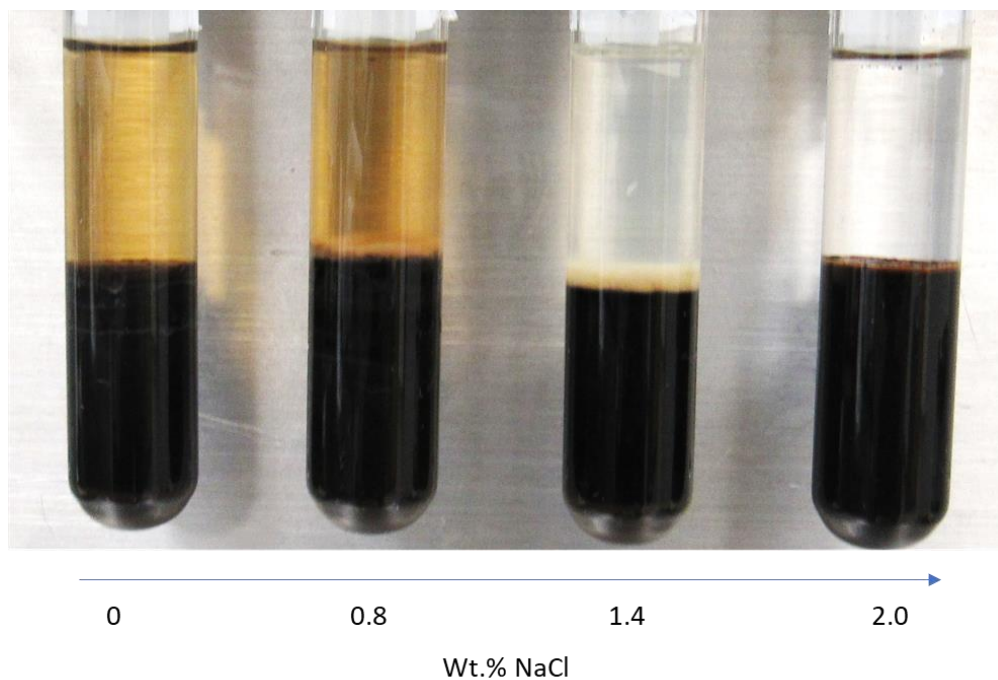


Figure 6-16: Surfactant screening tubes for 0.5 wt.% C12-13 sulfate (7 PO), 0.5 wt.% C12-13 AAS (13 PO), 1 wt.% 2-butanol, and 0.5 wt.% Na₂CO₃

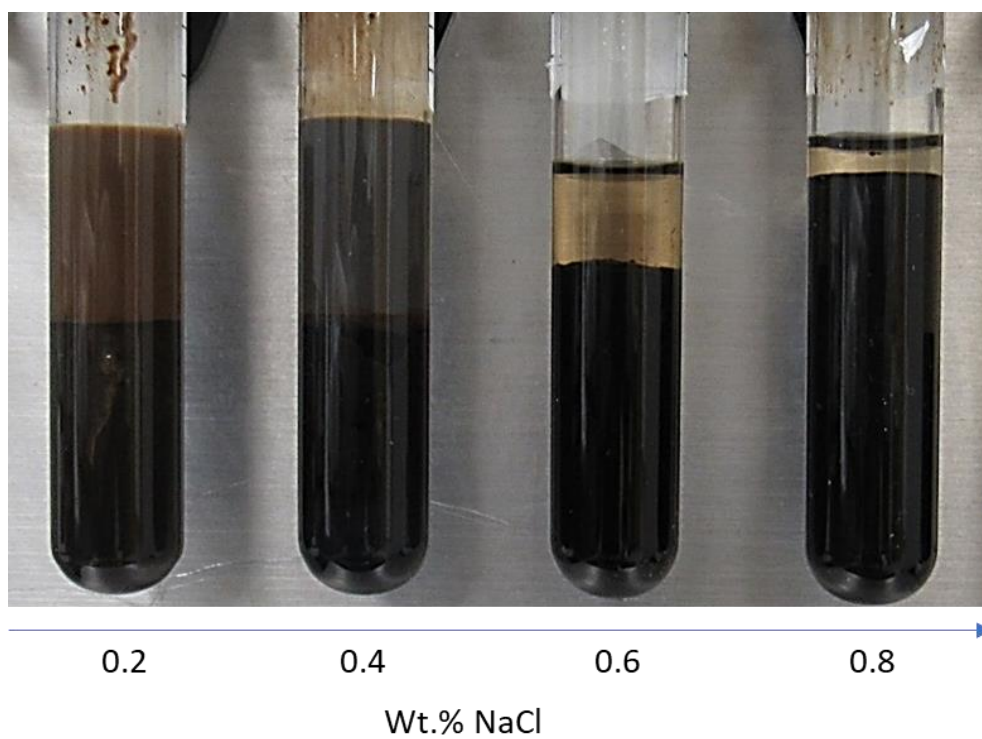


Figure 6-17: Surfactant screening tubes for 0.5 wt.% C20-24 IOS, 0.5 wt.% C13 13 PO sulfate, 1 wt.% 2-butanol and 0.5 wt.% Na₂CO₃

6.2.3.2 Salinity Scans

A salinity scan for the selected formulation was conducted keeping the NaCl concentration at 0.2 wt.% and varying the Na₂CO₃ only. Figure 6-18 is a photograph of the salinity scan of the selected formulation with varying amount of alkali (sodium carbonate) at a WOR 4. The microemulsion phase was analyzed with GC to estimate the amount of bitumen solubilized in the microemulsion phase. The GC calibration method and results are described in Appendix A2.

Additional investigation revealed that single phase microemulsion with high solubilization can be achieved using lower concentrations of the surfactants and the co-solvents (Figure 6-19). The new, optimized formulation (0.25 wt.% C20-24 IOS and 0.25 wt.% C13 13 PO alcoxy sulfate, 1 wt.% 2-butanol, with 0.5 wt.% Na₂CO₃ and 0.2 wt.% NaCl) was tested at several WOR to ensure the solubilization of bitumen is high under each condition (Figure 6-20). The bitumen solubilization was measured to be 82,000 mg/L for WOR 4, 156,000 mg/L for WOR 3, 210,000 mg/L for WOR 2, and 254,000 mg/L for a WOR 1. Based on these observations, the surfactant formulation of 0.25 wt.% C20-24 IOS and 0.25 wt.% C13 13 PO alcoxy sulfate, with 0.5 wt.% 2-butanol, 0.5 wt.% Na₂CO₃ and 0.2 wt.% NaCl – was selected for dynamic flow tests.

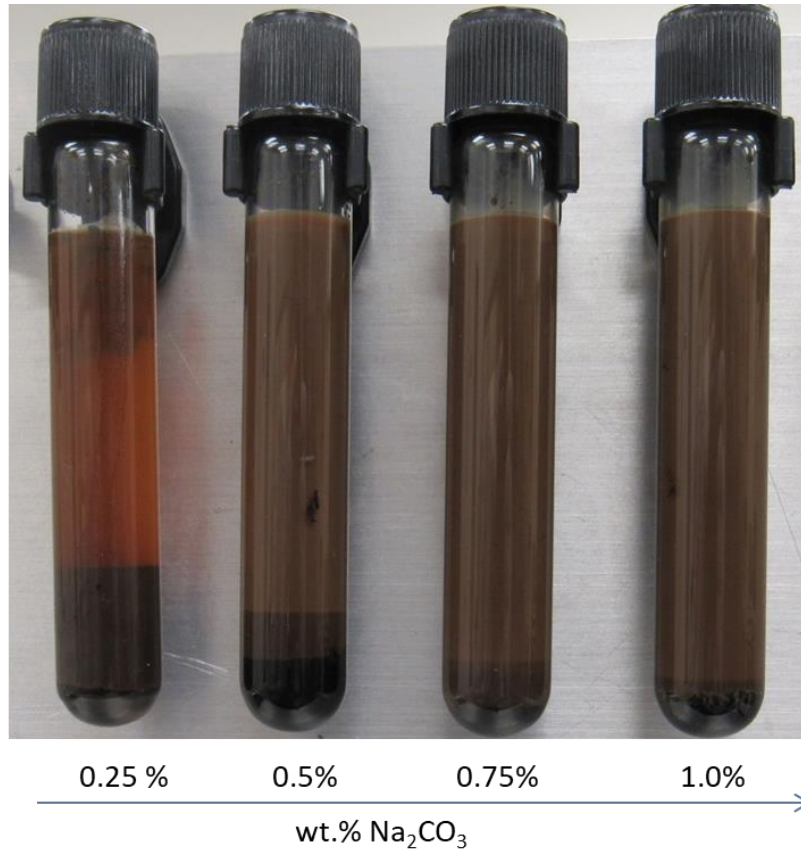


Figure 6-18: Salinity scan for 0.50 wt.% C20-24 IOS and 0.50 wt.% C13 13 PO alcoxy sulfate, with 1 wt.% 2-butanol and 0.2 wt.% NaCl with bitumen

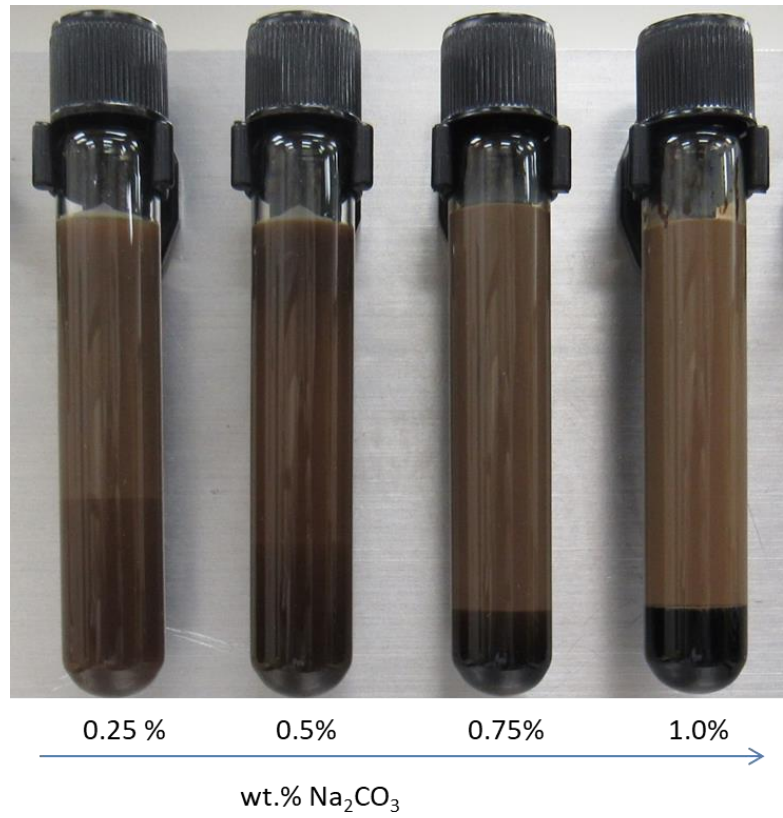


Figure 6-19: Salinity scan for 0.25 wt.% C20-24 IOS and 0.25 wt.% C13 13 PO alcoxy sulfate, with 0.5 wt.% 2-butanol and 0.2 wt.% NaCl with bitumen

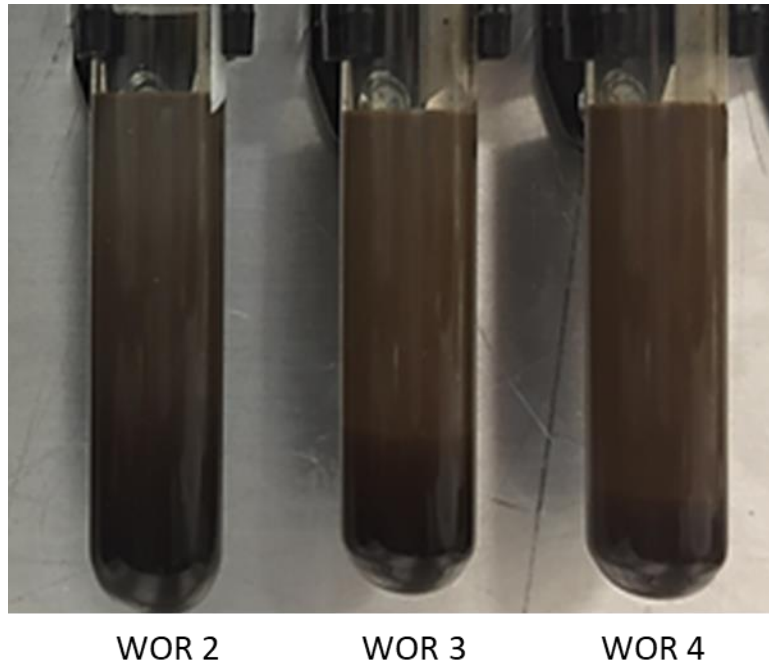


Figure 6-20: WOR scan for 0.25 wt.% C20-24 IOS and 0.25 wt.% C13 13 PO alcoxy sulfate, with 0.5 wt.% 2-butanol, 0.5 wt.% Na₂CO₃, and 0.2 wt.% NaCl with bitumen

6.2.3.3 Aqueous Stability

The selected surfactant formulation was prepared at a range of salinities to test the aqueous stability of the formulation. The formulation was stable for an extended amount of time; only for higher salinities (>3%) the solution became cloudy after mixing (Figure 6-21).

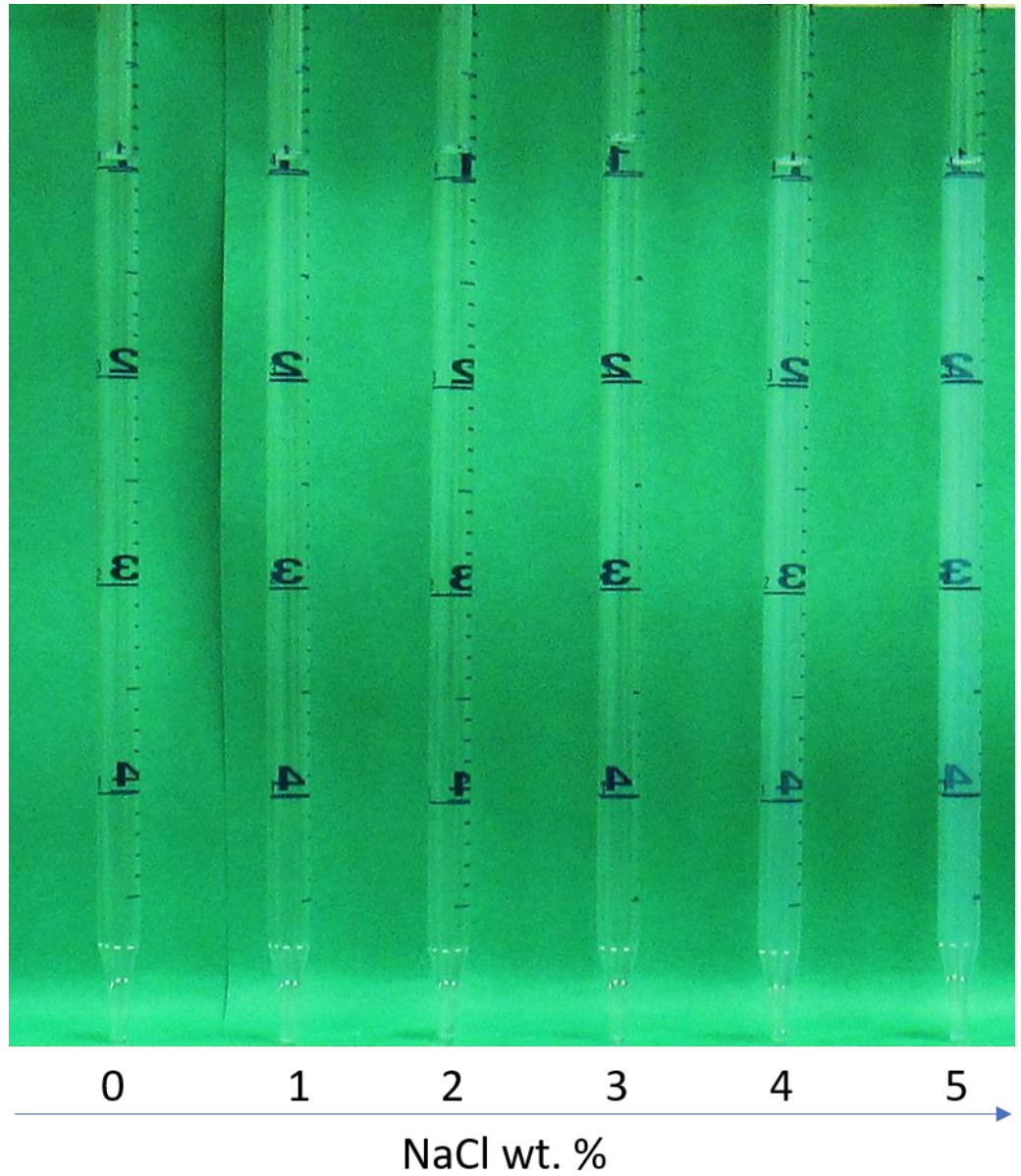


Figure 6-21: Aqueous stability tubes for surfactant formulation, notice cloudy solution for salinities 4 and 5 wt.% NaCl

6.2.4 Dynamic Tests 1 – 3

6.2.4.1 Dynamic Flow Test 1

This flow test was performed on a sandpack prepared with field-obtained oil sand.

Dynamic properties of the sandpack are listed in Table 6-4. Surfactant solution was

initially injected with a flow rate of 0.032 mL/min (1 ft/day intrinsic velocity) into the vertically-oriented column from top to bottom, column temperature was maintained at 20°C. Since the bitumen is heavier than water, any bitumen that was recoverable by means of viscous and gravity forces would be noted. No gel formation was observed and only microemulsion was produced. On visual examination, the produced microemulsion appeared to contain a low amount of bitumen in comparison with the phase behavior results. The samples were analyzed by GC and the analysis confirmed that the concentration of bitumen in produced fluid was approximately 12,000 mg/L at the time of surfactant breakthrough and reduced to 3500 mg/L, in contrast with the phase behavior where concentrations upwards of 200,000 mg/L was observed.

Based on these observations the experiment was shut-in at approximately 2 PV for approximately 8 hrs. Upon re-commencing surfactant injection, the flow direction was changed to be upwards, from bottom to top. The bitumen concentration in the produced samples increased to 7500 mg/L immediately after the shut-in period but decreased to 1500 mg/L after 2 PV of injection. The shut-in process was employed periodically, after every 1 PV injection, to understand whether rate-limited processes were affecting the results. Total bitumen recovery after 10 PV injected was 4.52% OOIP.

As a result of these observations, the flow rate was reduced to increase the contact time of the surfactant with the bitumen. Injection was started at a lower flow rate 0.017 ml/min (0.5 ft/day). A total of 7 PV of surfactant solution was injected; performance in terms of bitumen recovery continued to be low. To rule out the possibility of channeling with the sandpack or along the column walls, the next 3 PV of surfactant

solution included a viscosifier namely 400 ppm xanthan gum. Polymer addition increased the pressure drop of the system as expected, but the bitumen concentration in the produced microemulsion remained the same indicating that channeling was not likely the cause of the low bitumen solubilization. Overall incremental bitumen recovery for the second 10 PV injection was 2.97% OOIP.

Based on the unexpected results of this test, the next test was designed using synthetic oil sand.

Table 6-4: Results of Dynamic test 1

weight of oil sand	130 g
bulk water fraction	18.5%
PV	14.3 ml
permeability	20 darcy
% OOIP recovery	7.49%
highest solubilization	12,000 mg/L

6.2.4.2 Dynamic Test 2

The first synthetic oil sand flow experiment utilized the same setup as dynamic test 1. The purpose of this experiment was to eliminate the possibility that some components within the solids (clay minerals, silts or other materials) were interfering with the recovery processes. The flow rate was maintained at 0.017 ml/min (0.5 ft/day) and temperature of 20°C. A total of 16 PV solution was injected, and the bitumen concentration in effluent was measured to be 10000 ppm initially and dropped to 2000 ppm—again, significantly lower than the expected values from phase behavior. The total recovery of 4% OOIP was low and without explanation. Results of dynamic test 2 are

listed in Table 6-5. Figure 6-22 depicts the bitumen concentration and recovery history with respect to injected pore volumes.

All the previous flow experiments were done in the glass columns, where there was no confining stress applied to the sandpack. Confining stress helps keep the shape of the sandpack uniform and it will eliminate any possibility of channeling along the sides of the column (between sandpack and column wall). The result of this dynamic test observation was to re-design the experiment in a Hassler-type core holder so that confining stress could be applied to the sandpack.

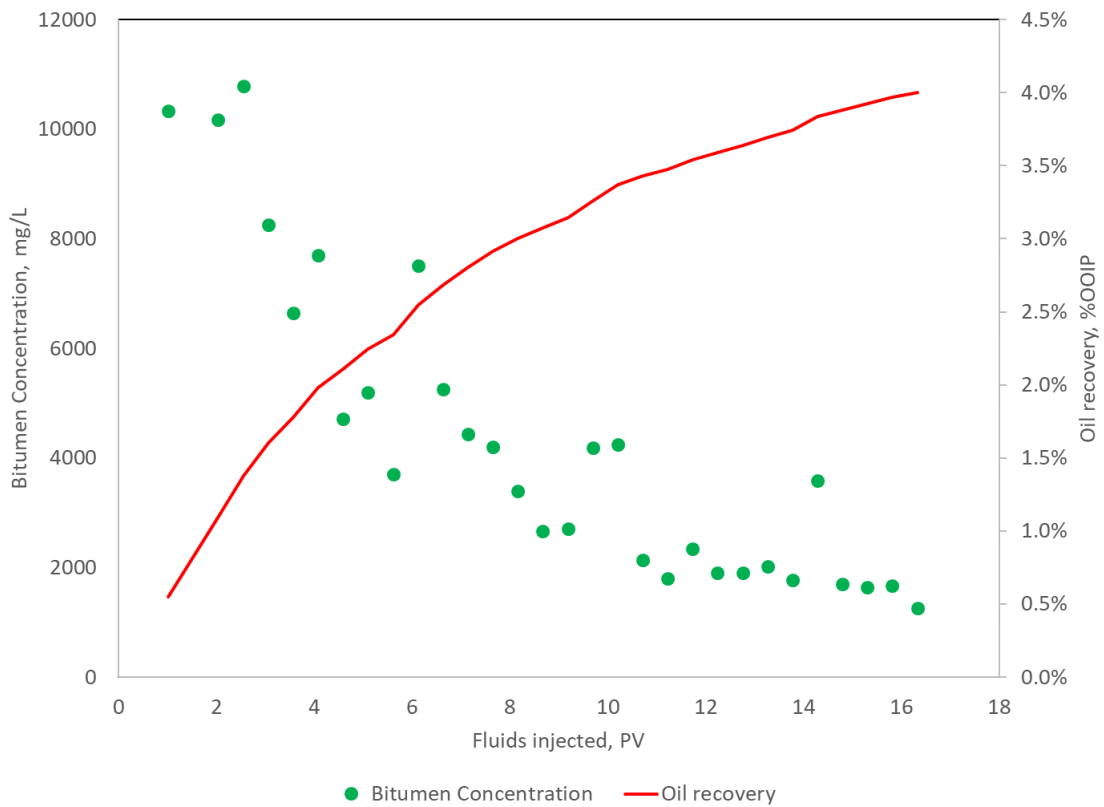


Figure 6-22: Bitumen concentration and oil recovery dynamic test 2

Table 6-5: Results of Dynamic test 2

weight of synthetic sand packed	148 g
bulk water fraction	13%
PV	10 ml
% OOIP recovery	4.00%
highest solubilization	10,000 mg/L

6.2.4.3 Dynamic Test 3

The surfactant solution injection was started at 0.015 ml/min which is equivalent to 0.5 ft/day based on initial bulk water fraction. The injection was continued for 5.44 PV and total 1.66% OOIP was recovered. The bitumen concentration at the outlet was in between 17500 mg/L to 3000 mg/L. The injection was shut-in for 24 hours once the outlet concentration fell. When injection was started again at the same flow rate, outlet concentration increased to 10000 mg/L but eventually decreased to 5000 mg/L. The flow rate was increased to 0.03 ml/min (1 ft/day) but no significant improvement in concentration. In the first dynamic test flow rate was decreased but had no effect on the degree of solubilization, so in this case it was increased to explore whether inertial forces are playing any part in the solubilization. The pressure differential and tar concentration are shown in Figure 6.23. Results are listed in Table 6-6.

Table 6-6: Results of dynamic test 4

weight of synthetic sand packed	330 g
bulk water fraction	11.8%
PV	20.5 ml
% OOIP recovery	5.75%
highest solubilization	17,500 mg/L

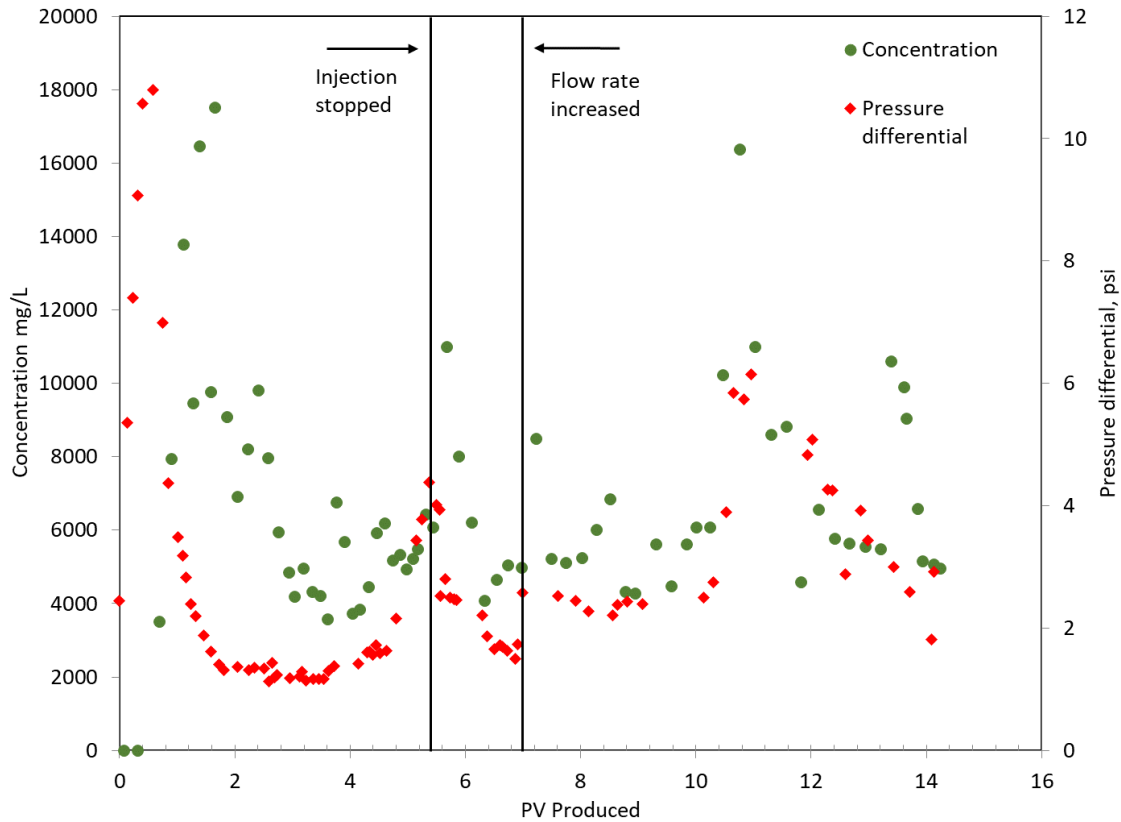


Figure 6-23: Concentration and pressure profile during dynamic test 3

Although phase behavior tests showed very promising results for this surfactant formulation, the dynamic test failed to reproduce the solubilization. Whether oil sand or synthetic oil sands were used, the degree of solubilization were much lower than expected and recoveries were not encouraging. It was decided to study surfactant phase behavior in presence of the solids.

6.2.5 Static Tests

Static tests were designed to study the surfactant phase behavior in presence of solids under static conditions. These tests were performed for both field-obtained and

synthetic oil sands samples. Ten grams of field-obtained oil sand was mixed with 10 ml of the selected surfactant formulation. This microemulsion resulted in only 4200 mg/L solubilization of bitumen (Figure 6-24). The photograph in Figure 6-24 display that, although bitumen has been cleaned off the sand, but surfactant formulation did not solubilize it and a layer of oil was present between the liquid and solid phases.



Figure 6-24: Static test result for oil sand mixed with 0.25 wt.% C20-24 IOS, 0.25 wt.% C13 13 PO sulfate, 1 wt.% 2-butanol and 0.5 wt.% sodium carbonate

Another static test was conducted with synthetic oil sand to understand the effect of bitumen content and solid surface on surfactant phase behavior. Synthetic oil sands samples were prepared with varying amounts of bitumen. These samples were mixed with the selected formulation surfactant formulation to maintain the same amount of bitumen (2 grams) in all the tubes, only the quantity of solids was varied. The

composition, amount, and microemulsion concentration of each test tube is listed in Table 6-7.

Table 6-7: Synthetic sand static test design and results

tube #	bitumen % in sand	sand weight, g	surfactant solution, ml	microemulsion bitumen concentration, mg/L
T9	9.1	22	10	3914
T13	16.6	12	10	2823
T17	13	15.3	10	3845
T23	23	8.7	10	860

The amount of bitumen solubilized was very low in all the cases and there does not appear to be a correlation with the amount of sand present in the mixture. Another possible cause for achieving limited solubilization is surfactant adsorption in the porous media. The next set of static tests were designed to study surfactant adsorption.

6.2.5.1 Surfactant Adsorption Studies

Static tests were insufficient in explaining the lower solubilization of bitumen in presence of oil. So, surfactant adsorption phenomenon was studied under static conditions with clean oil sand. The surfactant formulation which was used in dynamic tests 1-3 (0.25 wt.% C20-24 IOS and 0.25 wt.% C13 13 PO alcoxy sulfate, and 0.5 wt.% 2-butanol) was mixed with 5 grams of clean oil sand in centrifuge tubes, concentration of alkali (Na_2CO_3) was varied, keeping total liquid volume 10 ml. The tubes were mixed for 3 days and surfactant concentration was measured by HPLC afterwards. The results are listed in Table 6-8. Figure 6-25 displays trend of adsorption with sodium carbonate concentration. Note the sharp drop in adsorption at 2 wt.% sodium carbonate.

Table 6-8: Surfactant adsorption with respect to the amount of alkali added

tube #	wt.% sodium carbonate	adsorption (mg/g)	pH
1	0	23	11
2	0.5	24	11.61
3	1	22	11.49
4	1.5	24	11.87
6	2.5	5	11.91
7	3	7	11.89
8	3.5	1	11.98
9	4	2	12

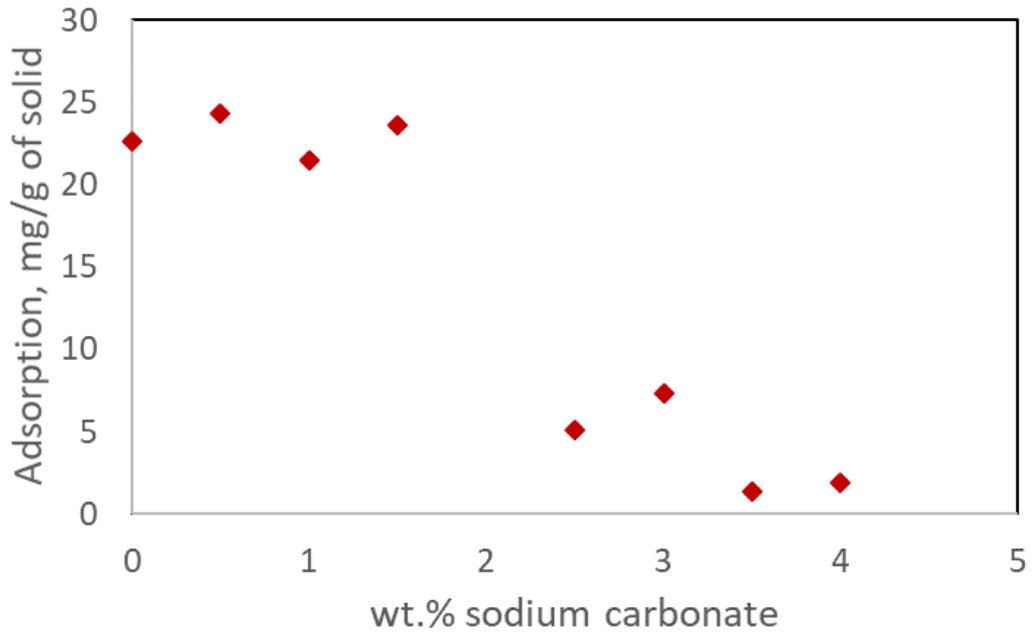


Figure 6-25: Surfactant adsorption with respect to sodium carbonate concentration, notice the inflection point at 2 wt.%

Adsorption tests exhibited that alkali concentration to reduce concentration might be critical for performance of surfactant formulation. Static tests were repeated with higher concentration of sodium carbonate, but the surfactant formulation was not

stable above 4 wt.% of sodium carbonate possibly due to salting out (Figure 6-26). Hence static tests with oil sands were repeated and only surfactant concentration, ratios, and co-solvent were changed while sodium carbonate concentration was maintained at 4 wt.%. Static tests demonstrated that as the amount of total surfactant increased, bitumen solubilization increased. Solubilization parameter for oil was highest with 1 wt.% C20-24 IOS and 1 wt.% C13 13 PO alcoxy sulfate, 1 wt.% TEGMBE, and 4 wt.% Na₂CO₃. Bitumen solubilization was 60,000 mg/L and solubilization parameter was 3 (for static test the highest solubilization possible was approximately 120,000 mg/L). Figure 6-27 displays the static test tube for this formulation. Based on these observations 1 wt.% C20-24 IOS and 1 wt.% C13 13 PO alcoxy sulfate, 1 wt.% TEGMBE, and 4 wt.% Na₂CO₃ surfactant formulation was used in all the subsequent flow experiments.

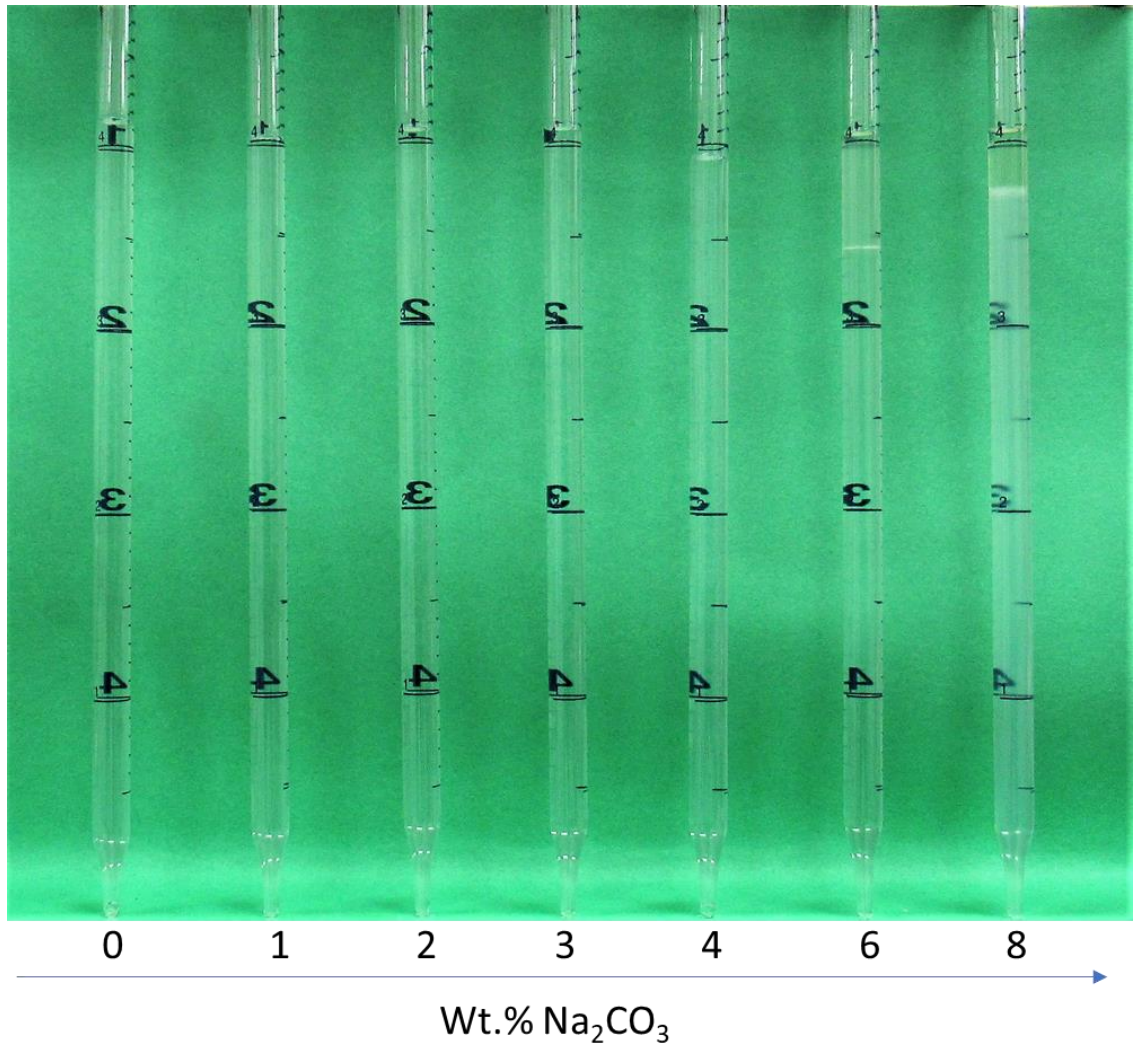


Figure 6-26: Alkali scan for 0.25 wt.% C20-24 IOS and 0.25 wt.% C13 13 PO alcoxy sulfate, and 0.5 wt.% 2-butanol, notice the phase separation in tubes higher than 4 wt.% Na₂CO₃



Figure 6-27: Static test for 1 wt.% C20-24 IOS and 1 wt.% C13 13 PO alcoxy sulfate, 1 wt.% TEGMBE, and 4 wt.% Na_2CO_3

6.2.6 Dynamic Tests 4 – 8

Static tests demonstrated that surfactant adsorption is significantly affecting the solubilization and adsorption can be significantly reduced with the use of alkali (Na_2CO_3). The surfactant formulation decided upon based on the static test was used for dynamic tests with field obtained oil sands. These tests were conducted on the flow setup described in section 5.2.6.1.

6.2.6.1 Dynamic Test 4

Sandpack dynamic properties were calculated and are listed in Table 6-9. The flow rate was maintained at 0.013 ml/min (0.9 ft/day) vertically upwards.

Table 6-9: Properties of sandpack in dynamic test 4

weight of sandpack	132.07 g
bitumen in sandpack	16.9 g
bulk water fraction	13.80%
pore volume	10.2 ml
permeability	10 Darcy
temperature	20°C

A total of 26 PVs was injected into the system. The highest bitumen concentration achieved was approximately 30,000 mg/L. The concentration profile normalized with highest concentration is shown in Figure 6-28. The pressure drops recorded while injecting was very low (0.04 psig on average). During the test it was visible through the glass that surfactant solution was interacting with bitumen and a darker microemulsion was moving upward within the column (Figure 6-29).

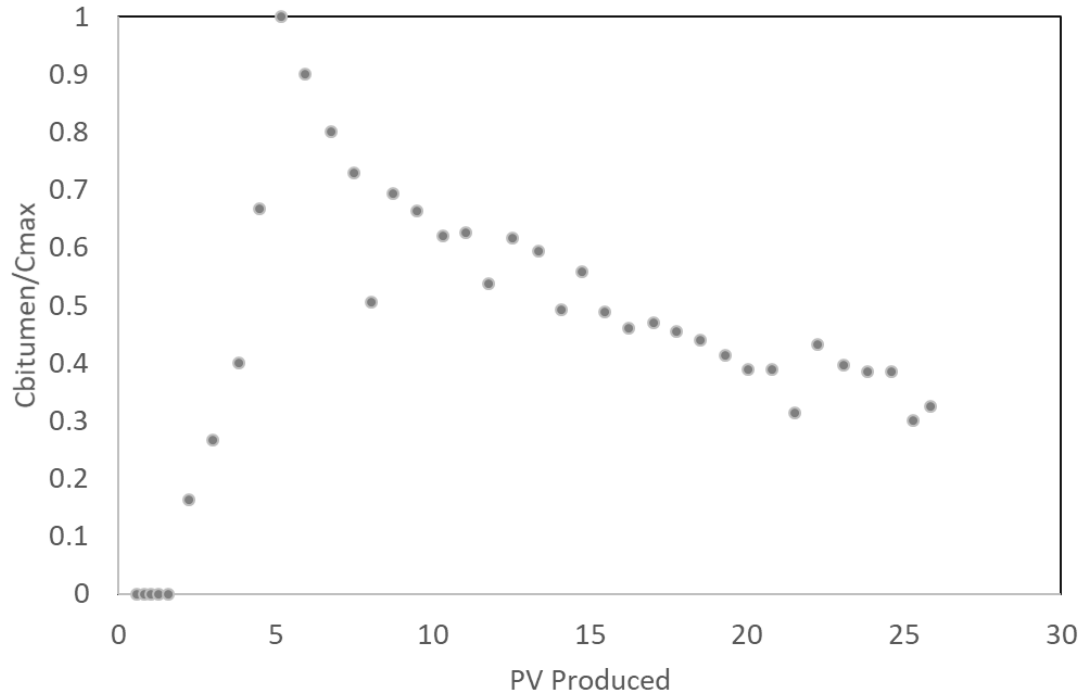


Figure 6-28: Concentration profile for bitumen in test 1, concentrations are normalized by the highest concentration which was 30,000 mg/L



Figure 6-29: Picture of the flow setup during the test. Notice the microemulsion moving through the column, circled in red

The recovery was calculated to be 46.14 % OOIP by gravimetric method, which was significantly improved from all the previous flow tests performed before adjusting for adsorption. bulk water fraction of the sandpack after the test increased to 22.8 % which translated to 40.33 % OOIP. After emptying the sand from the column, it was observed that sand was cleaner at the inlet in comparison to the outlet. Figure 6-30 highlights the difference between sand samples at the outlet and inlet. The sand near the outlet showed recovery occurred only along the outer periphery of the sandpack, which

indicate possible by-pass of the solution along the sides of the column as the solution moves upwards.

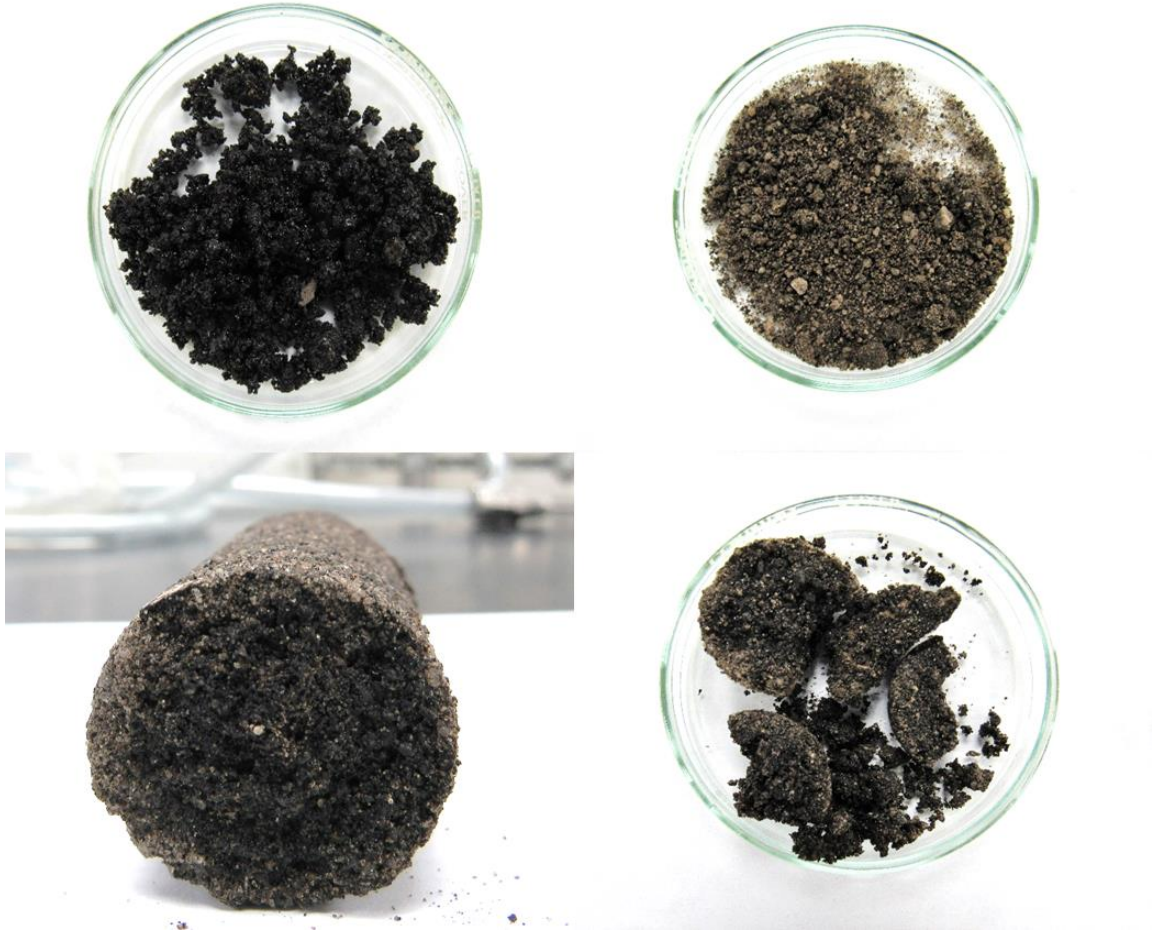


Figure 6-30: Top left – Original sand sample, Top right – Inlet sand sample after test, Bottom left – Side view of outlet sand sample, and Bottom right – Top view of outlet sand sample

6.2.6.2 Dynamic Test – 5

The composition and dynamic properties of the test-5 is listed in Table 6-10. This test was conducted with a thermal enhancement at 40°C.

Table 6-10: Properties of dynamic test - 5

weight of sandpack	137.7 g
bitumen in sandpack	17.63 g
bulk water fraction	13.80%
pore Volume	10.22 ml
permeability	44 Darcy
temperature	40°C

The flow rate was maintained at 0.013 ml/min (0.9 ft/day) vertically upwards. A total of 37 pore volumes were injected into the system. The highest bitumen concentration was measured to be approximately 37,700 mg/L. Figure 6-31 depicts the concentration profile during the test.

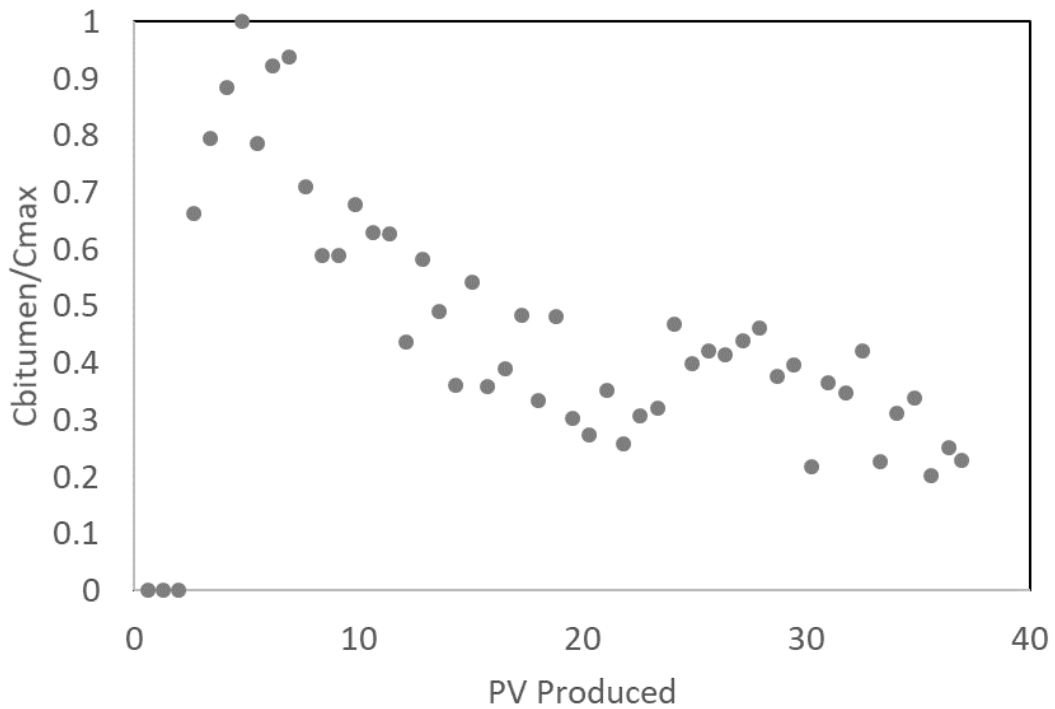


Figure 6-31: Concentration profile for test 5, concentrations are normalized by the highest concentration 37,700 mg/L

Bitumen recovery was calculated to be 61.07 % OOIP by gravimetric method. The bulk water fraction of the sandpack increased to 27.5% which translated to 58.12 % OOIP recovery. Sand was analyzed after removal from the sandpack. Note in Figure 6-32, both inlet and outlet sands look clean but the evidence of flow channeling specially towards the outlet can still be observed upon close examination.



Figure 6-32: Top – Original sand sample, bottom left – Inlet sand sample after test, and bottom right outlet sand sample after test

6.2.6.3 Dynamic Test – 6

This test was performed employing a soaking method, to provide more time for surfactant formulation interaction with bitumen. The surfactant formulation was injected

with 0.9 ft/day for 13 hours vertically upwards, after that the column was isolated for 13 hours to allow the surfactant formulation soak. The column temperature was maintained at 20°C for comparison against the test-4. Sandpack composition and properties are listed in Table 6-11.

Table 6-11: Sandpack composition and properties for test – 6

weight of sandpack	138.22 g
bitumen in sandpack	17.69 g
bulk water fraction	12.55%
pore volume	9.24 ml
permeability	38 Darcy
temperature	20°C

A total of 13 pore volumes of surfactant solution were injected from bottom to up. The highest bitumen concentration was measured to be approximately 35,500 mg/L. The concentration history is depicted in Figure 6-33.

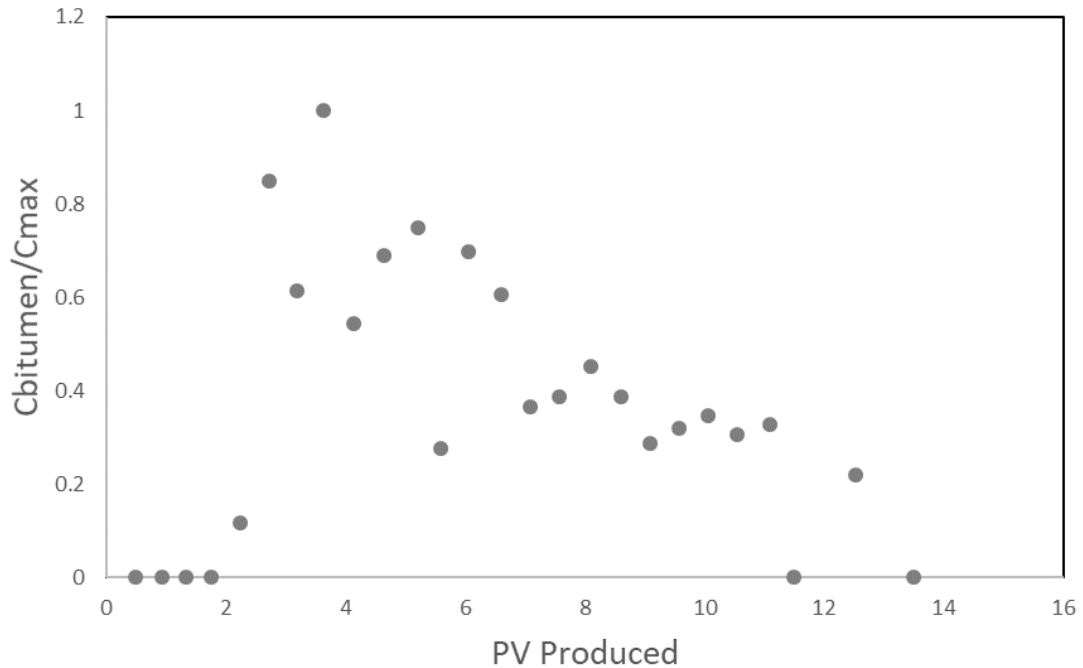


Figure 6-33: Concentration profile test 6, concentrations are normalized by the highest concentration 35,500 mg/L

The recovery was calculated to be 36.5 % OOIP by gravimetric method. The bulk water fraction of the sandpack increased to 19.69 %, which translates to 30.63 % OOIP recovery. Close examination of sand after the test also led to the same conclusion that recovery at the inlet is better than the outlet (Figure 6-34). Although the total recovery in this test was lower than the base case (dynamic test 4) since the stopping criteria for the test (i.e., the bitumen concentration dropped below 10,000 mg/L) was achieved sooner, the bitumen recovery per PV of the surfactant formulation injection was higher. This indicates that soaking process was able to achieve more solubilization in first few soaks but surfactant formulation didn't solubilize inaccessible bitumen as the process progressed.



Figure 6-34: Top left – original sand sample, top right – inlet sand sample after test, bottom left – side view of outlet sand sample, and bottom right – top view of outlet sand sample

6.2.6.4 Dynamic Test – 7

The dynamic flow test 7 was designed to understand recovery in presence of higher inertial forces. The injection rate for this test was increased to 0.027 ml/min (1.8 ft/day).

Table 6-12: Sandpack properties and composition for test 7

weight of sandpack	138.48 g
bitumen in sandpack	17.72 g
bulk water fraction	14.42%
pore volume	10.62 ml
permeability	44 Darcy
temperature	20°C

Total 15 PVs of surfactant formulation was injected. The highest bitumen concentration in produced microemulsion was measured to be approximately 35,000 mg/L.

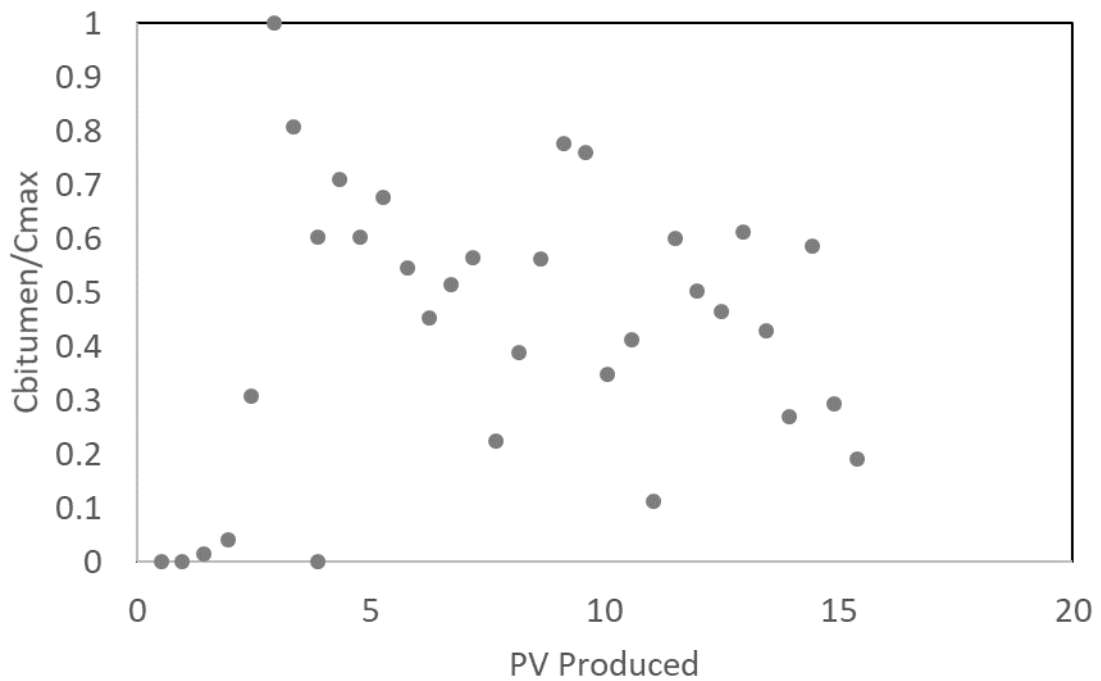


Figure 6-35: Bitumen concentration profile of test 7, concentrations are normalized by the highest concentration 35,000 mg/L

The recovery by gravimetric method was 36.11% and 30.68% by bulk water fraction difference method. The higher flow rate resulted in similar recovery to the soaking method. Sand analysis exhibited patterns similar to soaking test (Figure 6-36). Based on test 6 and 7, it was evident that, while dynamic processes are affecting bitumen recovery, the rate of solubilization was not the controlling factor. The recovery appears to be linked to the amount of bitumen contacted by the surfactant.



Figure 6-36: Top – Original oil sand, Bottom left – Inlet sand, and Bottom right – Outlet sand

6.2.6.5 Dynamic Test – 8

Based on the observations of all dynamic experiments, it was decided to test surfactant formulation at higher viscosity to increase sweep. The surfactant formulation viscosity was 2.24 cP at 20°C without any polymer present. Surfactant formulations were prepared with varying amounts of polymers to understand their characteristics with

polymer. The viscosities of these solutions were measured at 20°C, 40°C, and 60°C and at various shear rates. The results of viscosity at 20°C and s^{-1} shear rate are listed in Table 6-13.

Table 6-13: Viscosity of different polymer concentration solution at 20°C and 1/s shear rate

polymer concentration, ppm	viscosity, cP
0	2.24
2000	18.78
4000	85.55
6000	238.23
10000	831.97

All the polymer solutions passed the filtration test, so 2000 ppm polymer concentration was selected for injection. The flow rate was maintained at 0.9 ft/day and temperature was kept at 20°C. The dynamic properties of the sandpack are listed in Table 6-14.

Table 6-14: Sandpack properties and composition for test 8

weight of sandpack	147.31 g
bitumen in sandpack	18.85 g
bulk water fraction	14.10%
pore volume	10.38 ml
permeability	10 Darcy
temperature	20°C

During the test it was observed that due to the presence of polymer in microemulsion, the GC measurements were not accurate. The experiment was stopped after 26.5 PV injection, even though the GC concentration was indicating a value of approximately 20,000 mg/L, above the stopping criteria. The recovery from gravimetric

method was 34.9% OOIP and 26.33% OOIP from bulk water fraction method using a similar throughput as in the base case (dynamic test 4). The sand examination also revealed poor bitumen recovery, especially at the outlet of the column (Figure 6-37). The evidence suggests that the addition of polymer to the surfactant formulation may have interfered with the solubilization process and was not improved over the base case. This observation was confirmed with the static test performed with surfactant formulation injected in this test.



Figure 6-37: Top - original oil sand, bottom left – Inlet sand, and bottom right – outlet sand

Dynamic tests 4-8 resulted in a high recovery of bitumen compared to the dynamic test 1-3, which highlights the adverse effect of adsorption on the process and the importance of alkali for the process. These tests also helped in understanding the dynamics of recovery process, which is more affected by access to the pore space instead

of dynamic factors such as injection rates or contact time. Test 8 resulted in lower recovery which also highlighted that injecting with a higher viscosity polymer solution is not a good strategy until the effects of polymer on solubilization are studied.

6.3 Surfactant Recovery Experiments

6.3.1 Surfactant Behavior with pH Variations and Salt Concentration

Various surfactant stock solutions were observed for a range of pH to understand their behavior under both acidic and basic conditions.

6.3.1.1 Surfactant Behavior under Acidic Conditions

Sulfates are expected to undergo hydrolysis under acidic conditions at higher temperatures but at low temperature their behavior is different. Similarly, sulfosuccinates go through hydrolysis at both low and high pH but low pH hydrolysis is not complete (Batchu et al., 2014). According to Casero et al. anionic surfactant go through phase separation to achieve surfactant-rich phase in presence of hydrochloric acid (Casero et al., 1999).

A variety of anionic surfactants including sulfate, IOS, sulfosuccinates, etc. were studied for their behavior under low pH by adding a fixed amount of HCl in solution (1 ml). Table 6-15 lists the effect of acid addition on these surfactants. It was observed that surfactant with higher molecular weight showed phase separation. Surfactants which are stable under acidic conditions were eliminated from further investigations, they require higher concentration of hydrochloric acid for separation. The last formulation in Table 6-15 is the formulation used in dynamic tests; it exhibited no separation after acid addition,

but the solution became cloudy. Surfactants solutions that separated into two phases were analyzed further.

HPLC analysis of both the phases was conducted. The upper phase for all the surfactant solutions showed no trace of surfactants. In case of C12-13 7 PO sulfate, C12-13 13 PO AAS, C13-13 PO alcoxy sulfate, and sulfosuccinates surfactant-rich phase was at the bottom of the tube. Surfactant-rich bottom phase was removed and mixed with higher pH solution (water mixed with Na_2CO_3) to achieve the stable surfactant formulation again. This process exhibited that for certain anionic surfactants it is possible to produce a surfactant concentrate by acid addition.

Table 6-15: Observations of acid addition to surfactant stock solutions

surfactant type	pH of stock solution	pH after HCl addition	observation
propoxy sulfate	7.92	0.13	cloudy solution
C12-13, 7 PO Sulfate	7.97	0.2	phase separation, surfactant in bottom phase
C12-13 AAS, 13 PO	6.98	0.22	phase separation, surfactant in bottom phase
C15-18 IOS	11.47	0.05	no effect
sodium dioctyl sulfosuccinate	7.54	0.49	phase separation, surfactant in bottom phase
sodium dimyl sulfosuccinate	8.56	0.55	no effect
C20-24 IOS	11.89	0.52	cloudy solution
C13-13 PO alcoxy sulfate	10.17	0.54	phase separation, surfactant in bottom phase
octyl phenol ethoxylated	6.99	0.52	no effect
sodium dodecyl sulfate	6.02	0.26	no effect
1 wt.% C20-24 IOS and 1 wt.% C13 13 PO alcoxy sulfate, 1 wt.% TEGMBE, and 4 wt.% Na ₂ CO ₃	12.11	0.9	cloudy solution

6.3.1.2 Surfactant Behavior under Basic Conditions

Surfactants tested under acidic conditions were also tested under basic conditions by adding a fixed amount of NaOH (0.2g). The results are listed in Table 6-16. Observations from alkali addition was quite different from low pH case.

Alkali addition resulted in phase separation in some sulfates. Sulfosuccinates exhibited alkaline hydrolysis, so no surfactant was observed in the solution after base

addition. Another interesting observation was the precipitation of C20-24 out of solution, possibly because of the high pH is acting as though higher salinity to drive surfactant out of solution. The surfactant formulation used in the dynamic tests also exhibited phase separation, but the surfactant concentrate was in the upper phase (top of the tube).

Further investigations conducted on the dynamic test surfactant formulation showed that the formulation was stable below a pH 13.5 and at pH higher than 13.5, phase separation occurred. High pH behavior was more useful for microemulsion separation study because it was affecting the separation of surfactant formulation used in dynamic testing. Microemulsion produced from flow experiment was subjected to similar pH change to separate bitumen (section 5.3.2).

Table 6-16: Observations of base addition to surfactant stock solutions

surfactant type	pH of stock solution	pH after alkali addition	observation
C12-13, 7 PO Sulfate	7.97	13.71	no effect
C12-13 AAS, 13 PO	6.98	13.67	phase separation, surfactant in bottom phase
C15-18 IOS	11.47	13.85	no effect
sodium dioctyl sulfosuccinate	7.54	13.7	no surfactant
sodium dimyl sulfosuccinate	8.56	13.92	no surfactant
C20-24 IOS	11.89	13.75	precipitation
C13-13 PO alcoxy sulfate	10.17	13.75	no effect
octyl phenol ethoxylate	6.99	13.76	no effect
sodium dodecyl sulfate	6.02	13.56	no effect
1 wt.% C20-24 IOS and 1 wt.% C13 13 PO alcoxy sulfate, 1 wt.% TEGMBE, and 4 wt.% Na ₂ CO ₃	12.11	13.83	phase separation, surfactant in top phase

6.3.1.3 Surfactant Behavior under Salts Additions

Non-ionic surfactant exhibit salting out at higher salt concentrations. Phase behavior and static tests conducted with 4 wt.% octyl phenol ethoxylate (Triton X-100) showed good solubilization (40,000 mg/L) but was not selected for the dynamic tests. Triton X-100 was selected to study its behavior under a range of salt concentrations as a model non-ionic surfactant. A NaCl scan for Triton X-100 showed that at salinities above

17 wt.%, phase separation took place and the surfactant moved to a surfactant-rich phase on top of the aqueous phase. The volume of the surfactant-rich phase is dependent upon the amount of NaCl in the mixture; higher NaCl concentrations led to smaller vol of surfactant-rich phase. In other words, increases above 17 wt.% NaCl led to a more concentrated surfactant-rich phase. The lower phase did not contain any surfactant.

Triton X-100 was not affected by acid nor base addition, but it exhibited a phase separation with sodium carbonate addition. A sodium carbonate scan was conducted with Triton X-100 4 wt.% solution. It was observed that the surfactant solution separated into a surfactant-rich upper phase and a surfactant-less lower phase at sodium carbonate concentration of 5 wt.% and above. This observation was unique because it was not observed for the Triton X-100 solution when the pH was increased to 13.76. Sodium carbonate was changing the solubility of ethoxylated alcohol in aqueous solution as a result of salting out, and it was able to achieve phase separation at significantly lower concentration than sodium chloride.

6.3.2 Microemulsion Behavior with pH Variations

Based on the observations of surfactant behavior with pH variations and salt variations, similar tests were conducted using microemulsion. The microemulsion produced during the dynamic tests was mixed at both high and low pH. The expected result was to achieve microemulsion separation at high pH, since the surfactant formulation exhibited phase separation at higher pH. But microemulsion at lower pH showed clear separation (Figure 6-38). The separated oil was not floating on the surface as suggested from the figure, but it was adhered to the wall of the container. Separated

aqueous phase was analyzed, to detect any surfactant in mixture; but no surfactant was detected. The pH of the aqueous phase was increased and no surfactant was detected when it was analyzed again.

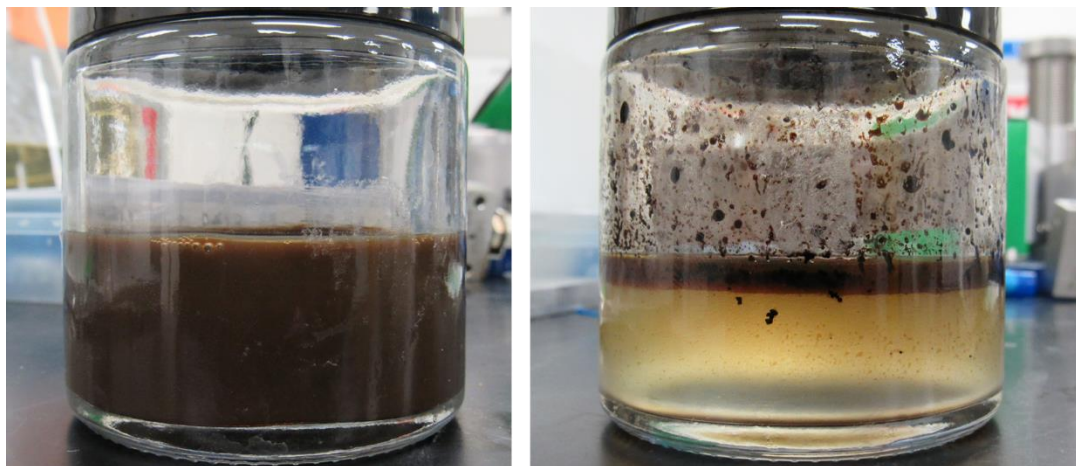


Figure 6-38: Left – Microemulsion mixture produced from dynamic test. Right – Separated phases after acid addition and equilibration

Similarly, another batch of produced microemulsion was mixed with sodium hydroxide to increase the pH above 13.5, which was the pH required to initiate phase separation based on the surfactant experiments. Increasing the pH was not as effective as acid addition because the separation was not clear (Figure 6-39). The microemulsion seemed to be destabilize but there was no separation of phases. Even after allowing several weeks to equilibrate, the solution did not separate into two phases.

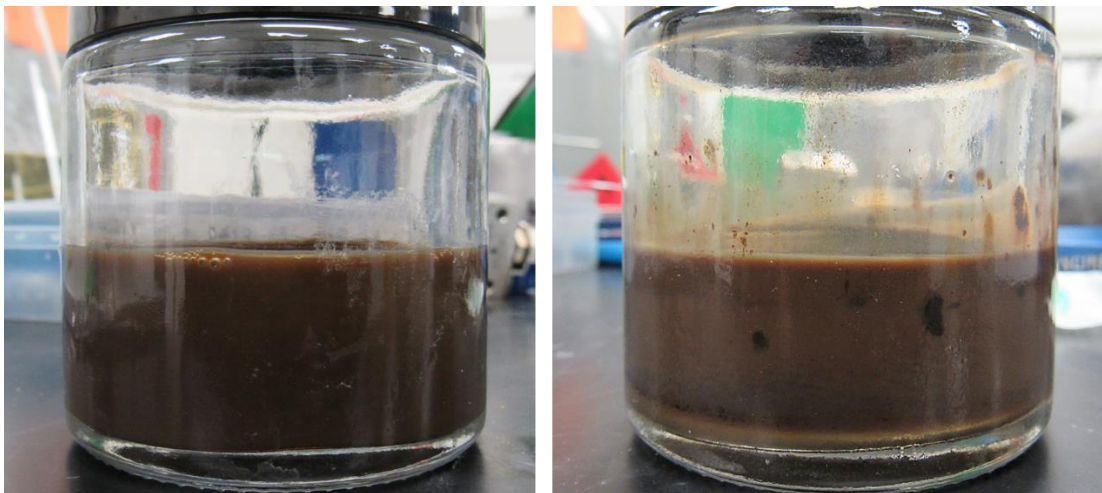


Figure 6-39: Left – Produced microemulsion from dynamic test. Right – Microemulsion after base addition, notice black droplet on the glass wall, indicating unstable solution

Triton X-100 static test microemulsion solution was used to study the effect of sodium carbonate addition to the microemulsion with non-ionic surfactant. Sodium carbonate solid was added in 0.1 g increment to 40 ml microemulsion until solution appeared to be destabilize. Sodium carbonate was able to achieve phase separation (Figure 6-40). Again, aqueous phase analysis did not show a trace of surfactant.

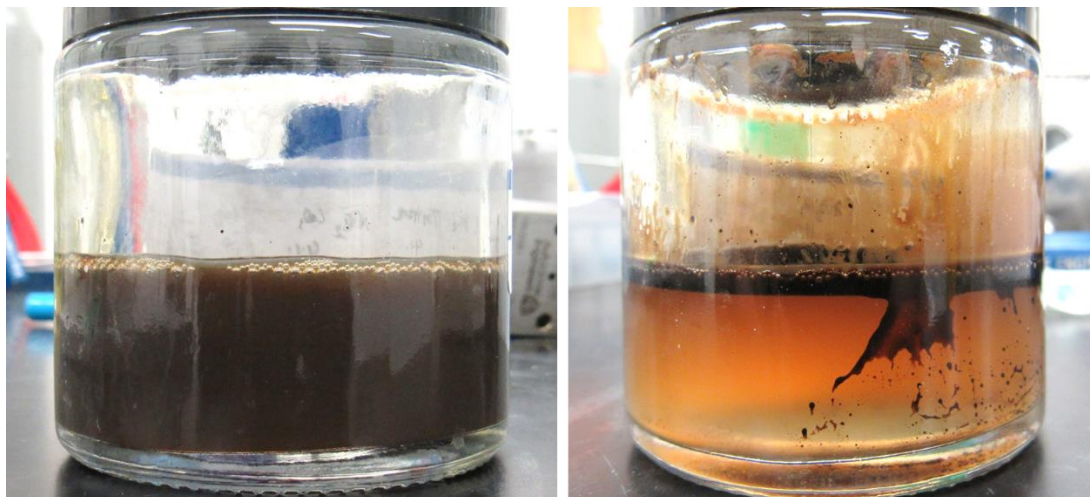


Figure 6-40: Microemulsion from Triton X-100 static tests. Right – Separated phases after salt addition and equilibration

Separation experiment conducted with microemulsion highlighted that in presence of oil phase, recovery of surfactant is more complex in comparison to the surfactant solution alone. Although surfactant-rich phase was separated for surfactant solutions but in the presence of oil the surfactant-rich phase was not observed.

Chapter 7

Summary, Conclusions and Recommendations

The research conducted as part of this dissertation conceptualized an approach to recover bitumen and extra heavy oil to meet a growing demand for a non-thermal process. The results of this work confirm the proof-of-concept, which was conducted with a synthetic oil sand composed of coal tar and quartz sand. When applied to actual oil sands, results were encouraging and required additional investigation to better understand the effects of both the actual sand and the actual bitumen. Finally, areas requiring further study are suggested.

7.1 Summary

7.1.1 Coal tar: Proof of Concept

Coal tar was used as a model oil because of the similarities in type of components present in coal tar and bitumen. The viscosity of coal tar is significantly lower than bitumen but the mechanism of recovery for cyclic surfactant solubilization is dependent on solubilization, which will be affected by oil composition. The results of the proof-of-concept study can be summarized as follows:

1. Surfactant formulation was selected with detailed phase behavior study and emphasis was on selecting formulation without any preferential solubilization.

2. Surfactant formulation of 4 wt.% alcohol propoxy sulfate, 4 wt.% sodium dioctyl sulfosuccinate, 4 wt.% tri-ethylene glycol mono-butyl ether, and 0.5 wt.% Na₂CO₃ was found to be suitable for coal tar.
3. Single phase microemulsion was produced without mobilizing the oil phase.
4. Microemulsion viscosity was significantly lower than the oil phase and was proportional to amount of oil solubilized.
5. Extremely high solubilization (300,000 mg/L and upwards) was achieved.
6. Pressure differential required for flow was extremely low, which was also an indication that oil is not mobilized.
7. Recovery of 78% OOIP was achieved despite higher flow rates.
8. This proof-of-concept demonstrated that cyclic surfactant solubilization can be feasible.

7.1.2 Bitumen

Based on the proof-of-concept study results, experiments related to cyclic surfactant solubilization of oil sands and extracted bitumen from oil sand were conducted. The results of these tests can be summarized as follows:

1. Phase behavior studies should be modified to handle highly viscous and dense materials. Solubilization measurement needs to be done based on GC analysis instead of conventional volumetric change approach.
2. Low surfactant adsorption onto the media is critical for effectiveness of the cyclic surfactant solubilization approach. Phase behavior and batch testing

conducted without taking surfactant adsorption into account will lead to extremely low recovery in 1-D flow experiments, and will likely affect the economics negatively when applied at field scale.

3. The clean sand after extracting bitumen, exhibited adsorption 23 mg of surfactant per gram of sand, which can be drastically reduced when alkali is included in the surfactant formulation.
4. A 2 wt.% alkali is found to be an inflection point for adsorption for the clean sand.
5. A surfactant formulation of 1 wt.% C20-24 IOS and 1 wt.% C13 13 PO alcoxy sulfate, 1 wt.% TEGMBE, and 4 wt.% Na₂CO₃ was found to be most effective at solubilizing bitumen without forming viscous gels.
6. When employing the formulation adjusted to reduce adsorption, it exhibited better recovery in dynamic tests no 4 to 8 (1-D flow experiments). The results of several dynamic tests are summarized in Table 7-1.
7. Dynamic test – 5 conducted at slightly elevated temperature of 60°C exhibited highest recovery of 61% OOIP.
8. Various modifications employed in the dynamic test design indicated that although the process is affected by dynamic parameters but it is not controlled by accessibility to bitumen.
9. The recovery was constrained by the adverse mobility of the surfactant formulation after solubilizing bitumen (microemulsion).

Table 7-1: Summary of dynamic tests

test number	type sand	approach	temperature
1	oil sand	continuous + soaking	20
2	synthetic oil sand	continuous injection	20
3	synthetic oil sand	continuous injection	20
4	oil sand	continuous injection	20
5	oil sand	continuous injection	40
6	oil sand	soaking	20
7	oil sand	continuous injection	20
8	oil sand	continuous injection	20

Table 7-2: Results summary of dynamic tests

test number	flow rate (ft/day)	PV injected	% OOIP recovery by bulk water fraction	% OOIP recovery by gravimetric method	recovery per PV
1	1	20	-	7.49	0.37
2	0.5	16	-	4	0.25
3	0.5	14	-	5.75	0.41
4	0.9	26	40.33	46.14	1.77
5	0.9	37	58.12	61.07	1.65
6	0.9 (soak)	13	30.63	36.5	2.81
7	1.8	15	30.68	36.11	2.41
8	0.9	26.5	26.33	34.9	1.32

7.1.3 Surfactant Recovery Experiments

Surfactant recovery experiments focused on first to separate solubilized bitumen and aqueous phase, second on recover surfactant for recycling. The experiments were designed to study surfactant behavior in aqueous phase and in microemulsion phase.

7.1.3.1 Surfactant Behavior in Aqueous Phase

Based on the evidence present in the literature, various surfactant formulations were exposed to pH variations (anionic) and salt concentration variations (non-ionic). The results of these experiments can be summarized as follows:

1. High molecular weight anionic surfactants showed phase separation into surfactant-rich and surfactant-less aqueous phases at low pH conditions (with hydrochloric acid).
2. Surfactant formulation used in the dynamic tests showed no separation at low pH but the solution became cloudy.
3. Sulfosuccinate surfactants were hydrolyzed under higher pH.
4. Surfactant formulation used in the dynamic tests showed phase separation at pH greater than 13.5, where surfactant-rich phase was present at the top layer.
5. Triton X-100 solution exhibited phase separation at 17 wt.% NaCl, and was also able to achieve the phase separation with only 5 wt.% sodium carbonate.

7.1.3.2 Microemulsion Behavior

Microemulsion produced during the dynamic and static tests were used to conduct surfactant separation tests. The results of these tests can be summarized as follows:

1. Produced microemulsion quickly separated into two very clear phases upon hydrochloric acid addition. The separated aqueous phase was surfactant poor, even after neutralizing with base.
2. Higher pH destabilized the microemulsion, but there was not clear separation.
3. Microemulsion of Triton X-100 (non-ionic surfactant) exhibited separation after addition of sodium carbonate. The aqueous phase did not contain a trace of surfactant.

7.2 Conclusions

Cyclic surfactant solubilization shows promise as a non-thermal and sustainable process to recover extra heavy oil and bitumen. The study results indicate that the proposed concept is feasible.

1. **The proof-of-concept studies with coal tar as a model oil displayed that a high degree of oil recovery is possible with proper surfactant selection**, even when employing very high flow rates that would be considered an extreme test of the approach.
2. **Phase behavior, performed with bitumen extracted from oil sand, identified the suitable surfactant formulation capable of a high degree of bitumen solubilization with minimum adsorption.**
3. **The adsorption-controlled surfactant formulation exhibited high bitumen recovery in dynamic flow tests.** The recovery was further improved with thermal enhancement. Dynamic tests also demonstrated that poor sweep of the surfactant

microemulsion due to mobility control is affecting the recovery rather than solubilization.

4. **Surfactant recovery experiments demonstrated that surfactant separation from an aqueous solution is achievable** by changing the pH (anionic surfactants) or salt concentration (non-ionic surfactants).
5. **For microemulsion solutions, it is possible to achieve separation of oleic and aqueous phase** but recovery of surfactant for re-use requires additional investigation.

7.3 Recommendations

This work has set-up a guideline to develop a cyclic surfactant solubilization process. Additional work on improving the surfactant formulations would be highly recommended. Optimizing the surfactant formulation may positively impact the process economics. A cost analysis for the process, comparing it with currently employed methods such as SAGD and open pit mining, would be beneficial. Cost analysis would help determine the cost imbalance of the cyclic surfactant solubilization process with respect to the amount of surfactant required, compared to advantages such as the: elimination of solvent addition for transportation; reduction in heating costs associated with thermal methods; reduction in water and tailings treatment costs, and; elimination of post-operation rehabilitation costs associated with strip mining. Cost analysis would also point out how effective should be surfactant recovery systems to make the process more effective.

Finally, surfactant recovery processes have not been well-studied at field scale. This work presents a brief analysis of surfactant behaviors, but further research would

not only help cyclic surfactant solubilization but also would be a benefit for the scale-up of other surfactant-based processes designed for the subsurface environment.

References

- Alboudwarej, Hussein, Joao Felix, Shawn Taylor, R Badry, C Bremner, B Brough, C Skeates, A Baker, D Palmer, K Pattison, M Beshry, P Krawchuk, G Brown, R Calvo, J a C Triana, R Hathcock, K Koerner, T Hughes, D Kundu, J L De Cárdenas, and C West. 2006. "Highlighting Heavy Oil." *Oilfield Review* 18 (2): 34–53.
https://www.slb.com/resources/publications/industry_articles/oilfield_review/2006/or2006sum03_highlighting_heavyoil.aspx%0Ahttp://www.scopus.com/inward/record.url?eid=2-s2.0-33750047195&partnerID=40&md5=76213b2719151416f2ba741951baf65b.
- Alvarez, Johannes, and Sungyun Han. 2013. "Current Overview of Cyclic Steam Injection Process." *Journal of Petroleum Science Research* 2 (3): 116–27.
- Araghi, Majid Nasehi. 2010. "Utilization of CO₂ for Improving the Performance of Waterflooding in Heavy Oil Recovery." University of Regina.
<https://doi.org/10.2118/2009-130>.
- Banerjee, Dwijen. 2012. *Oil Sands, Heavy Oil, & Bitumen*. Web. Tulsa, US: PennWell Corporation.
- Batchu, Sudha Rani, Cesar E. Ramirez, and Piero R. Gardinali. 2014. "Stability of Dioctyl Sulfosuccinate (DOSS) towards Hydrolysis and Photodegradation under Simulated Solar Conditions." *Science of the Total Environment* 481 (1): 260–65.
<https://doi.org/10.1016/j.scitotenv.2014.02.033>.
- Beliveau, Dennis. 2009. "Waterflooding Viscous Oil Reservoirs." *SPE Reservoir Evaluation*

& *Engineering* 12 (05): 689–701. <https://doi.org/10.2118/113132-pa>.

Bryan, Jonathan, and Apostolos Kantzas. 2007. “Enhanced Heavy - Oil Recovery by Alkali-Surfactant Flooding.” *Spe 110738*, 1–13. <https://doi.org/10.2523/110738-MS>.

———. 2009. “Potential for Alkali-Surfactant Flooding in Heavy Oil Reservoirs through Oil-in-Water Emulsification.” *Journal of Canadian Petroleum Technology* 48 (2): 37–46. <https://doi.org/10.2118/09-02-37>.

Butler, Roger M. 1994. “Steam-Assisted Gravity Drainage: Concept, Development, Performance And Future.” *Journal of Canadian Petroleum Technology* 33 (02): 44–50. <https://doi.org/10.2118/94-02-05>.

Casero, I., D. Sicilia, S. Rubio, and D. Pérez-Bendito. 1999. “An Acid-Induced Phase Cloud Point Separation Approach Using Anionic Surfactants for the Extraction and Preconcentration of Organic Compounds.” *Analytical Chemistry* 71 (20): 4519–26. <https://doi.org/10.1021/ac990106g>.

Chang, J, J Ivory, and R S V Rajan. 2009. “Cyclic Steam-Solvent Stimulation Using Horizontal Wells.” *Proceedings of Canadian International Petroleum Conference*, no. June: 1–29. <https://doi.org/10.2118/2009-175>.

D445-17a, ASTM Standard. 2016. “Standard Test Method for Kinematic Viscosity of Transparent and Opaque Liquids (and Calculation of Dynamic Viscosity).” *ASTM*. <https://doi.org/10.1520/D0445-17A>.

- Das, Swapan K. 1998. "Vapex: An Efficient Process for the Recovery of Heavy Oil and Bitumen." *SPE Journal* 3 (03): 232–37. <https://doi.org/10.2118/50941-PA>.
- Das, Swapan K., and Roger M. Butler. 1998. "Mechanism of the Vapor Extraction Process for Heavy Oil and Bitumen." *Journal of Petroleum Science and Engineering* 21 (1–2): 43–59. [https://doi.org/10.1016/S0920-4105\(98\)00002-3](https://doi.org/10.1016/S0920-4105(98)00002-3).
- Drews, AW. 2008. "Standard Test Method for Acid Number of Petroleum Products by Potentiometric Titration." *Manual on Hydrocarbon Analysis, 6th Edition*, 159-159–7. <https://doi.org/10.1520/mnl10848m>.
- Dwarakanath, Varadarajan, Konstantinos Kostarelos, Gary A. Pope, Doug Shotts, and William H. Wade. 1999. "Anionic Surfactant Remediation of Soil Columns Contaminated by Nonaqueous Phase Liquids." *Journal of Contaminant Hydrology* 38 (4): 465–88. [https://doi.org/10.1016/S0169-7722\(99\)00006-6](https://doi.org/10.1016/S0169-7722(99)00006-6).
- Emadi, Alireza, Mehran Sohrabi, Mahmoud Jamiolahmady, Shaun Irland, and Graeme Robertson. 2011. "Mechanistic Study of Improved Heavy Oil Recovery by CO₂-Foam Injection." <https://doi.org/10.2118/143013-ms>.
- Farouq Ali, S. M., J. M. Figueroa, E. A. Azuaje, and R. G. Farquharson. 1979. "Recovery of Lloydminster and Morichal Crudes By Caustic, Acid and Emulsion Floods." *Journal of Canadian Petroleum Technology*, no. 1: 53–59.
- Fassihi, Mohammad Reza, and Anthony R. Kavscek. 2017. *Low-Energy Processes for Unconventional Oil Recovery*.

Fortenberry, R., P. Suniga, S. Mothersele, M. Delshad, H. Lashgari, and Gary A. Pope.

2015. "Selection of a Chemical EOR Strategy in a Heavy Oil Reservoir Using Laboratory Data and Reservoir Simulation." *SPE Canada Heavy Oil Technical Conference*. <https://doi.org/10.2118/174520-MS>.

Fortenberry, Robert, Do Hoon Kim, Nabijan Nizamidin, Stephanie Adkins, Gayani W. P.

Pinnawala Arachchilage, Hee Song Koh, Upali Weerasooriya, and Gary A. Pope.

2015. "Use of Cosolvents To Improve Alkaline/Polymer Flooding." *SPE Journal* 20 (02): 255–66. <https://doi.org/10.2118/166478-PA>.

Gates, I.D., S. Larter, H. Huang, J. Adams, and B. Bennett. 2010. "The Origin, Prediction and Impact of Oil Viscosity Heterogeneity on the Production Characteristics of Tar Sand and Heavy Oil Reservoirs." *Journal of Canadian Petroleum Technology* 47 (01): 1–16. <https://doi.org/10.2118/08-01-52>.

Goldszal, Alexandre, and Maurice Bourrel. 2000. "Demulsification of Crude Oil Emulsions: Correlation to Microemulsion Phase Behavior." *Industrial and Engineering Chemistry Research* 39 (8): 2746–51.

<https://doi.org/10.1021/ie990922e>.

Hirasaki, George J., Clarence A. Miller, Olina G. Raney, Michael K. Poindexter, Duy T.

Nguyen, and John Hera. 2011. "Separation of Produced Emulsions from Surfactant Enhanced Oil Recovery Processes." *Energy and Fuels* 25 (2): 555–61.

<https://doi.org/10.1021/ef101087u>.

Hirasaki, George, Clarence A. Miller, and Maura Puerto. 2011. "Recent Advances in

Surfactant EOR." *SPE Journal* 16 (04): 889–907. <https://doi.org/10.2118/115386-PA>.

Holmberg, Krister, J Bo, and Bengt Kronberg. 2003. *Surfactants and Polymers in Aqueous Solution, 2nd Edition, John Wiley and Sons Ltd. West Sussex, UK.*
<https://doi.org/10.1002/0470856424>.

Huh, Chun. 1979. "Interfacial Tensions and Solubilizing Ability of a Microemulsion Phase That Coexists with Oil and Brine." *Journal of Colloid And Interface Science* 71 (2): 408–26. [https://doi.org/10.1016/0021-9797\(79\)90249-2](https://doi.org/10.1016/0021-9797(79)90249-2).

International Energy Agency. 2013. *Resources to Reserves 2013 - Oil, Gas and Coal Technologies for the Energy Markets of the Future* International Energy Agency, 2013. *Resources to Reserves 2013 - Oil, Gas and Coal Technologies for the Energy Markets of the Future. Doi:10.1787/9789264090705-.*
<https://doi.org/10.1787/9789264090705-en>.

Jennings, H.Y., C.E. Johnson, and C.D. McAuliffe. 1974. "A Caustic Waterflooding Process for Heavy Oils." *Journal of Petroleum Technology* 26 (12): 1344–52.
<https://doi.org/10.2118/4741-PA>.

Kaminsky, Robert D., Robert Chick Wattenbarger, Joe Lederhos, and Sergio Adrian Leonardi. 2011. "Viscous Oil Recovery Using Solids-Stabilized Emulsions" i.
<https://doi.org/10.2118/135284-ms>.

Koh, Heesong, Vincent B. Lee, and Gary A. Pope. 2017. "Experimental Investigation of

- the Effect of Polymers on Residual Oil Saturation." *SPE Journal* 23 (01): 001-017.
<https://doi.org/10.2118/179683-pa>.
- Kostarelos, Konstantinos, Sungho Yoon, and Kenneth Y. Lee. 2013. "Coal Tar Recovery Using Enhanced 'Pump-and-Treat.'" *Journal of Chemical Technology and Biotechnology* 88 (12): 2252–63. <https://doi.org/10.1002/jctb.4097>.
- Kumar, Rahul. 2013. "Enhanced Oil Recovery of Heavy Oils by Non-Thermal Chemical Methods."
- Kumar, Rahul, and Kishore K. Mohanty. 2010. "ASP Flooding of Viscous Oils." *Proceedings - SPE Annual Technical Conference and Exhibition* 6 (September): 19–22. <https://doi.org/10.2118/135265-MS>.
- Lee, Dal Heui, Robert D. Cody, and Dong Ju Kim. 2002. "Surfactant Recycling by Solvent Extraction in Surfactant-Aided Remediation." *Separation and Purification Technology* 27 (1): 77–82. [https://doi.org/10.1016/S1383-5866\(01\)00159-9](https://doi.org/10.1016/S1383-5866(01)00159-9).
- Liu, Q, M Dong, and S Ma. 2006. "Alkaline/Surfactant Flood Potential in Western Canadian Heavy Oil Reservoirs." *SPE/DOE Symposium on Improved Oil Recovery*, 1–10. <https://doi.org/10.2118/99791-MS>.
- Lowe, Donald F., Carroll L. Oubre, and Herb C. Ward. 2000. *Reuse of Surfactants and Cosolvents for NAPL Remediation*. CRC Press LLC. 1st ed. Lewis Publishers.
- McAuliffe, Clayton D. 1973. "Oil-in-Water Emulsions and Their Flow Properties in Porous Media." *Journal of Petroleum Technology* 25 (06): 727–33.

<https://doi.org/10.2118/4369-PA>.

Pei, Haihua, Guicai Zhang, J Ge, Lei Ding, Mingguang Tang, and Yufei Zheng. 2012. "A Comparative Study of Alkaline Flooding and Alkaline/Surfactant Flooding for Zhuangxi Heavy Oil." *Proceedings of SPE Heavy Oil Conference Canada*, 1–10. <https://doi.org/10.2118/146852-MS>.

Pei, Haihua, Guicai Zhang, Jijiang Ge, Lei Zhang, and Mingchao Ma. 2014. "Effect of the Addition of Low Molecular Weight Alcohols on Heavy Oil Recovery during Alkaline Flooding." *Industrial and Engineering Chemistry Research* 53 (4): 1301–7. <https://doi.org/10.1021/ie4028318>.

Peters, Kenneth E., Clifford C. Walters, and J Michael Moldowan. 1993. *The Biomarker Guide*. Cambridge University Press. Vol. 2. Cambridge: Cambridge University Press. [https://doi.org/10.1016/0146-6380\(93\)90028-a](https://doi.org/10.1016/0146-6380(93)90028-a).

Qi, Pengpeng, Daniel H. Ehrenfried, Heesong Koh, and Matthew T. Balhoff. 2017. "Reduction of Residual Oil Saturation in Sandstone Cores by Use of Viscoelastic Polymers." *SPE Journal* 22 (02): 447–58. <https://doi.org/10.2118/179689-PA>.

Renard G, Nauroy J.F., Bemmer E. n.d. *Heavy Crude Oils: From Geology to Upgrading An Overview*. Edited by Alain-Yves Huc. 2011th ed. Paris: Editions Technip.

Rhue, R. Dean, P. Suresh C Rao, and Michael D. Annable. 1999. "Single-Phase Microemulsification of a Complex Light-Nonaqueous-Phase- Liquid: Laboratory Evaluation of Several Mixtures of Surfactant/Alcohol Solutions." *Journal of*

Environmental Quality 28 (4): 1135–44.

<https://doi.org/10.2134/jeq1999.00472425002800040012x>.

Seright, Randall. 2010. "Potential for Polymer Flooding Reservoirs With Viscous Oils."

SPE Reservoir Evaluation & Engineering 13 (04): 730–40.

<https://doi.org/10.2118/129899-pa>.

Sheng, James. 2010. *Modern Chemical Enhanced Oil Recovery: Theory and Practice*.

Modern Chemical Enhanced Oil Recovery: Theory and Practice. Vol. 25. Gulf

Professional Publishing. <https://doi.org/10.1016/B978-1-85617-745-0.00013-9>.

Sheng, James J., Bernd Leonhardt, and Nasser Azri. 2015. "Status of Polymer-Flooding

Technology." *Journal of Canadian Petroleum Technology* 54 (02): 116–26.

<https://doi.org/10.2118/174541-PA>.

Sim, Steve Soo-Khoon, Fred Rolf Wassmuth, and Jen Jiang Bai. 2014. "Identification of

Winsor Type III Micro-Emulsion for Chemical EOR of Heavy Oil." *SPE Heavy Oil*

Conference-Canada, 1–11. <https://doi.org/10.2118/170018-MS>.

Sjöblom, Johan, Narve Aske, Inge Harald Auflem, Øystein Brandal, Trond Erik Havre,

Øystein Sæther, Arild Westvik, Einar Eng Johnsen, and Harald Kallevik. 2003. "Our

Current Understanding of Water-in-Crude Oil Emulsions. Recent Characterization

Techniques and High Pressure Performance." *Advances in Colloid and Interface*

Science 100–102 (SUPPL.): 399–473. <https://doi.org/10.1016/S0001->

8686(02)00066-0.

- Sobers, Lorraine, Tara LaForce, and Martin Blunt. 2010. "Optimizing Oil Recovery and Carbon Dioxide Storage in Heavy Oil Reservoirs" 2 (2005).
<https://doi.org/10.2523/132795-ms>.
- Somasundaran, P., and Zhang, L. 2006. "Adsorption of Surfactants on Minerals for Wettability Control in Improved Oil Recovery Processes." *Journal of Petroleum Science and Engineering* 52 (1–4): 198–212.
<https://doi.org/10.1016/j.petrol.2006.03.022>.
- Speight, James G. 2009. *Enhanced Recovery Methods for Heavy Oil and Tar Sands*. Elsevier. <https://doi.org/10.1016/C2013-0-15525-0>.
- Srivastava, Piyush, and Leo U. Castro. 2011. "Successful Field Application of Surfactant Additives to Enhance Thermal Recovery of Heavy Oil." In *SPE Middle East Oil and Gas Show and Conference*, 1–7. Society of Petroleum Engineers.
<https://doi.org/10.2118/140180-MS>.
- Sullivan, Andrew P., Nael N. Zaki, Johan Sjöblom, and Peter K. Kilpatrick. 2010. "The Stability of Water-in-Crude and Model Oil Emulsions." *The Canadian Journal of Chemical Engineering* 85 (6): 793–807. <https://doi.org/10.1002/cjce.5450850601>.
- Tang, Mingguang, Guicai Zhang, Jijiang Ge, Ping Jiang, Qinghua Liu, Haihua Pei, and Lifeng Chen. 2013. "Investigation into the Mechanisms of Heavy Oil Recovery by Novel Alkaline Flooding." *Colloids and Surfaces A: Physicochemical and Engineering Aspects* 421: 91–100. <https://doi.org/10.1016/j.colsurfa.2012.12.055>.

- Tyagi, V.K. 2006. "Sulfosuccinates as Mild Surfactants." *Journal of Oleo Science* 55 (9): 429–39. <https://doi.org/10.5650/jos.55.429>.
- Vogel, J.V. 1984. "Simplified Heat Calculations for Steamfloods." *Journal of Petroleum Technology* 36 (07): 1127–36. <https://doi.org/10.2118/11219-pa>.
- WEC. 2010. "World Energy Council - 2010 Survey of Energy Resources." *Atomic Energy*, 618.
- Winsor, P. A. 1948. "Hydrotrophy, Solubilisation and Related Emulsification Processes." *Transactions of the Faraday Society* 44 (4): 376. <https://doi.org/10.1039/tf9484400376>.
- Zhang, Haiyan, Mingzhe Dong, and Suoqi Zhao. 2010. "Which One Is More Important in Chemical Flooding for Enhanced Oil Recovery, Lowering Interfacial Tension or Reducing Water Mobility?" *Energy and Fuels* 24 (3): 1829–36. <https://doi.org/10.1021/ef901310v>.

Appendix A

A.1 Coal tar GC calibration

This section describes the calibration prepared to analyze the coal tar concentration in microemulsion. Dichloromethane (DCM) was used as a solvent, due to its low molecular weight it was less likely to interfere with the chromatograph. Coal tar diluted with DCM to create solutions with 500000, 250000, 125000, 62500, and 31250 mg/L coal tar concentrations. These solutions were analyzed in the GC-MS using the method described in section 5.1.2.1. The dilutions were created twice and analyzed in GC twice to ensure the consistency of the results. The two different analysis were done first in increasing order of concentration, then in decreasing order of concentration.

GC separated the various compounds present in coal tar based on molecular weight. MS was used to identify those compounds. Nine compounds were selected based on the quality of their peaks in gas chromatograph. These compounds and their respective retention times are listed in Table A-1.

Table A-1: Compound names and retention time for coal tar

compound name	retention time, min
azulene	9.932
2-methyl naphthalene	13.068
acenaphthene	17.98
dibenzofuran	18.626
fluorene	20.219
phenanthrene	25.024
fluoranthene	30.06
pyrene	31.099
benzopyrene	40.823

Peak areas for these compounds were calculated by integrating the chromatograph for each dilution. Peak area when plotted with coal tar concentration showed a linear trend. A straight line is fitted to the data, which related peak area with the concentration of coal tar. Straight line fit was done with keeping y-axis intercept to zero, which ensures that peak area is zero when coal tar concentration is zero. So straight line fit will provide a factor which can be used to convert peak area to coal tar concentration in mg/L. Figure A-1 shows the trend for azulene.

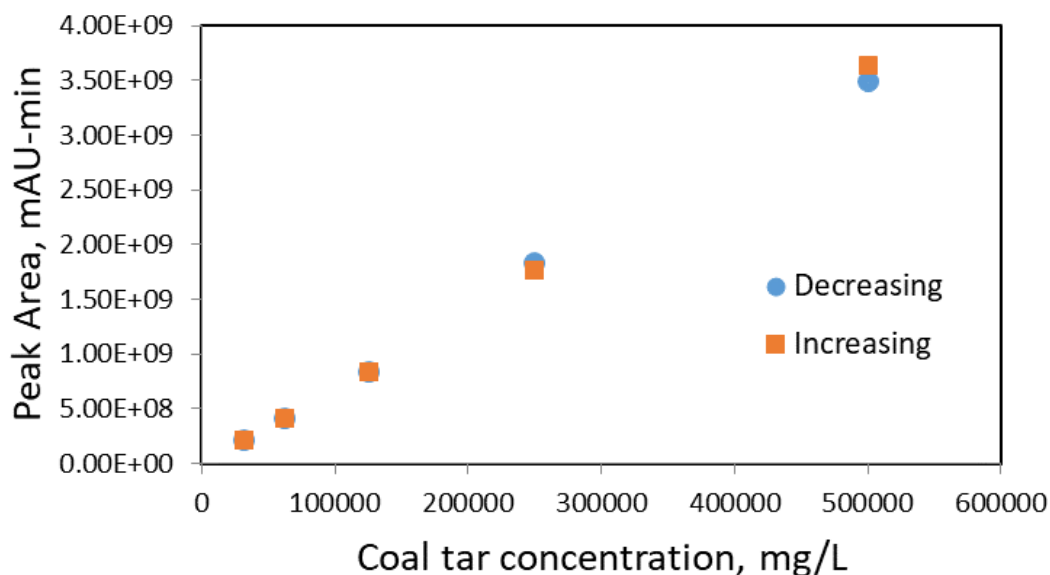


Figure A-1: Gas chromatograph peak area for azulene for different coal tar concentrations

The conversion factor for each of the selected nine compounds are listed in Table A-2. Ideally each compound should show approximately same concentration for coal tar but in case of preferential solubilization, preferentially solubilized compound will show a higher value.

Table A-2: Conversion factor for selected compound from coal tar

compound name	conversion factor, mAU-min/mg/L
azulene	7028
2-methyl naphthalene	13273
acenaphthene	15277
dibenzofuran	9263
fluorene	10934
phenanthrene	28950
fluoranthene	9574
pyrene	9710
benzopyrene	1552

A.2 Bitumen GC calibration

This section describes the calibration method used to analyze bitumen solubilized in microemulsion. DCM was used as a solvent for bitumen work too. Bitumen was diluted with DCM to create solutions with 500000, 250000, 125000, 62500, and 31250 mg/L bitumen concentration. These solutions were analyzed in GC using the method described in Table A-2. Bitumen contains numerous of compounds which are hard to separate through GC because they are very close in molecular weight. Instead from each chromatograph a collection of peaks, between retention time 20 mins – 40 mins, was selected for calibration. Two set of samples were prepared and tested in increasing and decreasing order for consistency.

Table A-3: Bitumen calibration GC method

GC-MS Method	
inlet	250°C
column	He Constant Flow 1 ml/min
oven	Initial temperature 50°C for 1 min ramp of 3°C per min to 300°C hold up time 40 mins
front detector	300°C, Hydrogen 30 ml/min, Air 350 ml/min
MS quad	150°C
MS source	230°C

Peak area for selected region was calculated by integrating the chromatograph for each dilution. Peak area when plotted with bitumen concentration showed a linear trend. A straight line is fitted to the data, which related peak area with the concentration of bitumen. Straight line fit was done with keeping y-axis intercept to zero, which ensures that peak area is zero when bitumen concentration is zero. So straight line fit will provide a factor which can be used to convert peak area to bitumen concentration in mg/L. Figure A-2 shows the trend of peak area with bitumen concentration. During the flow experiments the concentration of bitumen in produced microemulsion was lower than the lowest concentration used in calibration. Hence, another bitumen calibration was conducted based on lower concentrations 50000, 25000, 12500, 6250, and 3125 mg/L.

The GC method used for this calibration is described in Table 5-2. Figure A-3 shows the trend for lower concentration calibration.

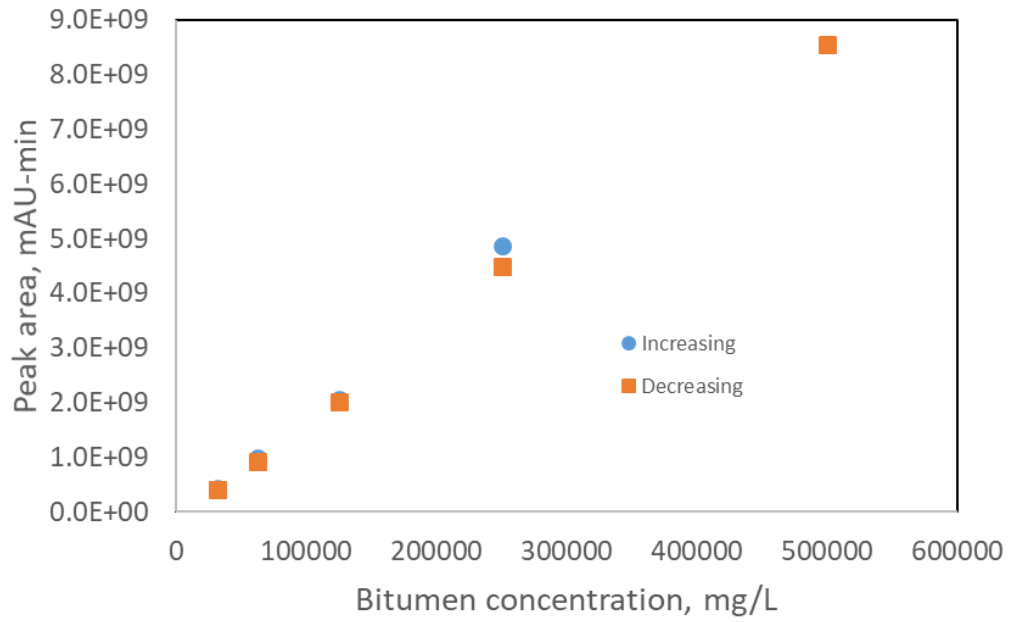


Figure A-2: Peak area for retention time 20-40 mins, for different bitumen concentration in DCM

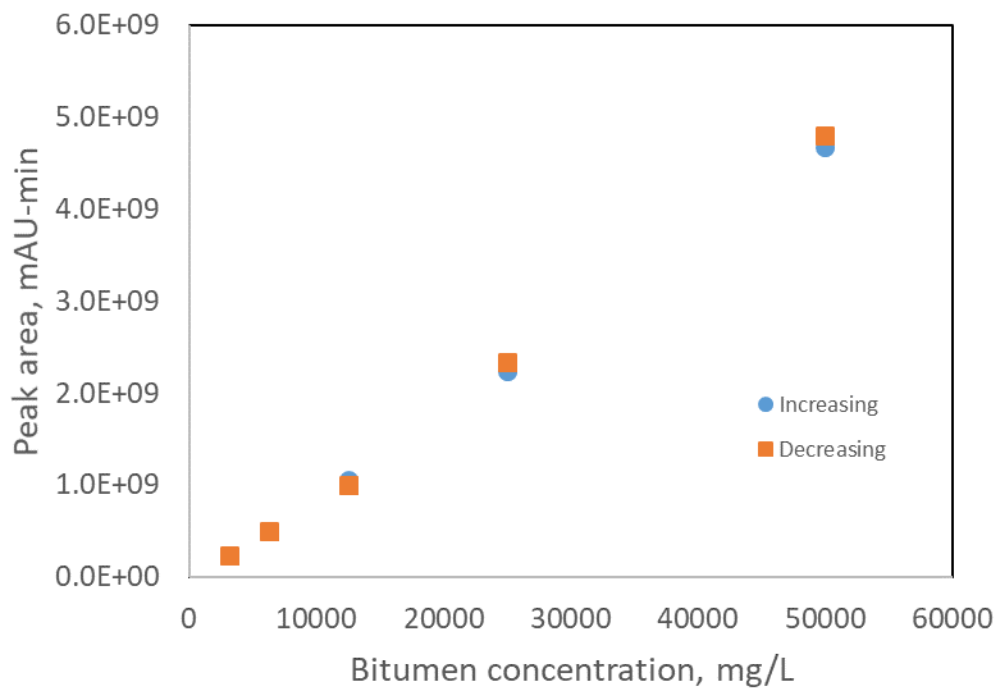


Figure A-3: Peak area for retention time 20-40 mins, for lower bitumen concentration in DCM

Based on these two calibrations, different conversion factors were calculated for both high and low bitumen concentration. For lower concentration conversion factor was 92103 mAU-min/mg/L and for high concentration 17338 mAU-min/mg/L.